

Realised Volatility Forecasting: Machine Learning via Financial Word Embedding

Eghbal Rahimikia, Stefan Zohren, and Ser-Huang Poon*

First version: July 29, 2021 • This revision: January 9, 2026

Abstract

We examine whether news can improve realised volatility forecasting using a modern yet operationally simple NLP framework. News text is transformed into embedding-based representations, and forecasts are evaluated both as a standalone, news-only model and as a complement to standard realised volatility benchmarks. In out-of-sample tests on a cross-section of stocks, news contains useful predictive information, with stronger effects for stock-related content and during high volatility days. Combining the news-based signal with a leading benchmark yields consistent improvements in statistical performance and economically meaningful gains, while explainability analysis highlights the news themes most relevant for volatility.

Keywords: Realised Volatility Forecasting, Machine Learning, Natural Language Processing, Large Language Models, Explainable AI.

JEL: C22, C45, C51, C53, C55, C58

*Eghbal Rahimikia (corresponding author) (eghbal.rahimikia@manchester.ac.uk) is affiliated with the Alliance Manchester Business School at the University of Manchester; Stefan Zohren (stefan.zohren@eng.ox.ac.uk) is with the Department of Engineering Science, University of Oxford; and Ser-Huang Poon (ser-huang.poon@manchester.ac.uk) is also at the Alliance Manchester Business School, University of Manchester. We are grateful to participants and discussants at the 2021 FMA Conference on Derivatives and Volatility, 2022 British Accounting and Finance Association (BAFA) Annual Conference, Economics of Financial Technology Conference, 12th Financial Markets and Corporate Governance Conference, 2022 FMA European Conference, 14th Annual SoFiE Conference, Advances in Data Science Conference, Greater China Area Finance Conference, 2022 FMA Annual Meeting, 3rd Frontiers of Factor Investing Conference, London-Oxford-Warwick Mathematical Finance Workshop, 2022 Cardiff Fintech Conference, 2023 International Finance and Banking Society (IFBS) Conference, Wolfe Research 6th Annual Quantitative and Macro Investment Conference, 2023 Market Volatility: NLP Trends in Research, Dow Jones, IFZ FinTech Colloquium at Lucerne University of Applied Sciences and Arts, Switzerland, and the Workshop on Financial Management and Technology for a Sustainable Future at Sheffield University Management School. We express sincere appreciation to the IT services of the University of Manchester for their continuous support and for providing the computational infrastructure utilised in this study. We extend our gratitude to Google for awarding an academic research grant in support of this study.

1 Introduction

Realised volatility forecasting in empirical finance has traditionally been dominated by econometric specifications that exploit the strong persistence of volatility while treating information arrivals only indirectly (Engle & Ng 1993), despite substantial evidence that the timing and incorporation of information are closely linked to volatility dynamics (French & Roll 1986). Media content and tone have also been shown to predict market activity and price pressure, consistent with news conveying economically relevant information beyond standard market variables (Tetlock 2007). However, despite the success of modern natural language processing (NLP) models in extracting signals from text in other fields, empirical finance has historically relied on relatively simple textual representations rather than modern language models, even as text-based methods have expanded rapidly across the broader economics literature (Gentzkow et al. 2019). Motivated by these advances, this study applies modern NLP models to news flow to forecast realised volatility and assesses whether this news-based approach can deliver effective forecasts relative to standard volatility-history benchmarks.

Most studies on realised volatility forecasting use historical realised volatility as the primary source of data for prediction within a linear framework. Heterogeneous autoregressive (HAR) models (Corsi 2009) are well-known, straightforward linear models for realised volatility forecasting that parsimoniously capture volatility persistence across multiple horizons. Further developments expanded the HAR-family with variations like HAR-J (HAR with jumps) and CHAR (continuous HAR) from Andersen, Bollerslev & Diebold (2007), SHAR (semivariance-HAR) from Patton & Sheppard (2015), and the HARQ model from Bollerslev et al. (2016). Bollerslev et al. (2018) extend these models by demonstrating that exploiting cross-asset volatility similarities improves out-of-sample forecasting performance, while Patton & Zhang (2025) show that further gains can be achieved by customising realised volatility measures. Also, during the last decade, there has been a growing number of studies on the theory and application of machine learning (ML) in finance. Recent evidence shows that ML models can outperform traditional financial models in asset pricing and return prediction (Gu et al. 2020), short-term price forecasting using high-frequency data (Sirignano & Cont 2019), and text-based financial forecasting using news articles (Adämmer & Schüssler 2020). More recently, Bybee et al. (2024) employ a latent Dirichlet allocation (LDA) topic model to analyse the textual content of Wall Street Journal articles, demonstrating that business news attention closely tracks economic activity and improves forecasts of macroeconomic dynamics.

In the context of realised volatility forecasting, Sermpinis et al. (2013), Rahimikia & Poon (2020), Christensen et al. (2023), and Han et al. (2025) show that ML models can outperform traditional

econometric approaches in predicting volatility. [Moreno-Pino & Zohren \(2024\)](#) introduce a realised volatility forecasting model using dilated causal convolutions and find that it improved prediction accuracy compared to traditional methods. [Li & Tang \(2025\)](#) introduce an automated volatility forecasting system that leverages a broad array of features and multiple algorithms, achieving superior out-of-sample forecasting performance across different horizons. A closely related strand of research shows that textual news can be processed automatically to quantify market reactions, with [Groß-Klußmann & Hautsch \(2011\)](#) demonstrating that machine-read news contains economically meaningful information for high-frequency market activity and volatility. Notwithstanding these advances, other studies caution that the empirical performance of ML models can be unstable and context-dependent ([Hillebrand & Medeiros 2010](#), [Audrino & Knaus 2016](#), [Branco et al. 2024](#), [Audrino & Chassot 2025](#)). Also, beyond realised volatility, there are a handful of studies that specifically focus on NLP and large language models (LLMs), such as [Van Binsbergen et al. \(2024\)](#), who employ ML techniques using word embeddings to construct a 170-year-long measure of economic sentiment from 200 million pages of US local newspapers, demonstrating its predictive power for GDP growth, employment, and monetary policy decisions. More recently, studies such as [Chen et al. \(2022\)](#), [Huang et al. \(2023\)](#), and [Rahimikia & Drinkall \(2024\)](#) have incorporated information extracted from advanced LLMs for various financial tasks.

Taken together, prior work has advanced realised volatility forecasting primarily by refining models that exploit the persistence of volatility and by expanding the predictor set with additional realised measures or broader ML feature sets. At the same time, text-as-data research shows that NLP and LLMs can extract economically meaningful signals from large corpora, but their role as dedicated, standalone forecasting models for realised volatility remains underexplored. This motivates four objectives that are central for both researchers and practitioners. First, we assess whether news alone, without lagged realised volatility or other market variables, can generate competitive realised volatility forecasts, and whether general-purpose language representations are sufficiently competitive for this task or specialised, finance-oriented NLP components are required. In doing so, we emphasise word embeddings as the core representation that converts unstructured news into quantitative inputs by encoding semantic and contextual similarity in a low-dimensional vector space; such embeddings also underpin modern LLMs as their representation layer, making them a transparent and practically relevant starting point for state-of-the-art NLP models in forecasting. Second, we examine whether any forecasting gains from news are stable across time and market conditions or concentrated in particular regimes. Third, we identify which components of news content drive predictability, distinguishing whether improvements arise primarily from stock-related or general news. Fourth, we evaluate the in-

cremental value of combining news-based signals with standard volatility-history benchmarks relative to using either information set in isolation. We address these objectives by developing a modern yet operationally simple NLP model that maps news directly into volatility forecasts. We evaluate it both as a news-only forecaster and as a complement to standard RV models, and use explainability analysis to identify the phrases and themes most responsible for predictive performance. We also extend the analysis to assess the economic gains of the proposed models.

We conduct a set of benchmarks to assess the quality and relevance of alternative word embeddings. At the language level, specialised financial word embeddings outperform general-purpose word embeddings in capturing economically meaningful relationships, particularly for stock-related financial analogies, even though they do not dominate on generic linguistic benchmarks. Turning to realised volatility forecasting, first, when we restrict the information set to news only, the NLP forecaster delivers competitive statistical accuracy relative to the HAR-family benchmarks even though it does not match the best volatility-history model in terms of loss ratio, with representative full out-of-sample loss ratios ranging from 1.106 to 1.187 under MSE and from 1.476 to 1.838 under QLIKE, relative to the best-performing HAR benchmark, and with realised utility in the range of 1.6280% to 2.1047% compared with 2.7540% for the benchmark model. Second, the contribution of news is strongly regime-dependent, becoming most informative during high volatility days. Third, the informativeness of news depends on its scope: stock-related (firm-specific) news yields consistently stronger performance than general news, and the advantage of specialised, finance-oriented language representations is most pronounced for stock-related inputs, with this pattern persisting both statistically and economically even when general-purpose representations remain broadly competitive. Fourth, combining the NLP news signal with the best HAR-family benchmark via a simple ensemble delivers systematic gains, reducing losses to between 0.961 and 1.020 under MSE and between 0.937 and 1.096 under QLIKE in the full sample, with particularly large improvements in high volatility days, and increasing realised utility to approximately 2.9321%. Finally, explainability analysis links these gains to economically intuitive phrases and themes, revealing distinct classes of news such as earnings announcements, corporate actions, macroeconomic releases, and policy-related developments that systematically contribute to volatility forecasts and help clarify which forms of information arrival contribute to predictive performance.

The remainder of the paper is organised as follows. [Section 2](#) outlines the theory and construction of word embeddings. [Section 3](#) presents the specialised word embeddings developed in this study and reports visualisation and evaluation results at multiple language levels. [Section 4](#) reviews realised volatility and the HAR-family of models and describes the proposed NLP framework for realised

volatility forecasting. [Section 5](#) reports the out-of-sample forecasting results, including both statistical performance and economic gain assessments, and summarises the accompanying explainability evidence. [Section 6](#) concludes by summarising the main findings and discussing directions for future research.

2 Word Embedding

Text data are inherently high-dimensional and unstructured, which makes them difficult to incorporate directly into statistical models. A central challenge is therefore to construct a numerical representation of text that is both low-dimensional and informative. Word embeddings address this challenge by mapping words to vectors in a continuous space, such that words used in similar contexts have similar representations. Earlier approaches relied on one-hot encoding, in which each word is represented by a binary vector with a single nonzero entry; under this representation, vectors corresponding to distinct words are orthogonal, which precludes any notion of similarity and limits the ability to capture structure in language. For example, while one-hot encoding treats words such as *stock* and *equity*, or *fell* and *declined*, as unrelated despite their similar economic meaning, word embeddings assign similar vectors to these words because they appear in comparable local contexts near words related to prices, markets, or volatility. This context-based representation captures economically meaningful similarities that are lost under one-hot encoding.

Let the text corpus be represented as an ordered sequence of tokens,

$$(w_1, w_2, \dots, w_T), \tag{1}$$

where a token is a sequence of characters corresponding to a unit of meaning, such as a word, number, or punctuation mark. Each token w_t takes a value in a finite set

$$\mathcal{V} = \{1, 2, \dots, N\}, \tag{2}$$

referred to as the vocabulary. Each token $w \in \mathcal{V}$ is associated with a vector

$$\mathbf{e}_w \in \mathbb{R}^d, \tag{3}$$

where d is the embedding dimension. Collecting these vectors yields an embedding matrix

$$E = (\mathbf{e}_1, \mathbf{e}_2, \dots, \mathbf{e}_N)', \tag{4}$$

with dimension $N \times d$. The vectors in E are estimated from the data and are not specified ex ante. In empirical applications, d is typically much smaller than N . The embedding matrix E is estimated using information on local co-occurrence patterns in the text. Tokens that tend to appear in similar textual environments are assigned similar vectors, so that distances or inner products between vectors provide a quantitative measure of similarity.

In this study, we focus on models that are explicitly designed to estimate word embeddings from text data. Although modern LLMs rely on word embedding layers, such representations form only one component of a substantially more complex architecture and are optimised jointly with many downstream layers for predictive performance rather than for standalone interpretability, making them difficult to isolate from an econometric perspective. By contrast, embedding-based models provide an explicit and reproducible mapping from raw text to numerical variables that is well suited for empirical finance. The resulting representations are low-dimensional, computationally tractable for large corpora, and easily aggregated within standard econometric frameworks. Efficient procedures for estimating such representations include Word2Vec and FastText, which are summarised in [Section 2.1](#) and [Section 2.2](#).

2.1 Word2Vec

Word2Vec is an unsupervised method for estimating the embedding matrix E in [Equation \(4\)](#) using local co-occurrence patterns in text ([Mikolov, Chen, Corrado & Dean 2013](#)). This method operates on the ordered sequence of tokens (w_1, \dots, w_T) defined in [Equation \(1\)](#) and is based on the idea that tokens appearing in similar local contexts should have similar embedding vectors.

Fix a context window of size k . For each token w_t , define its local context as the set of surrounding tokens within k positions of t . The embedding matrix E is estimated by maximising the following log-likelihood:

$$L(E) = \frac{1}{T} \sum_{t=1}^T \sum_{\substack{j=-k \\ j \neq 0}}^k \log p(w_{t+j} | w_t), \quad (5)$$

where the conditional probability is defined as

$$p(w_c | w_t) = \frac{\exp(\mathbf{e}'_{w_c} \mathbf{e}_{w_t})}{\sum_{l \in \mathcal{V}} \exp(\mathbf{e}'_l \mathbf{e}_{w_t})}. \quad (6)$$

The objective in [Equation \(5\)](#) corresponds to the skip-gram specification, in which the centre token w_t is used to predict each surrounding context token w_{t+j} . The continuous bag-of-words (CBOW) specification modifies this objective by reversing the prediction task. In CBOW, the centre token w_t

is predicted using the average of its context embeddings, so that \mathbf{e}_{w_t} in Equation (6) is replaced by

$$\bar{\mathbf{e}}_{\mathcal{C}_t} = \frac{1}{|\mathcal{C}_t|} \sum_{w_c \in \mathcal{C}_t} \mathbf{e}_{w_c}. \quad (7)$$

Under both specifications, the embedding vectors are estimated solely from local co-occurrence information. Tokens that appear in similar textual environments are assigned similar vectors, while tokens that appear in different contexts are placed further apart in the embedding space. When the vocabulary size N is large, evaluating the softmax probability in Equation (6) becomes computationally expensive. One approach to address this issue is hierarchical softmax, which replaces the flat softmax with a tree-based decomposition to reduce computational cost (Morin & Bengio 2005). Another approach is negative sampling, which reformulates the estimation problem as a set of binary classification tasks that distinguish observed word–context pairs from randomly sampled noise pairs (Mikolov, Sutskever, Chen, Corrado & Dean 2013).

2.2 FastText

FastText extends the Word2Vec framework by modifying how word representations are constructed, while retaining a similar estimation strategy (Bojanowski et al. 2017). As in Word2Vec, FastText estimates word embeddings using local co-occurrence patterns in the text and optimises a prediction-based objective function, such as the skip-gram or CBOW objective described in Section 2.1. The key difference lies in how each token is represented in the model.

In Word2Vec, each token is treated as an atomic unit and is associated with a single embedding vector. In contrast, FastText represents each token as a collection of smaller units, referred to as character n -grams. A character n -gram is a contiguous sequence of n characters extracted from a word. For example, when $n = 3$, the token *profit* is decomposed into overlapping character trigrams such as *pro*, *rof*, *ofi*, and *fit*. FastText also includes boundary symbols at the beginning and end of each token to distinguish complete words from character sequences that may appear as parts of other words. This ensures, for instance, that the standalone token *fit* is treated differently from the sequence *fit* appearing inside a longer word.

Formally, let a token w be decomposed into N character n -grams together with a whole-word token. FastText associates an embedding vector with each n -gram as well as with the token itself.

The representation of token w is then constructed as the sum of its component vectors,

$$\mathbf{e}_w = \sum_{i=0}^N \mathbf{u}_i, \quad (8)$$

where \mathbf{u}_0 denotes the vector associated with the token itself and \mathbf{u}_i , for $i \geq 1$, denotes the vector associated with the i th character n-gram. This composite vector \mathbf{e}_w replaces the single-token embedding used in Word2Vec. The estimation procedure in FastText is otherwise similar to that of Word2Vec. In both models, the embedding vectors are estimated by maximising a prediction-based objective defined on local co-occurrence patterns in the text. When the vocabulary size is large, direct evaluation of the softmax probability becomes computationally expensive. To address this issue, FastText adopts the same approximation techniques commonly used in Word2Vec.

This representation has important implications for rare and out-of-vocabulary (OOV) tokens. Because embeddings are constructed from character n-grams, FastText can generate meaningful vectors for tokens that appear infrequently or were not observed during training, provided their character components have been seen elsewhere in the corpus. This feature is particularly useful in settings with specialised terminology, abbreviations, or morphological variation. In contrast, Word2Vec can only assign embeddings to tokens that appear explicitly in the training data, which limits its ability to handle rare or unseen words.

3 Financial Word Embedding

At the time of writing, several well-known general-purpose word embeddings are available. A key characteristic used to compare such embeddings is the size of the corpus on which they are trained, commonly measured by the total number of processed tokens. Corpus size captures how much text the model is exposed to during estimation and is widely used as a proxy for the scale and generality of a word embedding, since larger corpora tend to encompass a broader range of language usage and contextual relationships. Prominent examples include the word embedding of Mikolov, Chen, Corrado & Dean (2013), trained using the Word2Vec algorithm described in Section 2.1 on the Google News dataset with approximately 100 billion tokens, and the WikiNews word embedding, trained using the FastText algorithm described in Section 2.2 on datasets such as Wikipedia, the UMBC web-based corpus, and the StatMT news dataset, comprising approximately 16 billion tokens.

Although general-purpose word embeddings have demonstrated strong performance in broad language tasks, it is important to consider the potential benefits of developing specialised word em-

beddings and to conduct a comparative evaluation with general-purpose alternatives at the language level. Financial language exhibits distinctive usage patterns, institutional references, and contextual relationships that are often absent from general text corpora. As a result, many tokens may carry meanings, associations, or economic implications that differ substantially from their usage in non-financial contexts. Using general-purpose word embeddings without prior validation may therefore introduce measurement error into text-based variables and weaken their economic interpretability. This consideration motivates the development and evaluation of specialised word embeddings tailored to financial language before employing them in downstream financial applications. [Section 3.1](#) describes the steps from data collection to the training of the financial word embedding, together with the associated design considerations, and [Section 3.2](#) subsequently presents the evaluation of both general-purpose and financial word embeddings using representation analysis and multiple language level benchmarks.

3.1 Design

To construct specialised word embeddings, the text used for training must be domain-specific, large in scale, and linguistically consistent, with minimal noise and redundancy. Prior research shows that the quality of word representations depends critically on corpus size, contextual richness, and stable domain usage ([Mikolov, Chen, Corrado & Dean 2013](#), [Pennington et al. 2014](#)). Moreover, the use of professionally produced financial text is essential for capturing economically meaningful language patterns and avoiding semantic distortions arising from generic corpora ([Loughran & McDonald 2011](#), [Gentzkow et al. 2019](#)). To satisfy these requirements, this study uses all news stories from the Dow Jones Newswires Text News Feed for the period from 1 January 2000 to 11 September 2015 to develop specialised word embeddings. The Dow Jones Newswires provide extensive, professionally edited coverage of financial markets and corporate events, making them particularly well suited for this purpose. A detailed description of the data cleaning and pre-processing steps applied to this corpus is provided in [Section A.1](#).

Moving to corpus size, the Google Word2Vec, WikiNews, and FinText corpora contain approximately 100 billion, 16 billion, and 4.32 billion words, respectively, implying that FinText relies on a substantially smaller corpus than these general-purpose word embeddings. Nevertheless, the FinText dataset expands substantially over time, with the number of monthly samples and the total word count exhibiting clear long-run growth over the 15-year period covered by the news archive, albeit with noticeable time variation, as illustrated in [Figure 1](#). Following all pre-processing steps, the resulting FinText corpus comprises 2,733,035 unique tokens.

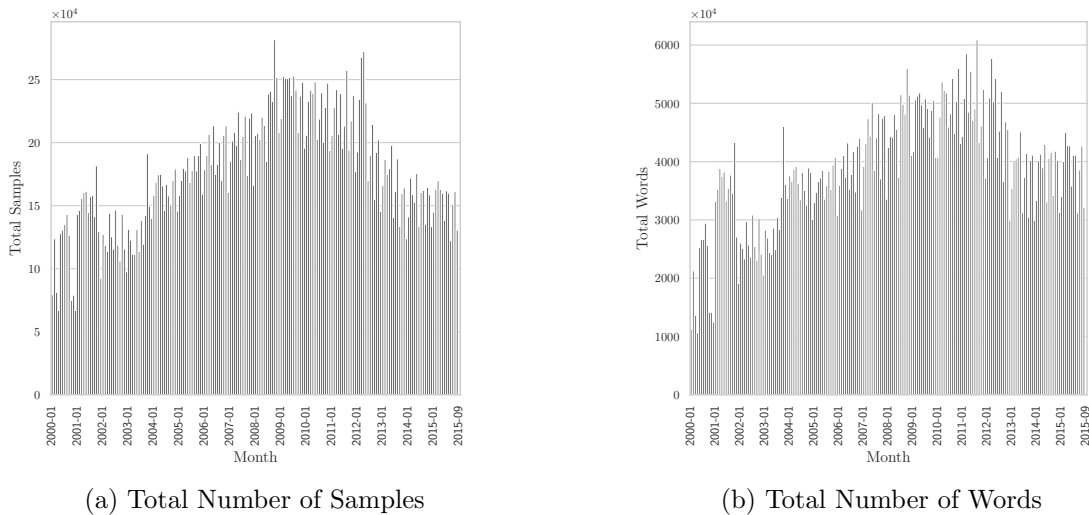


Figure 1: Monthly Corpus Sample and Word Count

Notes: The monthly total sample count and word count used for training the FinText word embedding, covering data from 1 January 2000 to 11 September 2015, are presented in figures (a) and (b), respectively.

The details of the word embedding construction, including model specifications and associated hyperparameter settings, are provided in [Section A.2](#). All pre-processing procedures and hyperparameter configurations closely follow the standard choices commonly adopted in the word embedding literature for general-purpose language models, ensuring methodological consistency across implementations. As a result, any observed differences in performance across word embeddings can be attributed to differences in the underlying corpus characteristics such as domain specificity, vocabulary composition, and contextual structure, rather than to variations in model architecture or hyperparameter selection.

In total, we trained four versions of the FinText word embedding: Word2Vec (skip-gram), Word2Vec (CBOW), FastText (skip-gram), and FastText (CBOW). In this notation, the first term indicates the underlying embedding algorithm, while the term in parentheses specifies the training architecture used to estimate the word representations. We consider all possible combinations of algorithms and training architectures in order to systematically assess their relative performance and to obtain a comprehensive understanding of how these design choices affect the resulting word embeddings. This approach is also consistent with the construction of widely used general-purpose word embeddings, which are themselves developed under different algorithm–architecture combinations.¹

¹Word embeddings trained from large text corpora may reflect biases inherent in the underlying data. In the present setting, this risk is partially mitigated by training on a long-span corpus of professionally edited news covering a large set of international news agencies, which reduces sensitivity to transient language, short-lived narratives, and idiosyncratic editorial perspectives.

Table 1: Word Embedding Comparison (Google Analogy)

Section	Word2Vec ^a			FastText		
	FinText ^b	FinText	Google	WikiNews	FinText	FinText
	(CBOW) ^c	(skip-gram)	(skip-gram)	(skip-gram)	(skip-gram)	(CBOW)
capital-common-countries	77.27	85.50	83.60	100	85.93	47.40
capital-world	63.60	75.87	82.72	98.78	71.06	35.79
currency	22.49	36.69	39.84	25.00	32.54	10.65
city-in-state	19.93	60.48	74.64	81.41	58.20	15.83
family	63.46	70.51	90.06	98.69	58.97	59.62
gram1-adjective-to-adverb	27.47	33.00	32.27	70.46	50.59	79.45
gram2-opposite	33.33	32.50	50.53	73.91	50.83	71.67
gram3-comparative	77.65	75.04	91.89	97.15	77.06	87.39
gram4-superlative	61.67	55.00	88.03	98.68	62.14	90.71
gram5-present-participle	62.30	61.24	79.77	97.53	70.63	76.06
gram6-nationality-adjective	88.11	93.23	97.07	99.12	94.05	79.05
gram7-past-tense	42.02	39.92	66.53	87.25	37.98	31.09
gram8-plural	59.23	62.46	85.58	98.69	70.92	79.54
gram9-plural-verbs	53.26	54.53	68.95	97.38	61.59	79.17
Overall	53.65	62.86	77.08	91.44	65.00	55.74

Notes: ^a To learn word embeddings from textual datasets, **Word2Vec** was developed by Mikolov, Chen, Corrado & Dean (2013), and **FastText**, an extension of the Word2Vec algorithm, was developed by Bojanowski et al. (2017).

^b The following word embeddings are utilised in this study: a financial word embedding developed specifically for this study (**FinText**); a publicly available word embedding trained on a portion of the Google news dataset (**Google**); and a publicly available word embedding trained on the Wikipedia dataset, UMBC web-based corpus, and StatMT news dataset (**WikiNews**). ^c CBOW and skip-gram are the unsupervised learning models proposed by Mikolov, Chen, Corrado & Dean (2013) for learning distributed representations of tokens.

3.2 Language Level Evaluation

We evaluate both general-purpose and specialised word embeddings using a combination of standard language benchmarks, visualisation techniques, and domain-specific tasks. The analysis begins with widely used general-purpose benchmarks to assess how different embedding algorithms and training architectures capture generic semantic relationships. We then examine the structure of the embedding spaces through low-dimensional visualisations to gain insight into how linguistic and sectoral information is organised. Finally, we turn to finance-oriented evaluations, including analogy tasks and a purpose-built gold-standard financial benchmark, to assess whether word embeddings trained on specialised financial corpora capture economically meaningful relationships that are not adequately represented by general-purpose models.

[Table 1](#) compares four versions of FinText against general-purpose word embeddings based on the Google Analogy benchmark. The Google Analogy benchmark is a widely used dataset for evaluating the quality of word embeddings. Each section in the Google Analogy benchmark contains a set of analogies. For example, under the ‘capital-common-countries’ section, the word embedding is challenged with questions such as ‘London to England is like Paris to ?’. From [Table 1](#), it is apparent that, except for ‘currency’ and ‘gram1-adjective-to-adverb’, WikiNews achieves the highest predictive accuracy. The overall evaluation score supports this observation. For this general-purpose benchmark, FinText is outperformed by Google under Word2Vec and by WikiNews under FastText. The individual

Table 2: Word Embedding Comparison (Gold-Standard Collections)

Benchmark	Word2Vec ^a			FastText		
	FinText ^b (CBOW) ^c	FinText (skip-gram)	Google (skip-gram)	WikiNews (skip-gram)	FinText (skip-gram)	FinText (CBOW)
WordSim-353 ^d (relatedness)	0.3821	0.4993	0.6096	0.6018	0.4425	0.1677
WordSim-353 (similarity)	0.6126	0.6436	0.7407	0.6713	0.6393	0.4722
SimLex	0.2657	0.2650	0.3638	0.3985	0.2772	0.2574

Notes: ^a To learn word embeddings from textual datasets, **Word2Vec** was developed by Mikolov, Chen, Corrado & Dean (2013), and **FastText**, an extension of the Word2Vec algorithm, was developed by Bojanowski et al. (2017). ^b The following word embeddings are utilised in this study: a financial word embedding developed specifically for this study (**FinText**); a publicly available word embedding trained on a portion of the Google news dataset (**Google**); and a publicly available word embedding trained on the Wikipedia dataset, UMBC web-based corpus, and StatMT news dataset (**WikiNews**). ^c CBOW and skip-gram are the unsupervised learning models proposed by Mikolov, Chen, Corrado & Dean (2013) for learning distributed representations of tokens. ^d WordSim-353 refers to the similarity and relatedness splits of the original WordSim-353 dataset, as re-annotated by Agirre et al. (2009), while SimLex (Hill et al. 2015) serves as another gold-standard dataset that focuses specifically on similarity.

and overall scores for FinText indicate that the skip-gram model performs better than CBOW.

Table 2 presents the predictive accuracy based on the gold-standard collections, namely WordSim-353 (Agirre et al. 2009) for measuring word relatedness and similarity, and SimLex (Hill et al. 2015), which focuses on similarity. Relatedness and similarity capture distinct types of relationships between words. Relatedness refers to an associative connection; words may be conceptually linked even if they do not share a direct meaning. For example, *doctor* and *hospital* are related because they appear in similar contexts but are not synonyms. Similarity, on the other hand, requires words to have a close or nearly identical meaning. For instance, *doctor* and *physician* are similar, as they essentially refer to the same concept. Accounting for these differences is crucial for language models, as it enables them to capture a broader range of semantic relationships between words. All these collections contain human-assigned judgements about the relatedness and similarity of word pairs. Performance is measured by Spearman’s rank correlation coefficient. It is evident from Table 2 that Google’s word embeddings outperform under WordSim-353, while WikiNews embeddings perform better under SimLex. As before, FinText is outperformed by Google under Word2Vec and outperformed by WikiNews under FastText. Additionally, for both Word2Vec and FastText algorithms, the skip-gram model is generally superior to the CBOW model, with only one exception.

To obtain a clearer understanding of how different word embeddings handle financial terminology, we illustrate their behaviour through a visualisation-based example that examines sectoral relationships among firm names. In this setting, tokens representing firms operating in similar sectors are expected to be embedded closer together, as their names tend to appear in comparable financial contexts. As discussed in Section 2, each token is represented by a 300-dimensional embedding vector,

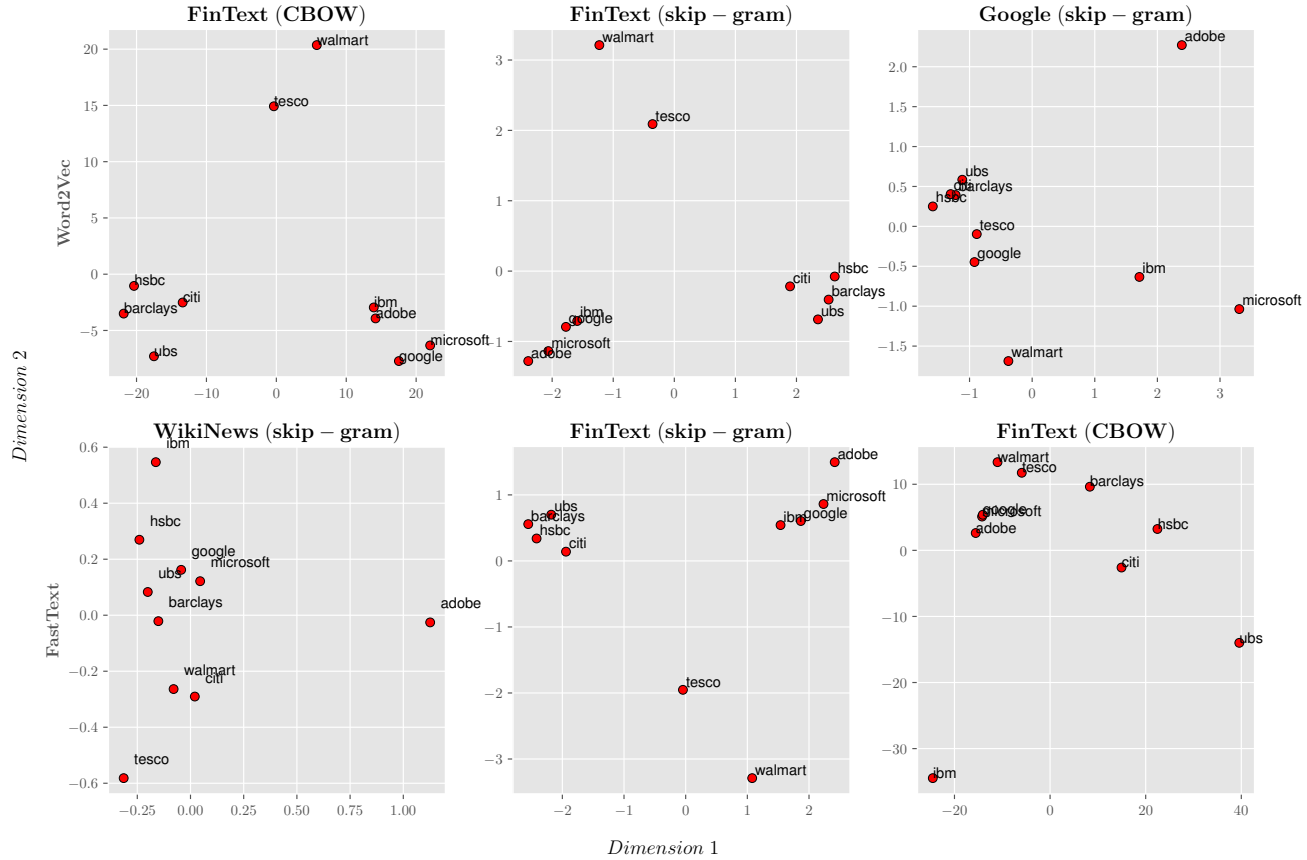


Figure 2: 2D Visualisation of Word Embeddings

Notes: This figure presents a two-dimensional visualisation of selected word embeddings obtained via PCA, which reduces the original 300-dimensional vectors to two dimensions. The selected tokens comprise technology firms (*microsoft*, *ibm*, *google*, *adobe*), financial services and investment banking firms (*barclays*, *citi*, *ubs*, *hsbc*), and retail firms (*tesco*, *walmart*). The first and second rows correspond to Word2Vec and FastText embeddings, respectively, estimated using FinText as well as publicly available Google Word2Vec and WikiNews embeddings. As principal components are identified only up to orthogonal rotation, the orientation and sign of the axes are arbitrary. The visualisation is therefore intended to illustrate relative clustering and separation patterns among embeddings rather than to support a literal interpretation of axis directions or distances.

Table 3: Financial Analogy Examples

Analogy	Word Embedding		
	Google	WikiNews	FinText ^a
debit:credit :: positive:X	positive	negative	negative
bullish:bearish :: rise:X	rises	rises	fall
apple:iphone :: microsoft:X	windows_xp	iphone	windows
us:uk :: djia:X	NONE ^b	NONE	ftse_100
microsoft:msft :: amazon:X	aapl	hmv	amzn
bid:ask :: buy:X	tell	ask-	sell
creditor:lend :: debtor:X	lends	lends	borrow
rent:short_term :: lease:X	NONE	NONE	long_term
growth_stock:overvalued :: value_stock:X	NONE	NONE	undervalued
us:uk :: nyse:X	nasdaq	hsbc	lse
call_option:put_option :: buy:X	NONE	NONE	sell

Notes: ^a Among the four variants considered, this table reports the FinText specification developed using the Word2Vec algorithm with a skip-gram model. ^b Not included in the vocabulary list.

which we project onto a two-dimensional space using principal component analysis (PCA) for visual inspection. Figure 2 presents the resulting projection for selected company tokens. Word2Vec results are shown in the top row, while FastText results appear in the bottom row. The projection suggests that, under FinText, technology firms such as *microsoft*, *ibm*, *google*, and *adobe*, financial institutions such as *barclays*, *citi*, *ubs*, and *hsbc*, and retail firms such as *tesco* and *walmart* appear more coherently grouped relative to the general-purpose word embeddings. This pattern suggests that domain-specific training enables FinText to capture sector-related usage of firm names.

Table 3 also reports a set of simple financial analogy tasks designed to assess whether different word embeddings capture financially meaningful relationships. Each row follows the structure ‘A is to B as C is to X’, where the correct answer reflects a standard financial association. Analogy tests provide a transparent and intuitive way to evaluate word embeddings, as they directly reveal whether economically meaningful relationships are encoded in the embedding space without relying on complex downstream models. For example, just as a *debit* is offset by a *credit*, a *positive* position should be offset by a *negative* one; similarly, *bullish* corresponds to rising prices, while *bearish* corresponds to falling prices. A word embedding performs well if it returns the financially intuitive counterpart rather than a token that is merely lexically similar. The results show that the general-purpose word embeddings frequently fail to return meaningful financial answers. In contrast, FinText consistently recovers the correct financial relationships, including exchange identifiers, trading concepts, and valuation terminology. Overall, these examples demonstrate that FinText encodes financial concepts and institutional knowledge that are not captured by general-purpose word embeddings.

While general-purpose language benchmarks provide useful information about overall linguistic competence, they are not sufficient in finance, where language encodes institutional facts and econom-

Table 4: Gold-Standard Financial Benchmark

Group	Word2Vec ^a			FastText		
	FinText ^b (CBOW) ^c	FinText (skip-gram)	Google (skip-gram)	WikiNews (skip-gram)	FinText (skip-gram)	FinText (CBOW)
Ticker to City (US)	14.74	23.68	0.26	0.00	15.00	1.05
Name to Ticker (US)	38.55	43.29	0.13	0.00	34.61	19.08
Name to Incorporation year (US)	25.70	28.86	0.09	0.00	23.07	12.72
Name to Exchange (US)	26.71	23.03	4.08	0.07	17.37	9.54
Name to State (US)	27.32	19.53	6.47	0.11	13.95	7.63
Name to Country (US & UK)	24.56	17.63	5.39	0.09	11.89	6.36
Name to Country (US, UK, China, & Japan)	21.84	15.75	4.62	0.08	10.94	5.45
Overall	25.63	24.54	3.01	0.05	18.12	8.83

Notes: ^a To learn word embeddings from textual datasets, **Word2Vec** was developed by Mikolov, Chen, Corrado & Dean (2013), and **FastText**, an extension of the Word2Vec algorithm, was developed by Bojanowski et al. (2017). ^b The following word embeddings are utilised in this study: a financial word embedding developed specifically for this study (**FinText**); a publicly available word embedding trained on a portion of the Google news dataset (**Google**); and a publicly available word embedding trained on the Wikipedia dataset, UMBC web-based corpus, and StatMT news dataset (**WikiNews**). ^c CBOW and skip-gram are the unsupervised learning models proposed by Mikolov, Chen, Corrado & Dean (2013) for learning distributed representations of tokens.

ically meaningful relationships. Also, visualisations and illustrative examples are helpful for intuition but remain qualitative and cannot provide a systematic assessment of whether word embeddings capture financial knowledge. This motivates the introduction of a gold-standard financial benchmark to rigorously evaluate finance-specific relationships. The benchmark is based on firm-level information from Bureau van Dijk’s Orbis database and consists of seven groups of financial analogy tasks covering different settings, with full construction details provided in Section A.3. Similar to the previous benchmarks, this benchmark evaluates word embeddings using simple financial analogies. For example, if *Apple* is associated with the ticker *AAPL*, then *Amazon* should be associated with *AMZN*; if *Microsoft* is listed on *NASDAQ*, then *IBM* should be listed on *NYSE*; and if *HSBC* is headquartered in the *UK*, then *JPMorgan* should be headquartered in the *US*. A word embedding performs well if it consistently recovers these known financial relationships.

The results are presented in Table 4. Each benchmark group contains 380 analogy questions, yielding a total of 2,660 financial analogies across all seven groups, and accuracy is reported as the proportion of correctly recovered relationships within each group and overall. The results show that general-purpose word embeddings perform poorly across all financial relationships, with near-zero accuracy in several benchmark groups. In contrast, FinText substantially outperforms these alternatives across all categories, achieving approximately eight times the performance of Google Word2Vec and more than 500 times that of WikiNews in overall accuracy. WikiNews attains an overall accuracy of just 0.05%, while Google Word2Vec reaches 3.01%. Among the FinText variants, Word2Vec with the CBOW architecture performs slightly better than its skip-gram counterpart. These results suggest that, despite their training on substantially larger corpora, general-purpose word embeddings do not adequately capture core financial relationships, while specialised financial word embeddings perform

markedly better on this language level financial benchmark.²

4 Realised Volatility Forecasting

A substantial body of literature establishes that financial market volatility is fundamentally driven by the arrival and interpretation of information. Seminal contributions such as [Engle & Ng \(1993\)](#) and [Andersen & Bollerslev \(1998\)](#), together with subsequent intraday evidence, show that information arrival and return innovations are closely linked to volatility clustering and sudden volatility episodes ([Gallo & Pacini 2000](#), [Kalev et al. 2004](#)). More broadly, this line of research emphasises that volatility dynamics reflect heterogeneous information flows operating across different horizons, which in turn generate the persistent behaviour commonly observed in financial markets ([Andersen, Bollerslev & Diebold 2007](#)). However, most empirical volatility forecasting models incorporate this information only indirectly, relying on past volatility measures as reduced-form summaries of how markets have responded to information arrivals. Although this approach has proven empirically successful, it abstracts from the underlying informational content and treats volatility persistence primarily as a time-series phenomenon. This provides motivation for testing the use of textual news as a direct proxy for information arrival.

4.1 Realised Volatility Forecasting and HAR Models

Assume that P_t denotes the stock price process, whose dynamics are given by

$$d \log(P_t) = \mu_t dt + \sigma_t dW_t + J_t dQ_t, \quad (9)$$

where μ_t is the drift component, assumed to be continuous, σ_t is the càdlàg volatility process, W_t is a standard Brownian motion, J_t denotes the jump size, and Q_t is a Poisson process. Over the interval $[t - 1, t]$, the integrated variance (IV) is defined as

$$IV_t = \int_{t-1}^t \sigma_s^2 ds. \quad (10)$$

Since IV_t is not directly observable, it is approximated by the realised variance,

$$RV_t \equiv \sum_{i=1}^M r_{t,i}^2, \quad (11)$$

²The FinText word embeddings and the gold-standard financial benchmark are available for download at [FinText.ai](#).

where $M = 1/\delta$ and the δ -period intraday return is defined as

$$r_{t,i} \equiv \log(P_{t-1+i\delta}) - \log(P_{t-1+(i-1)\delta}).$$

In the absence of jumps, this estimator is consistent as $\delta \rightarrow 0$ (Barndorff-Nielsen & Shephard 2002). Building on this framework, the HAR-family of models is employed to forecast realised variance (RV), which constitutes the main forecasting task of this study. To evaluate NLP models for RV forecasting, it is necessary to establish a strong and well-defined set of benchmark models. In general, these models can be written as

$$RV_{t+1} = f(\overline{RV}_{t-i}, J_t, \overline{BPV}_{t-i}, RV_t^+, RV_t^-, \overline{RQ}_{t-i}), \quad (12)$$

where \overline{RV}_{t-i} denotes the average RV over the previous i days. The jump component is defined as $J_t = \max(RV_t - BPV_t, 0)$, with bipower variation given by

$$BPV_t = \frac{\pi}{2} \sum_{i=1}^{\overline{M}-1} |r_{t,i}| |r_{t,i+1}|, \quad (13)$$

where \overline{M} denotes the maximum sampling frequency. The positive and negative realised semivariances are defined as

$$RV_t^+ \equiv \sum_{i=1}^M r_{t,i}^2 \mathbb{I}(r_{t,i} > 0), \quad RV_t^- \equiv \sum_{i=1}^M r_{t,i}^2 \mathbb{I}(r_{t,i} < 0), \quad (14)$$

where $\mathbb{I}(\cdot)$ is an indicator function. Finally, realised quarticity (RQ) is defined as

$$RQ_t \equiv \left(\frac{M}{3}\right) \sum_{i=1}^M r_{t,i}^4, \quad (15)$$

where \overline{RQ}_{t-i} denotes its average over the previous i days.

Within this setting, all models considered can be viewed as restricted versions of the general specification in Equation (12). The AR model restricts the information set to the daily realised variance RV_t only. The benchmark HAR model of Corsi (2009) extends this specification by including RV measured at heterogeneous horizons, namely the daily component RV_t and its weekly and monthly averages \overline{RV}_t^w and \overline{RV}_t^m , where the weekly component is defined as the average RV over the preceding five trading days and the monthly component as the average over the preceding twenty-two trading days. The SHAR model of Patton & Sheppard (2015) further augments the HAR specification by incorporating the signed realised semivariances RV_t^+ and RV_t^- defined in Equation (14). The HAR-J model extends the HAR framework by adding the jump component J_t , while the CHAR model replaces RV with the continuous volatility measure based on bipower variation as defined in Equation (13)

(Andersen, Bollerslev & Diebold 2007). To address measurement error in RV, the ARQ model extends the AR specification by including realised quarticity RQ_t defined in Equation (15). The HARQ model augments the HAR specification with average realised quarticity \overline{RQ}_{t-i} , and the HARQ-F model further extends the HARQ framework by incorporating RQ averaged over weekly and monthly horizons (Bollerslev et al. 2016).³

To formally implement the forecasting experiments, the sample periods, estimation procedure, and data construction are specified as follows. The in-sample period spans from 27 July 2007 to 11 September 2015, comprising 2,046 trading days, while the out-of-sample period extends from 14 September 2015 to 27 January 2022, comprising 1,604 trading days.⁴ RV is constructed from 5-minute intraday returns, consistent with Liu et al. (2015), who highlight the difficulty of significantly beating the 5-minute RV benchmark. Forecasts are generated using a daily rolling-window estimation scheme with a fixed window length of 2,046 days.⁵ RV is computed over NASDAQ trading hours from 9:30 AM to 4:00 PM Eastern Time using limit order book (LOB) data obtained from the LOBSTER database (Huang & Polak 2011). The empirical analysis is conducted on a cross-section of 23 stocks selected based on liquidity and data availability over the sample period.⁶ All data-cleaning procedures follow the guidelines of Barndorff-Nielsen et al. (2009), with a detailed description provided in Section A.4. Descriptive statistics for RV across these 23 stocks are presented in Table 5.

4.2 NLP for RV Forecasting

An NLP-based RV forecasting model is introduced in which textual information from news serves as the sole input and the next-day RV, RV_{t+1} , is the output. The news input consists of stock-related or general headlines released during the open-to-open interval associated with trading day t , reflecting information available to the market prior to the realisation of RV_{t+1} . Importantly, the

³As noted by Andersen, Bollerslev & Diebold (2007), one possible strategy for handling heavy-tailed distributions is to model the logarithm of RV. However, as discussed by Patton & Sheppard (2015), this approach effectively targets forecasts of log-volatility rather than volatility in levels, even though the latter is generally of greater relevance for most economic and financial applications. Accordingly, and consistent with the established literature on the HAR-family of models, this study focuses on forecasting RV in levels.

⁴The rolling estimation window comprises 2,046 trading days, corresponding to approximately eight years of daily observations. This choice reflects a standard bias–variance trade-off in volatility forecasting, providing sufficient observations for stable estimation while remaining responsive to gradual structural change. In unreported robustness checks, we also considered a window length equal to half this size and found no material differences in the relative performance of the HAR-family of models.

⁵As documented in Section 3.1, the FinText word embedding dataset covers the period from 1 January 2000 to 11 September 2015. The out-of-sample forecasting exercise is therefore free from look-ahead bias in the estimation and evaluation of the forecasting models, while the word embeddings are treated as fixed representations trained on a historical corpus.

⁶This study focuses on a sample of 23 large-cap U.S. equities. These stocks are selected to ensure high-quality and continuous LOB data, reliable RV measurement, and sufficiently rich and regular firm-specific news coverage over the sample period. The number of stocks included in the analysis is also consistent with the range commonly adopted in the empirical RV forecasting literature. Moreover, expanding the cross-sectional dimension beyond this level would impose substantially higher computational requirements that are beyond the scope of this study.

Table 5: RV Descriptive Statistics

Ticker	Min	Max	1 st quantile	Median	3 rd quantile	Mean	STD	Kurtosis	Skewness
AAPL	0.102	229.420	0.899	1.733	3.680	4.623	12.596	111.012	9.124
MSFT	0.067	216.181	0.829	1.449	2.814	3.237	8.125	194.004	11.275
INTC	0.030	318.697	1.103	1.873	3.577	4.299	11.628	294.963	13.982
CMCSA	0.004	237.387	0.910	1.632	3.320	3.821	9.697	192.169	11.462
QCOM	0.122	373.543	1.024	1.975	4.129	5.073	15.380	200.609	12.100
CSCO	0.047	343.946	0.886	1.561	3.028	4.115	13.160	212.453	12.258
EBAY	0.205	252.608	1.319	2.271	4.356	5.082	12.592	142.684	10.009
GILD	0.064	259.489	1.167	1.892	3.379	4.304	12.930	182.820	12.063
TXN	0.177	287.897	1.047	1.905	3.748	4.014	9.820	311.666	14.242
AMZN	0.065	547.030	1.305	2.336	4.808	6.200	19.359	242.205	12.735
SBUX	0.052	265.094	0.864	1.594	3.423	4.201	11.237	161.435	10.626
NVDA	0.159	1104.351	2.282	4.358	9.084	9.756	30.117	586.612	20.058
MU	0.292	484.388	3.570	6.246	11.912	12.818	25.734	89.141	7.960
AMAT	0.292	531.579	1.783	3.028	5.712	6.005	14.632	532.194	18.338
NTAP	0.119	462.821	1.503	2.587	5.154	6.289	18.008	201.510	11.934
ADBE	0.119	569.720	1.099	2.020	3.908	4.947	15.003	588.095	18.867
XLNX	0.229	265.374	1.296	2.363	4.787	5.005	11.941	194.718	11.764
AMGN	0.032	214.156	0.969	1.593	2.872	3.398	9.612	183.759	11.898
VOD	0.055	219.033	0.687	1.342	3.137	3.933	10.869	122.252	9.601
CTSH	0.189	485.894	0.984	1.764	4.161	5.288	15.757	325.214	14.287
KLAC	0.154	499.808	1.456	2.710	5.416	5.919	16.878	354.626	16.033
PCAR	0.039	389.930	1.157	2.162	4.633	5.125	12.108	313.338	13.010
ADSK	0.268	693.772	1.644	2.765	5.167	6.644	22.377	388.131	16.554

Notes: The period for the descriptive statistics spans from 27 July 2007 to 27 January 2022.

model does not incorporate any past RV or other market-based variables, allowing the predictive content of text to be examined in isolation. While HAR-type models summarise the market’s reaction to information arrivals through lagged volatility measures in [Section 4.1](#), the proposed NLP structure allows news content to enter the forecasting process explicitly and in a flexible manner. The model architecture is intentionally simple, computationally tractable, and easy to train, while remaining sufficiently expressive to capture nonlinear relationships between textual information and future RV.

Formally, let $\mathcal{X}_t = \{X_{(t,1)}, X_{(t,2)}, \dots, X_{(t,k_t)}\}$ denote the sequence of k_t tokens extracted from news headlines released on day t , where each token $X_{(t,i)}$ belongs to a finite vocabulary and is mapped to a fixed-dimensional word embedding vector $\mathbf{e}_{(t,i)} \in \mathbb{R}^d$ using a word embedding matrix. After padding the sequence to a fixed length K , the embedded tokens form a sentence matrix $\mathbf{S}_t \in \mathbb{R}^{K \times d}$, which provides a numerical representation of the information set available to the market prior to the realisation of RV_{t+1} . A nonlinear feature extraction operator $\Psi(\cdot)$, implemented via convolutional filters of varying window sizes followed by pooling operations, maps the sentence matrix \mathbf{S}_t into a low-dimensional latent feature vector $\mathbf{z}_t = \Psi(\mathbf{S}_t)$. The forecast of next-day RV is then obtained as

$$RV_{t+1} = f_{\text{NLP}}(\mathcal{X}_t) = \phi(\mathbf{z}_t; \boldsymbol{\theta}), \quad (16)$$

where $\phi(\cdot)$ denotes a nonlinear mapping with parameters $\boldsymbol{\theta}$. This formulation replaces the traditional HAR-family information set based on lagged components in [Equation \(12\)](#) with a direct, text-driven

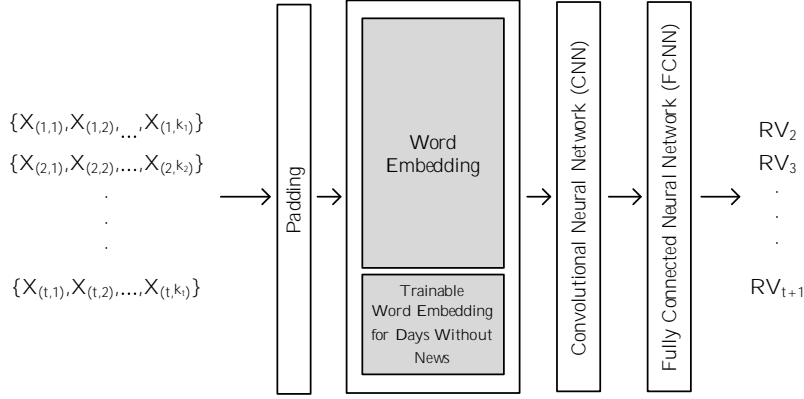


Figure 3: An Abstract Representation of the NLP Model

Notes: The set $X_t = \{X(t, 1), X(t, 2), \dots, X(t, k_t)\}$ consists of the sequence of tokens extracted from the news headlines observed on day t , where $X(t, k)$ represents the k -th token in the aggregated daily token sequence. Additionally, RV_{t+1} denotes the RV for day $t+1$ (i.e., the next day's RV). Padding up to a maximum length of 500 tokens (for stock-related news) is applied to ensure that all inputs to the model have a consistent length. The word embedding block comprises two distinct word embeddings; to accommodate days without any news, a trainable word embedding is employed.

representation of information arrival, allowing semantic patterns in news to enter the RV forecasting process explicitly and flexibly.

Figure 3 provides an abstract representation of the NLP forecasting structure. In implementation, the token sequence \mathcal{X}_t is padded to a fixed maximum length of 500 by appending the placeholder token NONE whenever $k_t < 500$. Padding is a standard procedure in NLP that ensures all inputs have a consistent length, which is required for efficient batch processing and stable model training. We use only news headlines rather than full news bodies, as aggregating complete articles generates extremely long token sequences even for a single day. Such sequences substantially increase computational demands and may lead to overfitting, particularly given the relatively limited size of the training sample. Moreover, news headlines are specifically designed to convey the most salient information contained in the full article.

As shown in Figure 3, the NLP model consists of three main components: a word embedding block, a convolutional neural network (CNN) block, and a fully connected neural network (FCNN) block. The word embedding block transforms each input token $X_{(t,k_t)}$ into a numerical vector representation. For days with news, each token is mapped to a fixed 1×300 word embedding vector. This word embedding is fixed and non-trainable to reduce model complexity and computational cost. The resulting 500×300 sentence matrix provides a structured numerical representation of the daily news input. On days without news, this matrix is initialised with randomly generated, trainable values to allow the model to learn a baseline representation in the absence of textual information. The CNN

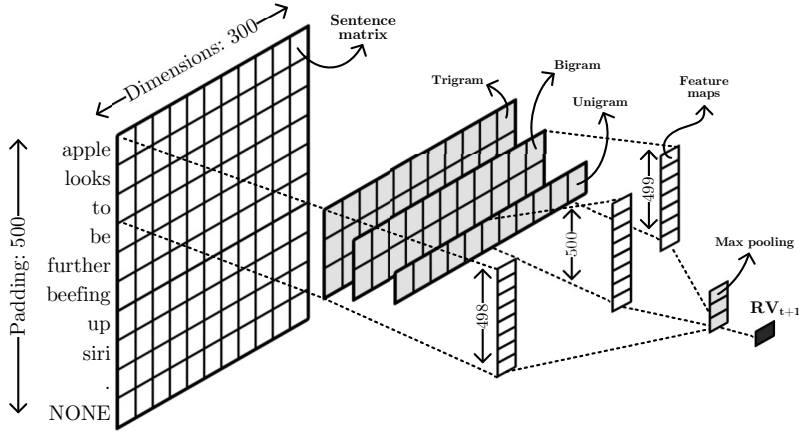


Figure 4: A Detailed Representation of the NLP Model

Notes: The sentence matrix is a 500×300 matrix with a maximum padding length of 500 (for stock-related news) and word embedding dimensions of 300. In this matrix, each token is represented by a vector of 300 values. This structure employs three filters of different sizes. The filters, with sizes of 1, 2, and 3, generate feature maps of dimensions 500, 499, and 498, respectively. Global max pooling is then applied, followed by a fully connected neural network (FCNN). The output of this network is the RV of the following day (RV_{t+1}).

block processes the sentence matrix by extracting informative local patterns and higher-level features from the embedded text. CNNs are well suited for this task because they efficiently capture local dependencies and hierarchical structures in sequential data through convolution and pooling operations (LeCun et al. 2015). The FCNN block then maps the extracted features to a single scalar output, producing the forecast of next-day RV. This layered architecture enables the model to capture nonlinear relationships between news content and future RV while maintaining a transparent and parsimonious structure.⁷

Figure 4 illustrates the detailed architecture of the NLP model using an example input. The input is a numerical sentence matrix constructed from the news headline ‘apple looks to be further beefing up siri,’ where each word is mapped to a fixed length numerical vector using a word embedding. The sentence matrix is processed by a CNN. Three sets of one-dimensional convolutional filters with window sizes $\{1, 2, 3\}$ are applied simultaneously, corresponding to unigram, bigram, and trigram representations based on one word, two consecutive words, and three consecutive words, respectively. The filters move across the sentence with a stride of one word, meaning that the filter window shifts forward by one token at a time and evaluates all overlapping word sequences, and the convolution is applied using valid padding, so filters are only evaluated where they fully overlap with the input sentence, resulting in output feature maps that are shorter than the original sentence representation. For each window size, 25, 50, 75, and 100 distinct filters are considered in separate model specifications, allowing the CNN to learn multiple types of unigram, bigram, and trigram patterns. When applied

⁷Apart from the reasons discussed in Section 2, the embedding-based CNN architecture is chosen to provide a transparent, reproducible, and computationally tractable mapping from news text to RV forecasts in a rolling out-of-sample setting. This design allows for regular retraining while retaining interpretability, which is central to the empirical objectives of this study.

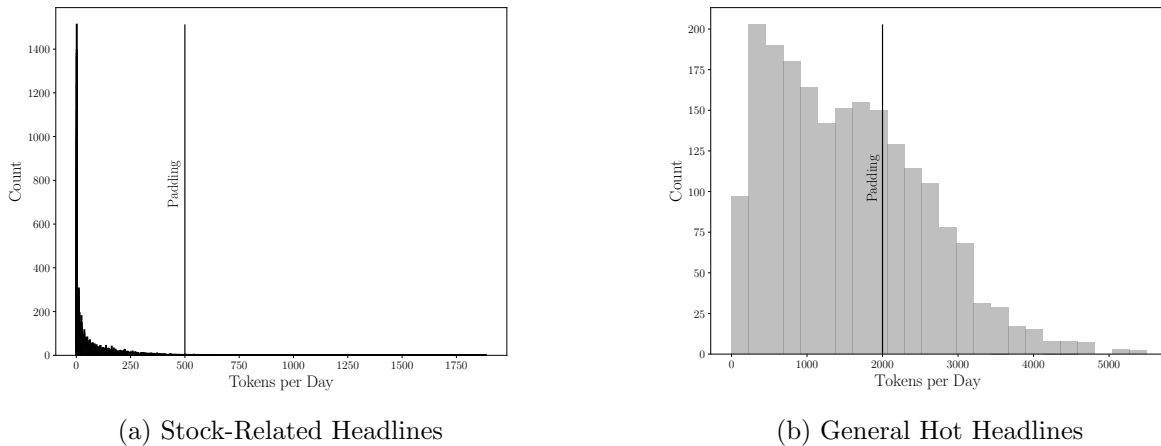


Figure 5: Distribution of Daily Tokens

Notes: The number of daily tokens is calculated, and their histograms are plotted for the stock-related news (left plot) and general hot news (right plot) (training data spanning 2,046 days). The vertical line represents the chosen maximum padding length. For clarity, ticker names are excluded from the left plot.

to a sentence of length 500 tokens, these operations produce three one-dimensional feature maps with lengths $\{500, 499, 498\}$.⁸ Each feature map is summarised using global max pooling, which retains the strongest filter response corresponding to the most informative word or phrase pattern in the headline. The pooled values form a fixed length feature vector that is passed to a FCNN, which combines the extracted features to produce a forecast of next-day RV. A detailed description of the model architecture and hyperparameter settings is provided in [Section A.8](#).

News headlines are aggregated over an open-to-open rolling window from 9:30 AM Eastern Time on day t to 9:30 AM Eastern Time on day $t + 1$, ensuring that the information set aligns with the trading period relevant for forecasting RV_{t+1} . Because daily re-estimation of the NLP model is computationally intensive, the model is retrained every thirty trading days and used for forecasting in the subsequent period. The Dow Jones Newswires Text News Feed assigns tags to news stories to indicate their relevance to specific stocks; for stock-related news, we use the ‘about’ tag, which denotes news stories in which the firm is a main subject. To examine the impact of broader information arrivals on RV, we additionally consider general hot news. According to their definition, ‘hot’ denotes news stories deemed important or timely under Dow Jones editorial standards. Additionally, we define a news story as ‘general’ when it is not associated with any specific stock. In summary, stock-related news comprises headlines in which the firm is the primary subject, such as earnings announcements, management changes, and firm-specific corporate events. General hot news consists of major market-moving headlines that are not attributable to any single firm but instead convey broader economic,

⁸When multiple headlines occur on the same day, they are concatenated into a single input sequence with a dedicated separator token inserted between consecutive headlines. This identifier prevents convolutional filters from spanning across unrelated news items and ensures that local n-gram features are learned within individual headlines rather than across headline boundaries.

5 Empirical Results

As a first step, we evaluate all models within the HAR-family in [Section 4.1](#) using both in-sample and out-of-sample performance to identify the best-performing specifications, which subsequently serve as benchmarks for further analysis. [Section A.5](#) reports the parameter estimates and in-sample performance measures for these models. The results indicate that the CHAR specification consistently delivers the strongest in-sample performance, attaining the highest adjusted R^2 and the lowest average MSE and QLIKE⁹ among all competing HAR-type models. In addition, following the modified test proposed by [Bollerslev et al. \(2016\)](#), we report the results of the reality check (RC), which evaluates the following hypothesis from the perspective of the model under evaluation, treating it as the benchmark and testing it against the best-performing competing model:

$$H_0 : \min_{k=1, \dots, n} \mathbb{E} \left[L^k(RV, X) - L^0(RV, X) \right] \leq 0, \quad (17)$$

$$H_1 : \min_{k=1, \dots, n} \mathbb{E} \left[L^k(RV, X) - L^0(RV, X) \right] > 0. \quad (18)$$

Let L^k (for $k = 1, \dots, n$) denote the value of the loss function for each of the n alternative models, and let L^0 represent the loss associated with the model under evaluation. As in [Bollerslev et al. \(2016\)](#), this formulation corresponds to a reversed version of the RC of [White \(2000\)](#), which focuses on whether the model under evaluation outperforms the best-performing competing specification. Following [White \(2000\)](#), the RC test is implemented using the stationary bootstrap procedure of [Politis & Romano \(1994\)](#), based on 999 resamples and an average block length of five.¹⁰ Failure to reject the null hypothesis indicates that there is insufficient statistical evidence to conclude that the model under evaluation outperforms all competing models in the candidate set. When reporting the RC results, each model is evaluated relative to all other specifications within the HAR-family. Accordingly, we implement the modified RC on a stock-by-stock basis. For each stock, the null hypothesis is that the model of interest does not outperform the best-performing model in the competing benchmark set. The RC is reported as the proportion of stocks for which this null hypothesis is rejected, indicating statistically significant outperformance of the model relative to all competing specifications. Throughout this study, RC is reported in percentage terms. Higher RC values therefore indicate that the model delivers statistically significant forecasting outperformance relative to the benchmark set for a larger fraction of stocks.

⁹The mean squared error (MSE) is defined as $MSE(RV_t, \widehat{RV}_t) \equiv (RV_t - \widehat{RV}_t)^2$. The quasi-likelihood (QLIKE) loss is defined as $QLIKE(RV_t, \widehat{RV}_t) \equiv \frac{RV_t}{\widehat{RV}_t} - \log\left(\frac{RV_t}{\widehat{RV}_t}\right) - 1$, where RV_t and \widehat{RV}_t denote the RV and its corresponding forecast at time t , respectively. As shown by [Patton \(2011\)](#), MSE, QLIKE, and their variants belong to the class of robust loss functions suitable for ranking RV forecasting models among competing HAR-type models.

¹⁰Our results show that the reported findings in this study are not sensitive to these choices; therefore, we follow the parameter values used in [Bollerslev et al. \(2016\)](#).

We further distinguish between normal and high volatility days when presenting the out-of-sample results. A day is defined as a high volatility day when RV for that day exceeds $Q3 + 1.5 IQR$, where $IQR = Q3 - Q1$, and $Q1$ and $Q3$ are the first and third quartiles of the RV distribution computed per stock over the out-of-sample period, respectively.¹¹ Normal volatility days are defined as all trading days not classified as high volatility days.¹² Turning to the out-of-sample results, the CHAR model again emerges as the best-performing specification. For details on the in-sample and out-of-sample results, the reader is referred to the [Section A.5](#)

Moving to the NLP models, the performance difference between NLP model j and CHAR, which serves as the best-performing specification within the HAR-family, is computed across stocks as

$$\rho_{MSE,j} = \text{Mean}_{i=1,\dots,23} \left[\frac{MSE_i(NLP_j)}{MSE_i(CHAR)} \right], \quad (19)$$

where the index i denotes an individual stock in the cross section, with a total of 23 stocks. Alternatively, the mean operator in [Equation \(19\)](#) can be replaced by the median to obtain a measure that is more robust to outliers. The MSE can also be replaced by the QLIKE loss. For both MSE and QLIKE, a value below one indicates that the NLP model outperforms the CHAR benchmark, whereas a value above one implies superior performance of the CHAR model. We also report results based on the RC as defined earlier. For the remainder of the analysis, we compare each NLP model against the full set of HAR-family of models, including AR, HAR, SHAR, HAR-J, CHAR, ARQ, HARQ, and HARQ-F.¹³

¹¹The threshold multiplier of 1.5 follows Tukey’s (boxplot) *inner-fence* convention for flagging unusually large observations using a robust, nonparametric cutoff (Tukey 1977, McGill et al. 1978). This convention is widely used in exploratory data analysis and standard software implementations, and it is particularly suitable for RV measures that are typically skewed and heavy-tailed.

¹²This classification is used exclusively for forecast evaluation and not for model estimation or forecast construction, thereby avoiding potential data-snooping concerns. By applying this criterion to the sample of 23 tickers, approximately 10% (160 days) of the out-of-sample period (1,604 days) are classified as high volatility days. Additional descriptive evidence is provided in [Section A.7](#), which illustrates the time series evolution of high volatility day counts across assets, revealing temporal variation, clustering during periods of heightened market volatility, and cross-sectional heterogeneity across tickers.

¹³We summarise out-of-sample forecasting performance from two complementary perspectives. Relative loss measures compare each NLP model to the single strongest benchmark over the evaluation period and quantify the magnitude of the associated forecast-error gap. By contrast, the RC statistic evaluates, on a stock-by-stock basis, whether the model under evaluation is not significantly outperformed by any model within a broader benchmark set, and reports the proportion of stocks for which this null hypothesis is rejected. Consequently, a model may exhibit a small loss compared to the best individual benchmark while still demonstrating widespread statistically significant gains over alternative benchmarks. The two metrics therefore capture distinct but complementary dimensions of forecasting performance: relative loss isolates shortfalls with respect to the top benchmark, whereas RC reflects the breadth of statistically significant improvements across competing models. Retaining both measures provides a more robust basis for model evaluation and mitigates the risk of model-selection bias.

5.1 Forecasting Performance of NLP Models

The NLP models analysed in this study differ along two dimensions: the word embedding specification and the underlying news information set. As described in [Section 3](#), we consider domain-specific FinText word embeddings constructed using Word2Vec (CBOW), Word2Vec (skip-gram), FastText (CBOW), and FastText (skip-gram). In addition, we include two general-purpose word embeddings: Word2Vec Google ([Mikolov, Chen, Corrado & Dean 2013](#)), hereafter referred to as Google for simplicity, and WikiNews. As discussed in [Section 4.2](#), we also distinguish between stock-related news and general hot news as separate inputs.¹⁴ [Table 6](#) reports out-of-sample forecasting results using stock-related news, while [Table 7](#) presents corresponding results based on general hot news. For each loss function, average and median values are reported as discussed in [Section 5](#). The tables also report out-of-sample RC results for six word embeddings, each evaluated with 25, 50, 75, and 100 filters, where a larger number of filters implies greater model complexity; RC denotes the percentage of tickers for which the NLP model outperforms all eight HAR-family of models at the 5% and 10% significance levels based on MSE and QLIKE. Finally, the top, middle, and bottom rows correspond to the full out-of-sample period, normal volatility days, and high volatility days, respectively.

[Table 6](#) and [Table 7](#) jointly show that the predictive value of NLP models depends critically on both the information set and the volatility regime. For stock-related news, the best-performing specifications rely on FinText embeddings. Over the full out-of-sample period, FinText Word2Vec with the skip-gram architecture delivers the lowest MSE ratios, corresponding to an average deterioration of approximately 10.6% (average MSE ratio of 1.106 using 25 filters) and a median deterioration of about 9.2% (median MSE ratio of 1.092 using 50 filters) relative to the CHAR benchmark. In terms of QLIKE, FinText FastText with the skip-gram architecture performs best, with average and median QLIKE ratios of 1.476 and 1.446 using 25 filters, implying loss increases of roughly 47.6% and 44.6%, respectively. Despite these higher loss ratios, RC results indicate economically meaningful cross-sectional gains, particularly under MSE, where FinText Word2Vec with the CBOW architecture outperforms all HAR-family benchmarks for more than 90% of stocks at the 5% significance level. When performance is decomposed by volatility regimes, stock-related news is only weakly informative on normal volatility days, but becomes substantially more informative on high volatility days. In this regime, the lowest average MSE and QLIKE ratios fall to 1.081 and 1.616, corresponding to loss increases of approximately 8.1% and 61.6%, respectively, while RC rates rise sharply, indicating broad cross-sectional improvements despite elevated loss levels.

¹⁴[Section A.6](#) documents the stability of news volume during the out-of-sample period. The monthly word count of both stock-related and general hot news remains broadly constant over time, with only a small number of highly visible stocks exhibiting persistently higher coverage.

In contrast, NLP models based on general hot news deliver weaker and less robust performance in [Table 7](#). Over the full out-of-sample period, FinText FastText with the CBOW architecture and 100 filters, attains average MSE and QLIKE ratios of 1.175 and 1.544, implying deteriorations of approximately 17.5% and 54.4%, respectively, with little RC support under QLIKE. Also, general hot news contributes primarily on normal volatility days, where WikiNews achieves average MSE ratios below one, with a minimum of 0.956 corresponding to an improvement of approximately 4.4%, and QLIKE ratio around 1.285, implying loss of 28.5%. However, general hot news performs systematically worse than stock-related news on high volatility days, with best average MSE and QLIKE ratios of 1.168 and 1.622, corresponding to loss increases of approximately 16.8% and 62.2%, respectively. Moreover, when general hot news is employed, general-purpose embeddings exhibit competitive performance and, in some cases, such as WikiNews, outperform alternative models in terms of QLIKE ratios. This result likely reflects the broader and more diverse semantic coverage of general-purpose word embeddings, which better capture the heterogeneous language and rapidly evolving content characteristic of general hot news. These results highlight the importance of word embedding specialisation. Specialised word embeddings are better suited to stock-related news, whereas general-purpose word embeddings become among the competitive models when general hot news is employed.¹⁵

¹⁵[Section A.11](#) reports a set of robustness checks that examine the sensitivity of the NLP forecasts to key architectural and aggregation choices, including the length of the news input window and the filter sizes. We show that extending the input window beyond one day or increasing textual granularity does not lead to systematic improvements in forecasting performance. Overall, the results indicate that volatility-relevant news effects are predominantly short-lived and that the baseline, parsimonious NLP architecture is sufficient for capturing the relevant information in news.

Table 6: Out-of-Sample RV Forecasting Performance: Stock-Related News

Full Out-of-Sample Period		p-value		FinText																Google				WikiNews			
				Word2Vec (CBOW)				Word2Vec (skip-gram)				FastText (CBOW)				FastText (skip-gram)				25	50	75	100	25	50	75	100
				25	50	75	100	25	50	75	100	25	50	75	100	25	50	75	100								
MSE ^a	Avg	1.146	1.146	1.153	1.144	1.106	1.108	1.108	1.107	1.116	1.117	1.118	1.117	1.118	1.118	1.118	1.118	1.108	1.110	1.109	1.109	1.169	1.187	1.178	1.182		
	Med	1.157	1.156	1.160	1.164	1.101	1.092	1.096	1.093	1.094	1.097	1.104	1.104	1.106	1.105	1.107	1.108	1.101	1.100	1.102	1.096	1.169	1.144	1.142	1.140		
RC ^c	0.05	91.30	86.96	91.30	86.96	82.61	82.61	82.61	82.61	65.22	65.22	65.22	65.22	56.52	60.87	60.87	60.87	86.96	86.96	86.96	86.96	73.91	78.26	65.22	65.22		
	0.10	100	100	100	100	100	100	100	100	95.65	95.65	100	95.65	95.65	91.30	91.30	91.30	100	100	100	100	95.65	91.30	95.65	91.30		
QLIKE ^b	Avg	1.838	1.744	1.782	1.740	1.566	1.640	1.571	1.571	1.500	1.520	1.513	1.519	1.476	1.489	1.492	1.486	1.567	1.564	1.571	1.569	1.829	1.701	1.609	1.636		
	Med	1.766	1.695	1.749	1.736	1.570	1.579	1.563	1.567	1.472	1.467	1.480	1.488	1.446	1.451	1.455	1.459	1.597	1.570	1.577	1.561	1.684	1.541	1.545	1.587		
RC	0.05	13.04	17.39	17.39	17.39	21.74	21.74	21.74	21.74	13.04	13.04	13.04	13.04	4.35	4.35	4.35	4.35	21.74	21.74	21.74	21.74	17.39	13.04	13.04	4.35		
	0.10	30.44	43.48	26.09	30.44	39.13	34.78	39.13	30.44	30.44	30.44	30.44	30.44	21.74	21.74	21.74	21.74	34.78	34.78	34.78	30.44	26.09	17.39	21.74	21.74		
Normal Volatility Days																											
MSE	Avg	2.383	2.426	2.194	2.102	1.683	1.703	1.702	1.690	1.510	1.503	1.497	1.507	1.384	1.381	1.383	1.384	1.685	1.715	1.708	1.705	1.763	1.450	1.337	1.300		
	Med	1.157	1.156	1.160	1.164	1.101	1.092	1.096	1.093	1.094	1.097	1.104	1.104	1.106	1.105	1.107	1.108	1.101	1.100	1.102	1.096	1.169	1.144	1.142	1.140		
RC	0.05	17.39	17.39	13.04	17.39	69.57	65.22	65.22	65.22	69.57	60.87	60.87	60.87	60.87	60.87	60.87	56.52	69.57	65.22	65.22	60.87	43.48	34.78	30.44	39.13		
	0.10	21.74	17.39	17.39	17.39	69.57	69.57	73.91	69.57	69.57	65.22	65.22	65.22	65.22	60.87	60.87	60.87	73.91	69.57	69.57	69.57	65.22	34.78	47.83	52.17		
QLIKE	Avg	1.584	1.562	1.586	1.534	1.345	1.370	1.363	1.354	1.329	1.327	1.340	1.330	1.337	1.341	1.339	1.334	1.342	1.340	1.351	1.357	1.515	1.415	1.421	1.434		
	Med	1.766	1.695	1.749	1.736	1.570	1.579	1.563	1.567	1.472	1.467	1.480	1.488	1.446	1.451	1.455	1.459	1.597	1.570	1.577	1.561	1.684	1.541	1.545	1.587		
RC	0.05	0.00	0.00	0.00	0.00	4.35	4.35	4.35	4.35	4.35	4.35	4.35	4.35	0.00	0.00	0.00	0.00	4.35	4.35	4.35	4.35	4.35	0.00	4.35	4.35		
	0.10	0.00	0.00	0.00	0.00	4.35	4.35	4.35	4.35	4.35	4.35	4.35	4.35	0.00	4.35	4.35	0.00	4.35	4.35	4.35	4.35	4.35	0.00	4.35	4.35		
High Volatility Days																											
MSE	Avg	1.097	1.095	1.111	1.107	1.081	1.082	1.082	1.082	1.097	1.099	1.100	1.099	1.105	1.106	1.105	1.105	1.082	1.083	1.082	1.082	1.145	1.175	1.171	1.176		
	Med	1.122	1.097	1.102	1.137	1.095	1.094	1.096	1.093	1.111	1.113	1.113	1.113	1.113	1.114	1.115	1.116	1.094	1.093	1.094	1.095	1.133	1.142	1.138	1.140		
RC	0.05	100	100	100	100	65.22	69.57	69.57	69.57	65.22	65.22	65.22	65.22	56.52	60.87	60.87	60.87	65.22	69.57	65.22	69.57	69.57	82.61	82.61	69.57		
	0.10	100	100	100	100	95.65	95.65	95.65	95.65	91.30	91.30	91.30	91.30	82.61	82.61	82.61	82.61	95.65	95.65	95.65	95.65	95.65	95.65	100	100		
QLIKE	Avg	2.123	1.947	1.996	1.965	1.804	1.960	1.794	1.812	1.665	1.704	1.675	1.699	1.616	1.637	1.649	1.641	1.804	1.813	1.788	1.804	2.135	1.997	1.796	1.823		
	Med	1.918	1.855	1.917	1.843	1.749	1.771	1.788	1.784	1.609	1.628	1.634	1.657	1.614	1.637	1.618	1.614	1.819	1.758	1.725	1.859	1.967	1.848	1.694	1.770		
RC	0.05	39.13	43.48	52.17	47.83	43.48	43.48	43.48	43.48	34.78	39.13	39.13	43.48	13.04	30.44	30.44	30.44	43.48	43.48	43.48	43.48	21.74	34.78	21.74	8.70		
	0.10	69.57	60.87	65.22	73.91	60.87	69.57	65.22	65.22	52.17	52.17	56.52	60.87	43.48	52.17	52.17	56.52	65.22	69.57	69.57	69.57	43.48	56.52	47.83	39.13		

Notes: ^a The ratio of the average (or median) MSE of the specified model to that of the CHAR model, averaged across 23 tickers. ^b The ratio of the average (or median) QLIKE of the specified model to that of the CHAR model, averaged across 23 tickers.

^c The RC denotes the percentage of tickers for which we reject, at the 5% (or 10%) significance level, the null hypothesis that the specified model does not outperform the best-performing model within the HAR-family benchmark set.

Table 7: Out-of-Sample RV Forecasting Performance: General Hot News

Full Out-of-Sample Period		p-value	FinText																Google				WikiNews			
			Word2Vec (CBOW)				Word2Vec (skip-gram)				FastText (CBOW)				FastText (skip-gram)				25	50	75	100	25	50	75	100
			25	50	75	100	25	50	75	100	25	50	75	100	25	50	75	100								
MSE ^a	Avg		1.195	1.181	1.180	1.177	1.185	1.185	1.183	1.181	1.179	1.181	1.178	1.175	1.183	1.183	1.182	1.180	1.180	1.181	1.181	1.181	1.175	1.176	1.176	1.178
	Med		1.175	1.146	1.139	1.142	1.156	1.153	1.151	1.144	1.141	1.154	1.141	1.137	1.159	1.154	1.154	1.150	1.153	1.157	1.159	1.159	1.144	1.145	1.143	1.144
RC ^c	0.05		21.74	13.04	13.04	17.39	43.48	34.78	39.13	39.13	39.13	39.13	39.13	39.13	34.78	34.78	34.78	39.13	43.48	39.13	34.78	39.13	26.09	30.44	30.44	34.78
	0.10		56.52	47.83	43.48	39.13	91.30	91.30	91.30	91.30	95.65	95.65	95.65	91.30	91.30	91.30	86.96	86.96	91.30	91.30	91.30	91.30	78.26	86.96	82.61	82.61
QLIKE ^b	Avg		1.814	1.583	1.606	1.588	1.888	1.856	1.793	1.718	1.579	1.651	1.563	1.544	1.862	1.838	1.805	1.721	1.670	1.685	1.687	1.684	1.680	1.683	1.677	1.683
	Med		1.725	1.543	1.513	1.515	1.876	1.863	1.789	1.707	1.537	1.565	1.508	1.499	1.794	1.824	1.756	1.679	1.660	1.688	1.651	1.728	1.636	1.667	1.653	1.619
RC	0.05		0.00	0.00	0.00	0.00	0.00	0.00	0.00	0.00	0.00	0.00	0.00	0.00	0.00	0.00	0.00	0.00	0.00	0.00	0.00	0.00	0.00	0.00	0.00	0.00
	0.10		0.00	0.00	0.00	0.00	4.35	4.35	4.35	4.35	4.35	4.35	4.35	4.35	4.35	4.35	4.35	4.35	4.35	4.35	4.35	4.35	0.00	0.00	0.00	4.35
Normal Volatility Days																										
MSE	Avg		1.875	1.486	1.457	1.336	1.288	1.363	1.324	1.414	1.430	1.460	1.407	1.312	1.226	1.282	1.312	1.345	1.070	1.078	1.088	1.101	0.956	0.968	0.995	1.082
	Med		1.843	1.351	1.459	1.316	1.142	1.325	1.243	1.381	1.366	1.421	1.319	1.315	1.144	1.210	1.359	1.357	1.105	1.094	1.094	1.085	0.918	0.914	0.944	1.097
RC	0.05		4.35	4.35	4.35	0.00	69.57	47.83	47.83	47.83	78.26	69.57	69.57	65.22	86.96	82.61	78.26	73.91	69.57	43.48	47.83	43.48	56.52	39.13	34.78	43.48
	0.10		4.35	8.70	8.70	8.70	73.91	47.83	52.17	47.83	78.26	73.91	73.91	73.91	86.96	86.96	86.96	82.61	73.91	52.17	52.17	43.48	56.52	39.13	47.83	43.48
QLIKE	Avg		1.728	1.497	1.508	1.459	1.425	1.487	1.468	1.514	1.509	1.513	1.479	1.458	1.419	1.434	1.464	1.479	1.284	1.296	1.310	1.316	1.285	1.293	1.299	1.348
	Med		1.640	1.450	1.456	1.427	1.371	1.455	1.437	1.506	1.498	1.488	1.470	1.432	1.364	1.403	1.438	1.452	1.297	1.295	1.323	1.312	1.262	1.286	1.275	1.327
RC	0.05		0.00	0.00	0.00	0.00	8.70	4.35	4.35	4.35	4.35	4.35	4.35	4.35	4.35	4.35	4.35	4.35	4.35	4.35	4.35	4.35	0.00	0.00	0.00	0.00
	0.10		0.00	0.00	0.00	0.00	8.70	4.35	4.35	4.35	4.35	4.35	4.35	4.35	4.35	4.35	4.35	4.35	8.70	4.35	4.35	4.35	0.00	0.00	0.00	0.00
High Volatility Days																										
MSE	Avg		1.168	1.168	1.169	1.169	1.180	1.178	1.178	1.172	1.168	1.169	1.169	1.168	1.181	1.179	1.177	1.174	1.183	1.183	1.183	1.182	1.182	1.182	1.181	1.181
	Med		1.138	1.139	1.140	1.137	1.139	1.135	1.140	1.137	1.138	1.137	1.137	1.137	1.154	1.152	1.159	1.151	1.152	1.152	1.152	1.153	1.153	1.153	1.150	1.150
RC	0.05		43.48	47.83	47.83	52.17	34.78	39.13	39.13	39.13	34.78	34.78	34.78	39.13	30.44	34.78	34.78	34.78	34.78	39.13	39.13	39.13	30.44	39.13	39.13	39.13
	0.10		65.22	91.30	91.30	86.96	69.57	69.57	69.57	69.57	69.57	73.91	73.91	73.91	60.87	60.87	60.87	60.87	69.57	69.57	69.57	69.57	56.52	82.61	73.91	69.57
QLIKE	Avg		1.907	1.660	1.699	1.705	2.370	2.245	2.149	1.936	1.648	1.782	1.642	1.622	2.326	2.253	2.168	1.968	2.049	2.063	2.058	2.050	2.068	2.075	2.058	2.017
	Med		1.709	1.653	1.654	1.612	2.246	2.194	2.052	1.896	1.692	1.620	1.555	1.547	2.144	2.325	2.151	1.912	1.987	1.945	1.920	2.029	1.934	2.048	1.961	1.899
RC	0.05		0.00	0.00	4.35	4.35	8.70	8.70	8.70	8.70	8.70	8.70	8.70	8.70	0.00	0.00	0.00	0.00	4.35	4.35	4.35	8.70	0.00	0.00	0.00	0.00
	0.10		8.70	4.35	8.70	17.39	17.39	17.39	21.74	21.74	17.39	17.39	21.74	26.09	13.04	13.04	17.39	17.39	21.74	17.39	21.74	21.74	8.70	17.39	4.35	4.35

Notes: ^a The ratio of the average (or median) MSE of the specified model to that of the CHAR model, averaged across 23 tickers. ^b The ratio of the average (or median) QLIKE of the specified model to that of the CHAR model, averaged across 23 tickers. ^c The RC denotes the percentage of tickers for which we reject, at the 5% (or 10%) significance level, the null hypothesis that the specified model does not outperform the best-performing model within the HAR-family benchmark set.

5.2 Forecasting Performance of Ensemble Models

Although [Section 5.1](#) shows that NLP models deliver promising results and that news content contains meaningful information for predicting RV across different market regimes, these models underperform the HAR-family of models in terms of standard forecasting metrics, particularly with respect to the magnitude of performance improvements. Combining forecasts from multiple models provides diversification gains and can improve predictive performance when individual forecasts rely on heterogeneous information sets or are subject to model uncertainty ([Bates & Granger 1969](#), [Timmermann 2006](#)). This naturally raises the question of whether, rather than serving as a replacement for the HAR-family of models, news-based NLP forecasts can provide complementary information. To this end, we define a straightforward ensemble model that combines forecasts from the CHAR model, which is the best-performing specification within the HAR-family in [Section 5](#), with forecasts generated by the NLP models. For each day, we compute the average of the two forecasts. This approach integrates the persistent dynamics captured by historical RV with short term information conveyed by recent news, potentially enhancing the robustness of daily RV forecasts.

The ensemble results for stock-related news in [Table 8](#) indicate that combining NLP forecasts with the CHAR yields systematic meaningful improvements in forecasting performance. Over the full out-of-sample period, most FinText-based ensemble specifications achieve MSE ratios below one, with the strongest performance delivered by FinText Word2Vec with the skip-gram architecture, for which the average MSE ratio declines to 0.961 and the median ratio to 0.980, corresponding to improvements of approximately 3.9% and 2.0% relative to CHAR. QLIKE ratios also fall substantially, reaching values as low as 0.937 on average and around 0.970 at the median, which implies loss reductions of roughly 6.3% to 3.0%. These improvements are accompanied by uniformly high RC rates under MSE, which reach 100% at both the 5% and 10% significance levels across nearly all FinText specifications, and remain high under QLIKE, frequently exceeding 90%. As expected, these gains are particularly pronounced during high volatility days. The MSE ratio reaches 0.959, corresponding to a 4.1% improvement in performance, supported by high RC values. Moreover, the ensemble reduces the average QLIKE ratio to as low as 0.763, representing an approximate 23.7% reduction, and delivers near-universal RC values. As in the standalone NLP analysis, variation in the number of filters has only a limited effect on ensemble performance.

For general hot news in [Table 9](#), the ensemble model delivers more mixed and regime-dependent results. Over the full out-of-sample period, average MSE ratios remain close to one, typically ranging between 1.018 and 1.023, corresponding to a deterioration of approximately 1.8% to 2.3% relative

to the CHAR benchmark, while average QLIKE ratios are moderately above one, implying losses that are roughly 7% to 12% higher. This indicates that, when evaluated across all trading days, general hot news provides limited incremental information beyond historical RV dynamics. However, when attention is restricted to normal volatility days, the ensemble exhibits clear and economically meaningful improvements. Several specifications achieve average MSE ratios well below one, with the best performance observed for WikiNews, where the minimum average MSE ratio of 0.765 corresponds to an improvement of approximately 23.5% relative to CHAR. These gains are accompanied by high RC rates under MSE, often exceeding 80%, indicating strong and pervasive cross-sectional improvements. In contrast, during high volatility days the ensemble based on general hot news performs close to, but generally not better than, the CHAR benchmark, with average MSE ratios around 1.02, implying performance losses of about 2%, and only modest and specification-dependent improvements under QLIKE. As with stock-related news, increasing the number of filters does not generate systematic performance gains, indicating that higher model complexity plays a secondary role.^{16 17}

Taken together, the ensemble results clarify and strengthen the conclusions drawn from the standalone NLP analysis in [Section 5.1](#). While the NLP models typically underperformed the best HAR-family specifications in terms of loss ratios, the ensemble approach successfully converts the informational content embedded in news text into statistically meaningful forecasting gains. This complementarity is strongest for stock-related news, particularly in high volatility days, consistent with the earlier finding that stock-related news is most informative during periods of market stress. For general hot news, the ensemble results mirror the regime dependence identified previously, with benefits concentrated on normal volatility days. Across both news types, the ensemble evidence reinforces the earlier conclusion that performance improvements are driven primarily by the combination of heterogeneous information sources rather than by increased model complexity. More importantly, these results indicate that news-based signals provide incremental predictive information for RV rather than fully substituting for volatility-history dynamics. Finally, similar to standalone NLP models in [Section 5.1](#), specialised word embeddings perform better for stock-related news, while general-purpose word embeddings perform better for general hot news.

¹⁶[Section A.9](#) evaluates dictionary-based textual signals within the same out-of-sample forecasting framework as the main analysis by augmenting the CHAR benchmark with Loughran and McDonald (LM) sentiment measures from [Loughran & McDonald \(2011\)](#) and a news-volume proxy. This comparison is important because it directly assesses whether moving from a simple textual method to more complex NLP model is warranted for RV forecasting. The out-of-sample results show that dictionary-based approaches perform close to CHAR, whereas the ensemble model that combines CHAR and NLP-based forecasts delivers systematically larger improvements across loss measures, supporting the need for richer language models when processing news.

¹⁷[Section A.10](#) evaluates whether nonlinear reformulations of the HAR-family of models, holding the information set fixed, can account for the forecasting and economic gains achieved by the proposed NLP and ensemble models. While nonlinear HAR specifications show improvements in performance during normal volatility days, they fail to deliver robust performance across volatility regimes and generate inferior realised utility.

Table 8: Out-of-Sample RV Forecasting Performance: Stock-Related News (Ensemble)

Full Out-of-Sample Period		p-value	FinText																Google				WikiNews			
			Word2Vec (CBOW)				Word2Vec (skip-gram)				FastText (CBOW)				FastText (skip-gram)				25	50	75	100	25	50	75	100
			25	50	75	100	25	50	75	100	25	50	75	100	25	50	75	100								
MSE ^a	Avg		0.971	0.973	0.978	0.977	0.961	0.961	0.961	0.962	0.974	0.975	0.977	0.975	0.980	0.980	0.980	0.980	0.962	0.962	0.962	0.962	1.003	1.019	1.017	1.020
	Med		0.993	0.992	0.988	0.995	0.981	0.980	0.981	0.980	0.993	0.993	0.994	0.993	1.000	1.001	1.001	1.001	0.984	0.982	0.984	0.984	1.027	1.024	1.020	1.025
RC ^c	0.05		100	100	100	100	100	100	100	100	100	100	100	100	100	100	100	100	100	100	100	100	91.30	95.65	95.65	95.65
	0.10		100	100	100	100	100	100	100	100	100	100	100	100	100	100	100	100	100	100	100	100	95.65	95.65	95.65	95.65
QLIKE ^b	Avg		0.972	0.965	0.991	1.002	0.937	0.938	0.937	0.939	0.959	0.959	0.966	0.959	0.967	0.970	0.968	0.968	0.938	0.938	0.939	0.940	1.038	1.086	1.088	1.096
	Med		1.015	0.994	1.011	1.036	0.969	0.968	0.970	0.972	0.983	0.983	0.989	0.988	0.996	1.006	1.010	1.000	0.969	0.972	0.970	0.972	1.058	1.079	1.076	1.081
RC	0.05		82.61	91.30	78.26	73.91	95.65	95.65	95.65	95.65	86.96	86.96	91.30	86.96	91.30	91.30	91.30	91.30	91.30	91.30	95.65	91.30	47.83	30.44	34.78	21.74
	0.10		95.65	95.65	86.96	82.61	95.65	95.65	95.65	95.65	91.30	91.30	91.30	86.96	91.30	91.30	91.30	91.30	95.65	95.65	95.65	95.65	56.52	34.78	34.78	39.13
Normal Volatility Days																										
MSE	Avg		1.164	1.181	1.127	1.107	0.976	0.981	0.982	0.979	0.946	0.942	0.942	0.943	0.916	0.914	0.915	0.915	0.977	0.985	0.984	0.982	1.009	0.942	0.923	0.919
	Med		1.134	1.145	1.018	1.058	0.917	0.923	0.917	0.911	0.861	0.860	0.864	0.859	0.863	0.860	0.860	0.861	0.906	0.926	0.901	0.903	1.036	0.926	0.946	0.936
RC	0.05		69.57	65.22	78.26	82.61	78.26	78.26	78.26	78.26	78.26	86.96	82.61	86.96	78.26	78.26	82.61	82.61	78.26	78.26	78.26	78.26	78.26	86.96	91.30	91.30
	0.10		78.26	82.61	82.61	86.96	78.26	78.26	78.26	78.26	86.96	86.96	86.96	86.96	82.61	82.61	82.61	82.61	78.26	78.26	78.26	82.61	82.61	91.30	91.30	91.30
QLIKE	Avg		1.125	1.133	1.142	1.149	1.112	1.113	1.115	1.114	1.130	1.126	1.131	1.127	1.136	1.135	1.134	1.134	1.111	1.113	1.115	1.114	1.123	1.164	1.176	1.182
	Med		1.127	1.134	1.143	1.151	1.106	1.100	1.102	1.098	1.126	1.119	1.122	1.123	1.137	1.129	1.126	1.128	1.109	1.105	1.102	1.104	1.110	1.157	1.167	1.179
RC	0.05		21.74	21.74	21.74	13.04	21.74	21.74	21.74	21.74	21.74	21.74	17.39	21.74	21.74	21.74	21.74	21.74	21.74	21.74	21.74	21.74	21.74	13.04	13.04	8.70
	0.10		30.44	26.09	21.74	21.74	21.74	21.74	26.09	21.74	21.74	26.09	21.74	21.74	21.74	21.74	21.74	21.74	21.74	21.74	21.74	21.74	30.44	17.39	13.04	13.04
High Volatility Days																										
MSE	Avg		0.962	0.964	0.971	0.972	0.959	0.959	0.959	0.960	0.974	0.975	0.977	0.975	0.981	0.982	0.981	0.981	0.960	0.960	0.960	0.960	1.002	1.021	1.020	1.023
	Med		0.976	0.982	0.985	0.987	0.973	0.975	0.973	0.972	0.992	0.993	0.993	0.993	1.001	1.003	1.003	1.001	0.975	0.975	0.971	0.976	1.023	1.025	1.026	1.028
RC	0.05		100	100	100	100	100	100	100	100	100	100	100	100	100	100	100	100	100	100	100	100	95.65	91.30	95.65	91.30
	0.10		100	100	100	100	100	100	100	100	100	100	100	100	100	100	100	100	100	100	100	100	95.65	95.65	95.65	95.65
QLIKE	Avg		0.821	0.798	0.840	0.859	0.765	0.766	0.763	0.767	0.788	0.792	0.802	0.792	0.800	0.806	0.804	0.803	0.769	0.767	0.765	0.768	0.952	1.006	0.996	1.006
	Med		0.858	0.832	0.875	0.895	0.787	0.776	0.775	0.788	0.810	0.830	0.835	0.831	0.822	0.825	0.826	0.823	0.799	0.783	0.806	0.807	0.963	0.992	0.983	0.991
RC	0.05		100	100	100	100	100	100	100	100	100	100	100	100	100	100	100	100	100	100	100	100	95.65	91.30	91.30	91.30
	0.10		100	100	100	100	100	100	100	100	100	100	100	100	100	100	100	100	100	100	100	100	95.65	91.30	91.30	95.65

Notes: ^a The ratio of the average (or median) MSE of the specified model to that of the CHAR model, averaged across 23 tickers.

^b The ratio of the average (or median) QLIKE of the specified model to that of the CHAR model, averaged across 23 tickers.

^c The RC denotes the percentage of tickers for which we reject, at the 5% (or 10%) significance level, the null hypothesis that the specified model does not outperform the best-performing model within the HAR-family benchmark set.

Table 9: Out-of-Sample RV Forecasting Performance: General Hot News (Ensemble)

Full Out-of-Sample Period		p-value		FinText																Google				WikiNews			
				Word2Vec (CBOW)				Word2Vec (skip-gram)				FastText (CBOW)				FastText (skip-gram)				25	50	75	100	25	50	75	100
				25	50	75	100	25	50	75	100	25	50	75	100	25	50	75	100								
MSE ^a	Avg	1.023	1.020	1.020	1.019	1.020	1.020	1.020	1.019	1.020	1.020	1.020	1.019	1.020	1.020	1.020	1.019	1.019	1.020	1.019	1.020	1.018	1.018	1.018	1.019		
	Med	1.029	1.021	1.022	1.023	1.022	1.023	1.022	1.024	1.023	1.027	1.021	1.021	1.024	1.022	1.023	1.022	1.023	1.024	1.024	1.024	1.023	1.022	1.021	1.023		
RC ^c	0.05	91.30	95.65	95.65	95.65	95.65	95.65	95.65	95.65	95.65	95.65	95.65	95.65	95.65	95.65	95.65	95.65	95.65	95.65	95.65	95.65	95.65	95.65	95.65	95.65		
	0.10	91.30	95.65	95.65	95.65	95.65	95.65	95.65	95.65	95.65	95.65	95.65	95.65	95.65	95.65	95.65	95.65	95.65	95.65	95.65	95.65	95.65	95.65	95.65	95.65		
QLIKE ^b	Avg	1.117	1.106	1.110	1.105	1.097	1.102	1.097	1.107	1.105	1.113	1.107	1.106	1.091	1.099	1.100	1.100	1.089	1.090	1.089	1.090	1.077	1.078	1.080	1.088		
	Med	1.107	1.098	1.098	1.094	1.099	1.099	1.096	1.091	1.091	1.111	1.097	1.091	1.087	1.091	1.089	1.083	1.081	1.078	1.078	1.080	1.082	1.079	1.078	1.082		
RC	0.05	21.74	21.74	26.09	26.09	21.74	21.74	26.09	26.09	34.78	30.44	34.78	26.09	26.09	17.39	21.74	21.74	30.44	17.39	26.09	30.44	26.09	21.74	21.74	26.09		
	0.10	26.09	21.74	26.09	26.09	39.13	26.09	30.44	34.78	52.17	52.17	34.78	39.13	30.44	34.78	34.78	30.44	43.48	26.09	39.13	43.48	26.09	21.74	26.09	26.09		
Normal Volatility Days																											
MSE	Avg	1.097	0.991	0.984	0.947	0.872	0.910	0.903	0.956	0.973	0.983	0.970	0.946	0.853	0.883	0.906	0.927	0.806	0.806	0.811	0.815	0.765	0.770	0.781	0.818		
	Med	1.167	0.928	0.971	0.942	0.837	0.899	0.901	0.936	0.968	0.962	0.937	0.947	0.850	0.869	0.931	0.923	0.826	0.823	0.832	0.828	0.747	0.735	0.747	0.818		
RC	0.05	65.22	78.26	78.26	82.61	95.65	91.30	91.30	86.96	100	100	100	95.65	95.65	100	95.65	95.65	95.65	91.30	91.30	82.61	82.61	78.26	82.61	78.26		
	0.10	69.57	82.61	78.26	82.61	95.65	91.30	91.30	86.96	100	100	100	95.65	100	100	100	100	95.65	91.30	95.65	95.65	82.61	82.61	82.61	82.61		
QLIKE	Avg	1.235	1.223	1.226	1.212	1.106	1.149	1.150	1.206	1.220	1.224	1.224	1.225	1.104	1.137	1.158	1.176	1.091	1.091	1.094	1.097	1.071	1.077	1.086	1.117		
	Med	1.227	1.208	1.220	1.215	1.114	1.121	1.140	1.200	1.211	1.212	1.216	1.212	1.093	1.125	1.155	1.176	1.105	1.105	1.105	1.113	1.068	1.074	1.101	1.107		
RC	0.05	0.00	0.00	0.00	4.35	8.70	4.35	4.35	0.00	39.13	39.13	39.13	21.74	30.44	26.09	26.09	30.44	13.04	8.70	8.70	4.35	0.00	0.00	0.00	0.00		
	0.10	0.00	0.00	0.00	4.35	17.39	4.35	4.35	0.00	39.13	39.13	39.13	21.74	30.44	26.09	30.44	30.44	17.39	8.70	8.70	8.70	0.00	0.00	0.00	0.00		
High Volatility Days																											
MSE	Avg	1.020	1.020	1.021	1.021	1.025	1.024	1.024	1.022	1.021	1.021	1.021	1.021	1.025	1.025	1.024	1.023	1.027	1.027	1.027	1.026	1.026	1.026	1.026	1.026		
	Med	1.025	1.025	1.027	1.027	1.030	1.029	1.029	1.027	1.026	1.027	1.024	1.025	1.032	1.033	1.032	1.028	1.032	1.034	1.034	1.033	1.033	1.031	1.032	1.031		
RC	0.05	95.65	91.30	91.30	91.30	86.96	86.96	82.61	86.96	73.91	69.57	78.26	73.91	69.57	73.91	73.91	73.91	86.96	82.61	82.61	86.96	91.30	91.30	91.30	91.30		
	0.10	95.65	95.65	95.65	95.65	95.65	95.65	95.65	95.65	91.30	86.96	91.30	91.30	86.96	86.96	86.96	82.61	95.65	95.65	95.65	95.65	95.65	95.65	95.65	95.65		
QLIKE	Avg	0.995	0.985	0.988	0.992	1.086	1.055	1.043	1.006	0.987	0.998	0.987	0.983	1.076	1.060	1.041	1.022	1.080	1.083	1.078	1.078	1.077	1.073	1.069	1.055		
	Med	0.977	0.974	0.982	0.962	1.067	1.071	1.041	1.008	0.972	0.991	0.980	0.968	1.050	1.071	1.048	0.999	1.056	1.071	1.061	1.069	1.064	1.056	1.047	1.034		
RC	0.05	95.65	91.30	95.65	91.30	73.91	78.26	82.61	91.30	65.22	73.91	73.91	82.61	69.57	73.91	73.91	69.57	73.91	78.26	82.61	91.30	95.65	91.30	95.65	95.65		
	0.10	100	100	100	100	82.61	91.30	95.65	95.65	78.26	78.26	78.26	86.96	73.91	73.91	73.91	73.91	82.61	91.30	86.96	91.30	95.65	95.65	100	100		

Notes: ^a The ratio of the average (or median) MSE of the specified model to that of the CHAR model, averaged across 23 tickers. ^b The ratio of the average (or median) QLIKE of the specified model to that of the CHAR model, averaged across 23 tickers.

^c The RC denotes the percentage of tickers for which we reject, at the 5% (or 10%) significance level, the null hypothesis that the specified model does not outperform the best-performing model within the HAR-family benchmark set.

5.3 Economic Gain

We evaluate the economic gain of models using the utility-based approach developed in [Bollerslev et al. \(2018\)](#). This setting considers a mean–variance investor who follows a risk-targeting strategy when trading assets with a constant Sharpe ratio (SR). Portfolio positions are dynamically scaled to maintain a fixed target level of volatility. In this environment, the quality of volatility forecasts plays a critical role in determining investor utility. Accurate forecasts enable the investor to closely adhere to the desired risk profile, whereas uncertainty induced by volatility-of-volatility generates fluctuations around the target risk level, leading to suboptimal portfolio scaling and lower expected utility.

The empirical assessment of expected utility is implemented by computing realised utility using out-of-sample volatility forecasts. Following this approach, we employ the utility-of-wealth (UoW) measure, which captures the realised utility associated with forecasts of RV. The measure is defined as

$$UoW^M = \frac{1}{T} \sum_{t=1}^T \left[8\% \frac{\sqrt{RV_{t+1}}}{\sqrt{\mathbb{E}_t^M(RV_{t+1})}} - 4\% \frac{RV_{t+1}}{\mathbb{E}_t^M(RV_{t+1})} \right], \quad (20)$$

where RV_{t+1} denotes the RV at time $t + 1$, $\mathbb{E}_t^M(RV_{t+1})$ represents the expectation from model M , that is, the RV forecast generated by model M at time t , and T denotes the number of days in the out-of-sample period. The coefficients 8% and 4% capture investor preferences for reward and penalty, respectively, and are calibrated using economically plausible assumptions regarding portfolio performance and risk aversion, as outlined in [Bollerslev et al. \(2018\)](#).¹⁸ Under this calibration, a perfectly specified risk model that accurately forecasts RV achieves a realised utility of 4%.

[Table 10](#) reports the realised utility of the NLP models presented in [Section 5.1](#) in the left panel and the ensemble models discussed in [Section 5.2](#) in the right panel. As a benchmark, the CHAR model attains a realised utility of 2.7540%.¹⁹ For ease of presentation, the reported realised utilities are averaged across model complexity settings. The realised utility results align closely with the statistical forecasting evidence in [Section 5.1](#) and [Section 5.2](#), thereby providing an economic validation of the model rankings obtained under MSE, QLIKE, and the RC results. When news is used in isolation (left panel), all NLP models deliver realised utilities substantially below CHAR, ranging from 1.6280% to 2.1047% for stock-related news and from 1.5550% to 2.0165% for general hot news. In this sense, the realised utility approach corroborates the earlier conclusion that news-only models, while informative, do not match the realised utility delivered by HAR-type benchmarks.

¹⁸The calibration assumes an annualised SR of 0.4, a coefficient of risk aversion equal to 2, and an investor targeting an annualised volatility of 20%.

¹⁹The realised utilities for the HAR-family of models are AR (2.4642%), HAR (2.6277%), HAR-J (2.7502%), CHAR (2.7540%), SHAR (2.6262%), ARQ (2.5611%), HARQ (2.6591%), and HARQ-F (2.5837%). Among these specifications, the CHAR model delivers the highest realised utility, consistent with the results reported in [Section 5](#).

Table 10: Realised Utility of NLP and Ensemble Models

NLP Models		Ensemble Models	
Model	Realised Utility	Model	Realised Utility
<i>Stock-related news</i>			
Word2Vec (CBOW)	1.6280	Word2Vec (CBOW)	2.8677
Word2Vec (skip-gram)	1.8949	Word2Vec (skip-gram)	2.9321
FastText (CBOW)	1.7772	FastText (CBOW)	2.7148
FastText (skip-gram)	1.9347	FastText (skip-gram)	2.9299
Google	2.0437	Google	2.9013
WikiNews	2.1047	WikiNews	2.8928
<i>General hot news</i>			
Word2Vec (CBOW)	1.9180	Word2Vec (CBOW)	2.6866
Word2Vec (skip-gram)	1.5550	Word2Vec (skip-gram)	2.6675
FastText (CBOW)	2.0165	FastText (CBOW)	2.6878
FastText (skip-gram)	1.7363	FastText (skip-gram)	2.6684
Google	1.7334	Google	2.6722
WikiNews	1.7363	WikiNews	2.6578

Notes: This table reports realised utility values from the utility-based approach for the NLP models in the left panel and the ensemble models in the right panel. In Equation (20), the maximum attainable realised utility is 4%. For ease of presentation, the reported realised utilities are averaged across model complexity settings with 25, 50, 75, and 100 filters. All values are expressed in percentage terms.

By contrast, the economic gain of news becomes apparent once it is combined with the RV dynamics captured by CHAR: for stock-related news, five out of six ensemble variants exceed the CHAR utility, with the best-performing Word2Vec (skip-gram) ensemble achieving 2.9321%, a gain of 0.1781%, in line with the loss reductions and strong RC evidence reported for the corresponding ensemble models in Table 8. Importantly, the utility ranking across word embedding algorithms is broadly consistent with the forecasting performance results. In contrast, general hot news ensembles remain below CHAR in realised utility (between 2.6578% and 2.6878%), which matches the full out-of-sample evidence in Table 9 showing loss ratios modestly above one despite improvements on normal volatility days. Overall, realised utility confirms that news is best viewed as a complementary signal, with the strongest economic gains arising from combining stock-related news with the HAR-family benchmark.²⁰

5.4 Explainable AI (XAI)

Over recent years, considerable efforts have been made to better understand ML models, which are often described as black-box. In this study, we explore one of the prominent XAI methods, Shapley additive explanations (SHAP), to analyse the explanatory power of specific phrases in RV forecasting. Lundberg & Lee (2017) propose the SHAP method based on coalition game theory. Shapley values, denoted as ϕ_i and defined below, reveal the importance of a model input S (a set of tokens in daily

²⁰The results presented in Section A.9 show that dictionary-based models yield realised utilities that are largely indistinguishable from the CHAR benchmark, indicating limited economic gains. By contrast, the ensemble models deliver consistently higher realised utilities, demonstrating that combining conventional RV forecasting models with richer textual representations generate larger economic gains than relying solely on sentiment measures extracted from news.

news headlines) given the model output $f(S)$, which in this case is the RV forecast. Specifically:

$$\phi_i = \frac{1}{|N|!} \sum_{S \subseteq N \setminus \{i\}} |S|! (|N| - |S| - 1)! [f(S \cup \{i\}) - f(S)], \quad (21)$$

where $f(S \cup \{i\}) - f(S)$ captures the marginal contribution in RV forecast of adding token i to the set S , N contains all model inputs, $|S|!$ shows the number of different ways the chosen set of tokens may be presented, and $(|N| - |S| - 1)!$ is the number of different ways that the remaining tokens could have been added.²¹ As tokens are added to the set, changes in the RV forecast reflect their relevance. The advantages of the SHAP method include a solid theoretical foundation in game theory and no requirement for differentiable models. However, it is computationally intensive and, like other permutation-based approaches, does not consider feature dependencies, potentially leading to misleading results.²² Here, we use a high-speed approximation algorithm, Deep SHAP based on DeepLIFT (Shrikumar et al. 2017), to calculate Shapley values.²³

For each stock, we obtained the Shapley values for the constituent n-grams of all the textual information used to forecast RV for that stock during the out-of-sample period. To identify the volatility drivers for the entire sample of 23 stocks, we first store, for each stock, the top five n-grams with the highest absolute Shapley values across the full out-of-sample period. This process results in 23 groups of five n-grams, with some overlapping n-grams among them. Next, for each n-gram, we count the number of occurrences t , where $t = 1 : 23$. An n-gram with $t = 23$ indicates that this specific n-gram appears among the top five n-grams for all 23 stocks.²⁴

²¹The Shapley values ϕ_i indicate the magnitude and sign of the average contribution of token i ; these satisfy three properties, namely local accuracy (additivity), which means that the sum of individual token attributions is equal to the forecasted RV; missingness (nonexistence or null effect), which implies that a missing token has no attributed impact ($\phi_i = 0$); and consistency (symmetry), which means that if a change in a specific token has a greater impact on the first model compared to the second model, the importance of this token should be higher for the first model than for the second model.

²²Following Zhao et al. (2020), SHAP is applied to the classification block of the model (FCNN). In this instance, the inputs are outputs from the global max pooling layer, and the final output is the forecasted RV in Figure 4. Consequently, the number of inputs is equal to $3h$, where h is the number of filters, and 3 corresponds to the three filter sizes (unigram, bigram, and trigram). Applying SHAP to the full model can lead to misleading results because non-existent words may mistakenly receive high scores. However, by applying SHAP specifically to the classification block, the permutation operates over features extracted from the filters, meaning the Shapley values are attributed directly to the unigrams, bigrams, and trigrams. Moreover, the duplication of filters is common in CNNs, particularly for large h values (RoyChowdhury et al. 2017), which could result in similar n-grams being generated. To prevent this, a de-duplication step is implemented by removing repeated n-grams and recalculating the Shapley value by summing the corresponding Shapley values. Zhao et al. (2020) propose two steps for de-duplication, namely ‘exact de-duplication’ (employed in this study) and ‘merge de-duplication’. In ‘merge de-duplication’, overlapping n-grams are merged, and their Shapley value is determined by summing the Shapley values of the constituent n-grams. Given the generally shorter input text length, our experiments indicate that incorporating ‘exact de-duplication’ alone is sufficient to achieve more granular results.

²³An overview of the DeepLIFT is provided in Section A.12.

²⁴In analysing stock-related news, we employ FinText word embedding trained using the FastText (skip-gram) specification, while general hot news is represented using WikiNews word embedding. Both models are configured with 50 filters. These configurations are among the best-performing models, separately, for stock-related and general hot news, as reported in Section 5.1. Our results indicate that alternative model complexity choices do not materially affect performance; therefore, we adopt a consistent number of filters for both stock-related and general hot news analyses. Also,

We examine the primary RV drivers for stock-related news in [Table 11](#) and general hot news in [Table 12](#) across the entire sample of 23 stocks during the out-of-sample period. As explained, we have a merged list of the top five n-grams from each stock along with the repetition count for each n-gram. An n-gram with $t = 23$ indicates that the specific n-gram appears among the top five n-grams for all 23 stocks. For stock-related news, a threshold of $t = 13$ repetitions is set to select the n-grams that influence the RV for more than half of the 23 stocks. For general hot news, a threshold of $t = 20$ repetitions is applied, as there are more n-grams and fewer repetitions for each.²⁵ There is no difference in importance among the n-grams within each group and across groups in these tables.²⁶

In [Table 11](#), we grouped the stock-related volatility drivers into ‘Analyst opinion’, ‘Event’, ‘Verb’, ‘Market’, ‘Abbreviation’, ‘Country/Company’, ‘Announcement’, ‘Numeric’, ‘Calendar’, ‘Insider’, and ‘Mixed’.²⁷ The key findings can be summarised as follows: (i) ‘Analyst opinion’ and ‘Event’ contain the majority of volatility driver n-grams. This outcome is anticipated, as it clearly demonstrates the importance of analyst opinions concerning a company’s earnings calls and financial reports. Among others, popular n-grams in this group include *registers*, *announces*, *files*, *raises*, and *surrenders*. (ii) ‘Market’ includes market-related n-grams such as *stocks to buy*, *premarket*, and *stock market opens*. (iii) *China* is the only country in the volatility drivers list for stock-related news, underscoring the relevance of news related to this country. The remaining classes contain fewer n-grams and exhibit less commonality; however, it is evident that these n-grams in stock-related news convey varying levels of information about stocks, the market, and the economy.

[Table 12](#) presents the volatility drivers in general hot news, grouped into ‘Person’, ‘Place’, ‘Legal entity’, ‘Level’, ‘Verb’, ‘Index’, ‘Data’, ‘Numeric’, and ‘Mixed’, and is revealing in several ways. The ‘Person’ category is dominated by prominent political and policy figures, including U.S. presidents Donald Trump, Barack Obama, and Joe Biden, New York City mayor Bill de Blasio, senior political actors such as Mark Meadows, Mitch McConnell, Mike Pompeo, and Nancy Pelosi, as well as key Federal Reserve officials, including Chair Jerome Powell, Janet Yellen, and Federal Reserve Bank presidents James Bullard of St. Louis, Loretta Mester of Cleveland, John C. Williams of New York, Neel Kashkari of Minneapolis, and Raphael Bostic of Atlanta, underscoring the central role of political and monetary policy communication in driving market volatility. International political figures such as

results based on alternative word embedding specifications are generally consistent with those reported here.

²⁵Further analysis indicates that varying t does not substantially alter the defined groups of volatility drivers for both stock-related and general hot news.

²⁶Numerical n-grams hold a prominent position in both tables, underscoring the importance of retaining numerical values during data cleaning, as discussed in [Section A.1](#). While numerical information is fully retained in the modelling stage, numerical n-grams are anonymised in [Table 11](#) and [Table 12](#) for readability and are represented by *NUMBERS*.

²⁷It is important to note that this classification is based on our judgement. However, we believe that reassigning some of the n-grams between groups would not alter the fundamental informational content of these groups.

Table 11: Volatility Drivers (Stock-Related News)

Analyst opinion	outperform by	price target	of earnings	sees #q adj	jumps	rtgs	<i>NUMBERS</i> ^c
equal-weight	neutral by	price target raised	earnings call	other events ζ	rises	chmn	Calendar
overweight	equal-weight by	price target announced	earning call transcripts	filing ζ	sues	dir	week ended
neutral	equal-weight from	price target cut	transcript	report	unveils	corp	week ended MONTH ^d
cut to neutral	overweight by	target announced	transcript, ζ	compensation filing	Market	shrs	ended MONTH
maintained at equal-weight	outperform from	target raised	events ζ	profit	stock market opens	yr	review for week
maintained at overweight	overweight from equal-weight	target announced at	earning season	revenue	premarket	Country/Company	for week ended
maintained at outperform	overweight from neutral	announces at	earnings preview	Verb	stock falls	china	Insider
maintained at neutral	equal-weight from overweight	cut to hold	earnings tomorrow	sees	stock surges	goldman sachs	insider review
from neutral	perform from outperform	raised to neutral	earnings DAY	announces	stock soars	moody's	insider review for
from hold	to neutral	raised to outperform	u.s. earnings DAY	registers	stocks to watch	credit suisse	insider sales
buy from neutral	to neutral from	raised to buy	u.s. earnings	appoints	stocks to buy	nasdaq	substantial insider sales
buy from hold	to outperform	outlook	earnings beat	assigns	to watch	cfa	Mixed
hold from buy	to outperform from	outlook stable	reports earnings tomorrow	soars	tech stocks	wsj	long-term
from equal-weight	neutral from	outlk	reports earnings	surrenders	chip stocks	Announcement	technology
from outperform	neutral from buy	analyst says	for u.s. earnings	release	morning movers	announces completion of	growth
from neutral by	neutral from overweight	from hold	conference (transcript)	update	morning report	moody's announces	sales
from overweight	outperform from	Event	holders, #q	acquires	on the street	agreement	sales: morning
at outperform	outperform from neutral	# ^a q	files 8k	backs	Abbreviation	definitive agreement	shares
at overweight	initiated at outperform	fourth quarter	13f	declares	inst	entry into definitive	correction
at overweight by	initiated at neutral	second quarter	dividend	files	inst holders	deal	price
at equal-weight	initiated at equal-weight	quarter	cash dividend	launches	inc	Numeric	stake
at neutral	overweight by keybanc	ζ ^b	rev	completes	mgmt	billion	results
at neutral by	overweight by morgan	#q, YEAR	eps	raises	exec	bln	new
at equal-weight by	equal-weight by morgan	holders #q	adj eps	boosts	exec mgmt	million	vs
at outperform by	outperform	earnings	#q adj eps	gains	changes exec mgmt	mln	

Notes: ^a # indicates number. ^b ζ commonly indicates quantities in news stories, especially the news headlines about financial reports and earning calls. ^c For clarity, the numerical n-grams are removed and replaced by *NUMBERS* in this table. ^d *MONTH* represents different months.

Dominic Cummings in the United Kingdom and Kim Jong-un of North Korea also appear as important volatility drivers, while the presence of Jim Cramer, a prominent financial media commentator, is notable but unsurprising given the influence of news coverage on market sentiment. In contrast, the appearance of William G. Kaelin, a Nobel prize winning physician scientist, and Reinhard Genzel, an astrophysicist, does not align with the economic and financial focus of the remaining n-grams in this category, illustrating that XAI methods are not error free and that their outputs must be interpreted with caution.

Further analysis of [Table 12](#) highlights the significance of places in our analysis and underscores the role of a group of countries, including *China*, as drivers of volatility. The term ‘Legal entity’ encompasses a variety of major offices, departments, commissions, and companies. The presence of the *health organization* and *CDC* (centres for disease control and prevention) could likely be attributed to the COVID-19 pandemic.²⁸ The next significant class, with a high number of n-grams, is labelled ‘Level’, encompassing a range of levels and changes, percentages, currency values, and specific terms like *below*, *above*, *fall*, and *under*, all referencing certain quantitative expectations. Moving to the subsequent groups, similar to stock-related news, the ‘Verb’ and ‘Numeric’ groups in general hot news underscore the relevance of these particular verbs and numbers as volatility drivers. The ‘Mixed’ group includes a variety of n-grams, such as *SPAC*²⁹, *Payroll-tax cut*, *Airstrike*, *Shutdown*, *Coalitions*, *Crisis*, *Trade Speech*, *Attorney General*, and *Hearing*. Finally, the ‘Index’ and ‘Data’ groups underscore the importance of changes in the S&P500 index and various financial and economic indicators such as *inflation*, *GDP*, and *deficit* as key n-grams. A detailed analysis of all n-grams is beyond the scope of this study; however, we believe that most of these n-grams align with expectations.

These results are broadly consistent with the view that volatility reflects variation in the rate at which economically relevant information is incorporated into prices. The recurrent importance of stock-related n-grams classified as ‘Analyst opinion’, ‘Event’, and ‘Market’, which include recommendation changes, earnings-related events and transcripts, corporate filings and announcements, and market-opening or premarket references, accords with classic empirical evidence that trading volume is closely linked to the magnitude of price changes and return variability ([Karpoff 1987](#)), that volume accounts for a non-trivial share of conditional heteroskedasticity in daily stock returns by proxying for the intensity of information arrivals ([Lamoureux & Lastrapes 1990](#)), and with no-arbitrage theory implying that price volatility scales with the rate of information flow ([Ross 1989](#)). The prominence of ‘Analyst opinion’ terminology is similarly consistent with event-study evidence showing that changes

²⁸As expected, the word COVID-19 does not appear, as it was not in the corpus before 2015.

²⁹Special-purpose acquisition company.

Table 12: Volatility Drivers (General Hot News)

Person	saudis	fall #%	% rate	ranks	payroll-tax cut	vacancies
trump (ref. Donald Trump) ^a	japan	fell #%	% food	correct	shutdown	problems
donald (ref. Donald Trump)	eu	raising #%	high	win	offering	major
obama (ref. Barack Obama)	u.k	above \$ ^c	still high	update	speech	minor
joe biden (ref. Joe Biden)	spain	at \$	higher	search	trade speech	source
biden (ref. Joe Biden)	asia	in \$	min	influence	hearing	week (wk)
powell (ref. Jerome Powell)	north korea	of \$	dip	becoming	us crude	global
yellen (ref. Janet Yellen)	Legal entity	on \$	up	Index	gold	approval
de blasio (ref. Bill de Blasio)	gop (ref. Republican Party)	than \$	down	s&p500 down	crisis	leverage
cummings (ref. Dominic Cummings)	ism (ref. Institute of Supply Management)	from \$	low	s&p500 falls	coalitions	standard
bullard (ref. James B. Bullard)	doe (ref. Department of Energy)	to \$	least	s&p500 drops	airstrike	tremendous
cramer (ref. Jim Cramer)	opec	up to \$	Verb	s&p500 gains	shifting coalitions	obstruction
mester (ref. Loretta J. Mester)	fed (ref. Federal Reserve)	around \$	seen	s&p500 rises	campaign staffer	analysis
meadows (ref. Mark Meadows)	omb (ref. Office of Management and Budget)	by #	sees	s&p500 up	law	statement
williams (ref. John C. Williams)	health organization	% over	forces	s&p500 adds	lawmakers	sources
mcconnell (ref. Mitch McConnell)	u.s. treasury	% target	achieve	s&p500 climbs	attorney general	adversity sources
pompeo (ref. Mike Pompeo)	treasury	% from	cut	s&p500	trump administration	advisor
pelosi (ref. Nancy Pelosi)	cdc (ref. Centers for Disease Control and Prevention)	% rate	grows	Data	compensation	emails
kim (ref. Kim Jong-un)	occ (ref. Options Clearing Corporation)	% vs	resigns	ex-autos (ref. Retail Sales ex Autos)	banks	state tv
kashkari (ref. Neel Kashkari)	sec (ref. Securities and Exchange Commission)	% through	says	inflation	economy	companies
bostic (ref. Raphael Bostic)	wsj (ref. The Wall Street Journal)	about \$	charges	jobs	police	opioid companies
g kaelin (ref. William G. Kaelin)	st. louis (ref. Federal Reserve Bank of St. Louis)	under \$	dies	gdp	dodd_frank	relationships
genzel (ref. Reinhard Genzel)	bloomberg	for \$	passes	deficit	rico's	sru_related problems
Place	wolfe (ref. Wolfe Research)	yr to \$	propose	Numeric	corridors	first
us	Level	% on \$	releases	trillion	officials	chance
korea	below # ^b %	% to \$	triggers	billion	organization	groups
syria	above #%	% at #	proceed	million	pm	house
israel	to #%	% in	totaled	mln bbl	program	direction
china	up #%	% on	transferred	<i>NUMBERS</i> ^d	schools	dreamers'
iran	achieve #%	% to	pass	Mixed	prison	others
russia	slide #%	% on year	talk	spac	groups	speaker

Notes: ^a The most likely full phrase to which the specified n-gram refers. ^b # indicates number. ^c The symbol \$ denotes monetary values in U.S. dollars. ^d For clarity, the numerical n-grams are removed and replaced by *NUMBERS* in this table.

in brokerage recommendations convey information that is rapidly incorporated into prices and generate sharp contemporaneous market reactions (Womack 1996). Finally, the salience of general hot-news n-grams classified as ‘Person’, ‘Place’, ‘Legal entity’, ‘Index’, and ‘Data’, tied to macroeconomic, monetary policy, and geopolitical developments, aligns with a large literature demonstrating that scheduled macroeconomic announcements and unanticipated policy actions generate sharp contemporaneous market reactions in volatility (Ederington & Lee 1993, Andersen, Bollerslev, Diebold & Vega 2007, Bernanke & Kuttner 2005), and with text-based evidence that news-implied measures of economic and political risk co-move closely with implied volatility and broader measures of market uncertainty (Manela & Moreira 2017, Caldara & Iacoviello 2022).

Overall, the SHAP-based XAI analysis demonstrates that the NLP models extract economically meaningful and interpretable information from news text, rather than relying on opaque or spurious patterns. By attributing RV forecasts to specific n-grams, the results show that stock-related news is primarily driven by analyst opinions, earnings related events, and firm-specific announcements, while general hot news is dominated by macroeconomic indicators, political developments, and policy communication. This clear separation mirrors the earlier regime dependent forecasting results, with firm-specific language being most informative during high volatility days and market-wide information matters more during normal volatility days. Importantly, the SHAP attributions provide transparency comparable to dictionary-based models, confirming that the forecasting gains are grounded in identifiable and theoretically consistent textual signals, thereby strengthening the economic credibility of the proposed framework.³⁰

6 Conclusions

This study develops and evaluates a news-driven RV forecasting framework that uses modern NLP to transform news into predictive signals. The core empirical design tests whether a text-only NLP forecaster can produce competitive one-day-ahead RV forecasts relative to established volatility-history benchmarks, and whether combining news-based signals with standard RV models yields incremental predictive value. We further compare general-purpose and specialised language representations and apply explainability analysis to attribute forecast variation to specific phrases and themes in the news.

Overall, the evidence indicates that news contains useful information for RV forecasting. A news-only NLP model delivers meaningful out-of-sample performance relative to the standard HAR-family

³⁰The results in Section A.9 show that the NLP models rely on a heterogeneous set of economically interpretable n-grams whose effects on RV vary in sign and magnitude across stocks and news types. In contrast to dictionary-based models, which impose a fixed and uniform sentiment interpretation, the SHAP analysis reveals substantial cross-sectional and contextual heterogeneity in how identical words affect RV forecasts.

benchmarks, although volatility-history models remain strong performers on average. Predictive content varies with coverage, with stock-related news typically more informative than general news. When combined with a standard RV benchmark, the news-based signal improves both statistical performance and economic-gain measures, indicating that text-based information complements rather than substitutes for established econometric models. The explainability analysis makes it possible to trace RV forecasts back to the underlying news content and to distinguish clearly between stock-related news and general hot news. Stock-related news is mainly associated with analyst opinions and firm-level events and announcements, while general hot news is linked to broader macroeconomic and policy-related categories, including political actors, institutions, economic indicators, and market-wide developments.

Future research could integrate news text and numerical inputs, such as lagged RV, within a unified model to exploit complementarities across information sources and to improve robustness across regimes. It would also be valuable to assess whether news-based signals enhance cross-asset and bespoke-volatility frameworks (Bollerslev et al. 2018, Patton & Zhang 2025). Another direction is to account for potential changes in the semantic meaning of words over time, which are not explicitly modelled in this study due to computational limitations. Moreover, this line of research can be extended to related finance applications, including return forecasting and credit risk assessment. The development of broader and larger specialised language models for finance represents another promising avenue for future research.

A Appendix

A.1 Data Cleaning Details

All duplicate news stories, as well as those without headlines and bodies, are removed as an initial filtering step. Given the heterogeneous nature of raw news data, extensive pre-processing of the textual content is required to eliminate redundant characters, sentences, and structural artefacts that do not convey semantic information. This cleaning process aims to standardise the text, reduce noise, and ensure that only meaningful content is retained for subsequent analysis. [Table A1](#) provides a structured overview of the textual data cleaning rules applied in this study. Each rule is implemented using a regular expression and may include multiple variations in order to capture differences in formatting and presentation across news sources; however, for clarity and brevity, only one representative variation of each rule is displayed. *XX* denotes an arbitrary sequence of characters of variable length, used as a placeholder to illustrate the general form of the corresponding regular expression pattern.

The text cleaning procedures are grouped into five main categories: 1) Primary, 2) Begins with, 3) Ends with, 4) General, and 5) Final checks. The *Primary* rules focus on fundamental transformations of the raw data, including extracting the body of news from extensible markup language (XML), removing XML-encoding characters (XMLENCOD), converting XML content into plain text through parsing, transforming upper-case letters into lower-case, and removing embedded tables. These steps ensure that the core textual content is isolated and normalised before applying more specific pattern-based cleaning rules. This category forms the foundation of the cleaning pipeline and prepares the text for further refinement.

The remaining categories target recurring non-informative patterns commonly found in news articles. The *Begins with* and *Ends with* rules remove boilerplate segments that appear at the start or end of articles, such as copyright notices, contact information, source attributions, subscription prompts, and references to external content. The *General* category addresses patterns that may occur anywhere within the text, including social media references, repeated disclaimers, attachments, and promotional content. Finally, the *Final checks* perform a last-stage clean-up by removing links, email addresses, phone numbers, short news stories containing fewer than 25 characters, and leading or trailing spaces. All five categories of cleaning rules are applied separately to both news headlines and news bodies to ensure consistent pre-processing across different textual components.

Due to the importance of numerical information in accounting and finance, all numbers are preserved. This design choice is essential for maintaining sentence integrity, particularly in settings where

token order conveys economically meaningful information rather than merely contributing to word counts. For example, removing numbers from the sentence ‘Over 540,000 apps wiped from Apple App Store in Q3 reaching lowest number in 7 years’ yields ‘Over apps wiped from Apple App Store in Q reaching lowest number in years,’ which materially alters the meaning and weakens the informational content.

Table A1: Textual Data Cleaning Rules

Primary	
Extracting body of news from XML Converting XML to text (parsing) Removing tables	Removing XML-Encoding Characters (XMLENCOD) Converting uppercase letters to lowercase letters
Begins with	
(END) XX for (more—further) (information—from marketwatch), please visit: XX (EMAIL; @XX) copyright XXXX, XX URL (more to follow) XX end of (message—corporate news) XX source: XX URL XX contributed to this article XX view source version on XX (=—————) view original content with multimedia XX readers can alert XX view original content: XX media inquiries: XX readers: send feedback to XX follow us on XX contact(s): XX please refer to URL XX find out more at URL XX XX enquiries: XX -by XX, dow jones newswires XX	(email—e-mail): XX (phone—fax—contact—dgap-ad-hoc—dgap-news): XX image available: XX source: XX to read more, visit: XX (view source—view original content) (with—on) XX (investor relations—investor contact) XX like us on XX (copyright—(c)—©) XX XX can be found at URL XX by dow jones newswires XX (write to—follow) XX at EMAIL (phone—tel—telephone—mobile—contact—inquiries—comment): XX (contact information—media contact—contact client services—internet) XX click here to subscribe to XX to learn more about XX (website—web site): URL XX contact us in XX to receive news releases by (e-mail—email) XX full story at XX
Ends with	
(more to follow) (fax—tel—contact—dgap-ad-hoc—dgap-news): ratings actions from baystreet: cannot parse story lipper indexes: to subscribe to for full details, please click on	view original content XX: (contacts—web site): (=— -—_—→) for notes, kindly refer following is the related link:
General	
(linkedin—facebook—fb): XX (twitter—ig): XX (attachment—attachments): XX please visit XX follow us on XX All rights reserved	(URL (and—&) XX) (EMAIL (and—&) EMAIL) this information was brought to you by XX write to EMAIL to receive our XX URL more at, XX URL
Final checks	
Removing links and emails Removing both the leading and the trailing space(s)	Removing news shorter than 25 characters Removing phone numbers

A.2 Word Embedding Development Details

After cleaning the raw news data following the steps described in [Section A.1](#), each headline and news body is tokenised into an ordered sequence (w_1, \dots, w_T) , as defined in [Equation \(1\)](#). Each token takes a value in the vocabulary \mathcal{V} defined in [Equation \(2\)](#), and is ultimately mapped to a vector representation $\mathbf{e}_w \in \mathbb{R}^d$ as introduced in [Equation \(3\)](#). Many economic concepts are expressed as multi-word phrases rather than individual words, and treating their components separately may dilute their economic meaning. To address this issue, frequently occurring two-word expressions are identified using the phrase-detection procedure of [Mikolov, Sutskever, Chen, Corrado & Dean \(2013\)](#). This method evaluates adjacent word pairs based on their empirical co-occurrence frequency relative to what would be expected under independence. Specifically, for any adjacent token pair (w_i, w_j) , an association score is computed as

$$\text{Score}(w_i, w_j) = \frac{C(w_i, w_j) - \delta}{C(w_i)C(w_j)}, \quad (\text{A1})$$

where $C(w_i, w_j)$ denotes the number of times the pair appears consecutively in the corpus, $C(w_i)$ and $C(w_j)$ are unigram counts, and δ is a discounting constant that penalises infrequent co-occurrences. In practice, this discounting is enforced implicitly by the phrase-detection procedure through minimum co-occurrence requirements and is not tuned. A threshold value of ten is applied as a separate selection criterion, consistent with standard implementations of the phrase-detection algorithm, so that only strongly associated word pairs are retained. Retained bigrams are merged into a single token by joining the two words with an underscore (e.g., `financial_statement`), allowing the word embedding models described in [Section 2.1](#) and [Section 2.2](#) to learn a unified vector representation for economically meaningful concepts.

To reduce estimation noise and improve the stability of the embedding matrix E defined in [Equation \(4\)](#), tokens that appear fewer than five times in the entire corpus are removed. Very infrequent tokens provide insufficient contextual information for reliable vector estimation and may introduce unnecessary variance. Following pre-processing, Word2Vec and FastText models are estimated using a context window of size five, as defined in [Section 2.1](#). This choice implies that the representation of each token is learned from the five tokens preceding and the five tokens following it in the text, so that local co-occurrence patterns drive the estimation of the embedding matrix E .

Model estimation relies on negative sampling, which is introduced conceptually in [Section 2.1](#) as an approximation to the full softmax likelihood in [Equation \(6\)](#). Rather than comparing each observed token–context pair with the entire vocabulary, the model contrasts it with a small number of artificially

generated noise pairs. In this study, five negative samples are used for each observed pair. Negative samples are drawn from a smoothed unigram distribution,

$$P_n(w) \propto C(w)^{0.75}, \tag{A2}$$

following Mikolov, Sutskever, Chen, Corrado & Dean (2013), where $P_n(w)$ denotes the probability of drawing token w as a negative sample and $C(w)$ is the total number of occurrences of token w in the training corpus. The exponent of 0.75 smooths the empirical frequency distribution by down weighting extremely common tokens, such as function words, while still assigning relatively higher probability to frequent and economically relevant terms, thereby improving estimation stability and representation quality.

All models are trained for five epochs, meaning that the entire corpus is processed five times during estimation. The learning rate is initialised at 0.025 and decays linearly to a minimum value of 0.0001 to ensure numerical stability and convergence. Each token is represented by a 300-dimensional vector, corresponding to the word embedding dimension M in Equation (3), which is a commonly adopted standard in general-purpose word embeddings, including the off-the-shelf Word2Vec and FastText word embeddings used in this study.

A.3 Gold-Standard Financial Benchmark Details

Each analogy follows the structure A is to B as C is to X, where the objective is to recover X by preserving the same financial relationship. For example, the analogy *AAPL* is to *Cupertino* as *MSFT* is to *Redmond* tests whether a word embedding links a firm’s ticker to its headquarters city; *Apple* is to *AAPL* as *Amazon* is to *AMZN* captures the mapping between company names and tickers; *Amazon* is to *1994* as *Google* is to *1998* relates firms to their incorporation years; *Microsoft* is to *NASDAQ* as *IBM* is to *NYSE* links firms to their primary stock exchanges; *Tesla* is to *California* as *Boeing* is to *Illinois* reflects US headquarters states; *HSBC* is to *UK* as *JPMorgan* is to *US* captures countries of headquarters; and *Toyota* is to *Japan* as *Alibaba* is to *China* extends this relationship to a global setting.

The benchmark is constructed in several systematic steps. First, firm-level data are collected separately for the United States, the United Kingdom, China, and Japan. Firms are filtered to retain only publicly listed companies with complete and consistent information on key attributes such as name, ticker, headquarters location, exchange, country, and incorporation year. Company names are standardised by removing legal suffixes and formatting inconsistencies to ensure that each entity is represented by a single, unambiguous token. To avoid confounding effects, only unigram representations are retained, and firms with duplicate or ambiguous identifiers are excluded.

Second, firms are classified by size using the Orbis size classification, and the benchmark focuses exclusively on very large companies to ensure reliable coverage in the underlying text corpora. The benchmark includes firms from four countries: the United States, the United Kingdom, China, and Japan, representing major equity markets. For US-only benchmarks, the top 20 very large US companies are selected and used across all US benchmarks, covering relationships involving company names, tickers, headquarters cities, incorporation years, stock exchanges, and US states. To extend the evaluation beyond a single country while maintaining sufficient firm coverage, a cross-country benchmark combines the top 10 very large firms from the United States and the United Kingdom. Finally, to assess whether word embeddings capture country-level relationships in a broader international setting, a global benchmark is constructed using the top 5 very large firms from each of the four countries.

Third, each benchmark group is defined by a specific financial relationship: ticker to headquarters city, company name to ticker, company name to incorporation year, company name to stock exchange, company name to US headquarters state, company name to country of headquarters in a US–UK setting, and company name to country of headquarters in a global setting. Within each group, all ordered permutations of the selected firms are generated to form analogy questions. This means that

every firm is systematically paired with every other firm in the same group, ensuring that each financial relationship is tested exhaustively rather than through a small number of hand-picked examples. For each permutation, the known attribute of one firm is used to infer the corresponding attribute of another firm under the same relationship structure. This procedure yields 380 unique analogies per group and 2,660 analogies in total. For evaluation, a prediction is considered correct if the true answer appears among the top five candidates returned by the word embedding model. We found five to be a fair and balanced choice, as a smaller cutoff would make the benchmark more restrictive, while a larger cutoff would make it more permissive.

A.4 RV Cleaning Procedures

We implemented the relevant data-cleaning procedures proposed by [Barndorff-Nielsen et al. \(2009\)](#), adapting them to a LOB setting. The procedures applied below use the following notation: P denotes the full dataset, Q refers exclusively to quote data, and T denotes trade data only.

- **P2:** Delete entries with a bid, ask or transaction price equal to zero.
- **T4:** Delete entries with prices that are above the ‘ask’ plus the bid-ask spread, or below the ‘bid’ minus the bid-ask spread.
- **Q1:** When multiple quotes share the same timestamp, they are replaced by a single entry using the median bid price, median ask price, the sum of all volumes, and the last snapshot of the LOB is selected as the LOB associated with the merged message data. For messages with different directions (buy or sell), the message data and the LOB with the same direction are grouped according to the buy side or sell side. The procedure mentioned above is then applied to the message data and the last snapshot of the LOB of the group.
- **Q2:** Delete entries for which the spread is negative.
- **Q3:** Delete entries for which the spread is more than 50 times the median spread on that day.
- **Q4:** Delete entries for which the mid-quote deviated by more than 10 mean absolute deviations from a rolling centred median (excluding the observation under consideration) of 50 observations (25 observations before and 25 after).

[Table A2](#) presents the summary statistics of the data cleaning process. This table indicates that approximately 40% of the samples (ticks) were discarded in the cleaning phase. Notably, T4 was responsible for the removal of a significant portion of the data, amounting to nearly 89.33% (i.e., 35.78/40.05) of the total data excluded. The filtering rules are applied uniformly across all stocks and all time periods. While filtering reduces the number of observations, it is designed to remove stale or erroneous records rather than information-bearing trades. To assess the impact of these cleaning procedures on the calculated RVs, we further analysed the LOB data without implementing the cleaning procedures. The comparative statistics and the correlation between RVs calculated with and without these data cleaning procedures are detailed in [Table A3](#). It is evident that the descriptive statistics without the application of cleaning procedures closely align with those presented in [Table 5](#). In all instances, the correlation remains significantly high, thereby affirming the robustness of the calculated RVs.

Table A2: Data Cleaning Summary Statistics

Name	Ticker	Sample Size	Removed (%)	P2 (%)	T4 (%)	Q1 (%)	Q2 (%)	Q3 (%)	Q4 (%)
Apple	AAPL	4174971328	34.22	0.00	29.88	4.34	0.00	0.00	0.00
Microsoft	MSFT	3827824574	35.88	0.01	30.18	5.69	0.00	0.00	0.00
Intel	INTC	2807965330	38.59	0.01	31.79	6.78	0.01	0.00	0.01
Comcast	CMCSA	2390133817	45.18	0.01	39.59	5.58	0.00	0.00	0.01
Qualcomm	QCOM	2086295132	41.46	0.00	36.46	4.98	0.00	0.00	0.01
Cisco Systems	CSCO	2296179428	40.46	0.01	33.50	6.94	0.00	0.00	0.01
eBay	EBAY	1683001942	40.73	0.01	35.68	5.03	0.00	0.00	0.01
Gilead Sciences	GILD	1404574567	41.68	0.00	38.41	3.25	0.00	0.00	0.01
Texas Instruments	TXN	1485049597	39.45	0.00	35.14	4.29	0.00	0.00	0.01
Amazon.com	AMZN	1201210867	23.06	0.00	19.89	3.15	0.00	0.00	0.02
Starbucks	SBUX	1564221129	44.04	0.01	39.95	4.07	0.00	0.00	0.01
Nvidia	NVDA	1548447223	35.47	0.01	30.40	5.05	0.00	0.00	0.01
Micron Technology	MU	2110482619	35.99	0.00	31.11	4.86	0.00	0.00	0.01
Applied Materials	AMAT	1616466522	39.70	0.01	34.41	5.27	0.00	0.00	0.01
NetApp	NTAP	1015914054	44.99	0.01	41.14	3.82	0.00	0.00	0.02
Adobe	ADBE	1083392595	37.76	0.01	34.35	3.39	0.00	0.00	0.02
Xilinx	XLNX	1172584895	40.24	0.01	36.97	3.26	0.00	0.00	0.02
Amgen	AMGN	863464001	38.62	0.01	34.73	3.86	0.00	0.00	0.02
Vodafone Group	VOD	1012861232	47.20	0.01	44.23	2.95	0.00	0.00	0.02
Cognizant	CTSH	928987253	46.22	0.01	43.28	2.91	0.00	0.00	0.02
KLA Corporation	KLAC	783931409	42.63	0.01	39.83	2.77	0.00	0.00	0.02
Paccar	PCAR	775954122	45.74	0.01	42.98	2.73	0.00	0.00	0.03
Autodesk	ADSK	803552017	41.73	0.01	38.96	2.74	0.00	0.00	0.02
Average			40.05	0.01	35.78	4.25	0.00	0.00	0.01

Notes: **P2:** Delete entries with a bid, ask or transaction price equal to zero, **T4:** Delete entries with prices that are above the ‘ask’ plus the bid-ask spread, or below the ‘bid’ minus the bid-ask spread, **Q1:** When multiple quotes share the same timestamp, they are replaced by a single entry using the median bid price, median ask price, the sum of all volumes, and the last snapshot of the LOB is selected as the LOB associated with the merged message data. For messages with different directions (buy or sell), the message data and the LOB with the same direction are grouped according to the buy side or sell side. The procedure mentioned above is then applied to the message data, and the last snapshot of the LOB of the group, **Q2:** Delete entries for which the spread is negative, **Q3:** Delete entries for which the spread is more than 50 times the median spread on that day, **Q4:** Delete entries for which the mid-quote deviated by more than 10 mean absolute deviations from a rolling centred median (excluding the observation under consideration) of 50 observations (25 observations before and 25 after).

Table A3: RV Descriptive Statistics (Without Cleaning)

Ticker	Min	Max	1 st Quantile	Median	3 rd Quantile	Mean	STD	Kurtosis	Skewness	Correlation ^a
AAPL	0.101	229.529	0.898	1.737	3.702	4.623	12.579	110.333	9.093	0.9999
MSFT	0.096	216.486	0.828	1.458	2.810	3.240	8.119	194.967	11.294	0.9997
INTC	0.030	318.118	1.099	1.876	3.592	4.300	11.615	295.828	14.000	0.9999
CMCSA	0.006	237.387	0.913	1.631	3.344	3.833	9.773	190.221	11.459	0.9994
QCOM	0.123	368.449	1.025	1.980	4.140	5.076	15.363	197.106	12.012	0.9999
CSCO	0.038	343.946	0.884	1.564	3.031	4.117	13.170	213.266	12.287	0.9999
EBAY	0.215	259.723	1.328	2.263	4.361	5.111	12.745	142.560	10.028	0.9974
GILD	0.063	261.664	1.170	1.895	3.375	4.312	12.933	184.066	12.094	0.9999
TXN	0.183	289.765	1.046	1.895	3.713	4.006	9.928	310.664	14.275	0.9986
AMZN	0.066	551.566	1.307	2.342	4.833	6.203	19.355	246.159	12.802	0.9998
SBUX	0.048	265.554	0.864	1.594	3.441	4.209	11.227	161.691	10.615	0.9997
NVDA	0.159	1104.483	2.280	4.342	9.098	9.760	30.112	586.751	20.055	1.0000
MU	0.288	484.388	3.575	6.281	11.964	12.821	25.726	89.478	7.966	0.9990
AMAT	0.312	529.508	1.773	3.031	5.730	6.014	14.615	526.901	18.237	0.9999
NTAP	0.114	463.545	1.508	2.606	5.180	6.301	18.020	201.869	11.942	0.9998
ADBE	0.120	575.498	1.096	2.001	3.874	4.810	14.784	661.002	20.309	0.9998
XLNX	0.231	265.372	1.300	2.374	4.791	5.022	11.950	193.951	11.739	0.9990
AMGN	0.039	212.485	0.962	1.580	2.860	3.311	9.225	202.622	12.391	0.9995
VOD	0.043	217.091	0.684	1.334	3.081	3.693	9.500	149.567	10.122	0.9998
CTSH	0.186	493.255	0.979	1.743	4.085	5.218	15.843	339.283	14.667	0.9997
KLAC	0.149	499.806	1.451	2.701	5.412	5.820	16.308	384.071	16.516	0.9933
PCAR	0.029	389.021	1.157	2.172	4.657	5.137	12.123	309.547	12.928	0.9998
ADSK	0.268	696.615	1.642	2.770	5.176	6.660	22.503	389.706	16.604	0.9999

Notes: ^a Correlation between two sets of calculated RVs with and without the implementation of the cleaning procedures. The RV descriptive statistics computed on the cleaned dataset are presented in [Table 5](#).

A.5 HAR-Family of Models: In-Sample and Out-of-Sample Results

All HAR-family of models are estimated following the rolling-window forecasting design described in [Section 4.1](#). The in-sample period spans from 27 July 2007 to 11 September 2015 and contains 2,046 daily observations for each stock, while the out-of-sample period covers 1,604 trading days. For each of the 23 stocks, model parameters are estimated by ordinary least squares (OLS) using a fixed-length rolling window of 2,046 observations. At each out-of-sample date, the estimation window is advanced by one day, the model is re-estimated using the most recent observations, and a one-step-ahead forecast of RV is generated. This procedure yields 1,604 rolling estimations per stock and a total of 36,892 estimations per model across the full cross-section. Also, following [Bollerslev et al. \(2016\)](#), when the forecasted RV exceeds (falls below) the maximum (minimum) value observed in the estimation sample, it is replaced with the sample mean of RV from the estimation period.

The in-sample results in [Table A4](#) summarise coefficient estimates and performance measures obtained from 36,892 rolling regressions across assets and time. The table shows that coefficient estimates largely conform to expected volatility dynamics. The AR specification delivers the weakest fit, whereas introducing heterogeneous horizons via HAR leads to a clear improvement in adjusted R^2 and loss measures, with further extensions providing additional but uneven gains. Among all specifications, the CHAR model stands out as the best-performing in-sample, achieving the highest average and median adjusted R^2 and the lowest average and median MSE and QLIKE. The out-of-sample forecasting results reported in [Table A5](#) provide a comprehensive comparison of the HAR-family of models using both loss-based metrics and the RC across the full out-of-sample period and across different volatility regimes. The RC statistics report the percentage of tickers for which a given model is not outperformed by any competing specification, where each model is evaluated relative to all other HAR-family of models under the chosen loss function at the 5% and 10% significance levels. Over the full out-of-sample period, clear performance differences emerge. The AR specification performs the worst under both MSE and QLIKE, while HAR leads to sizeable improvements. Further extensions yield additional gains, but the ranking is consistent across average and median losses: the CHAR model delivers the lowest average and median MSE and QLIKE among all competitors. This superior performance is reinforced by the RC results, where CHAR achieves rates of (100%, 100%) across tickers at both the 5% and 10% significance levels under both loss functions, indicating that it is not outperformed by any alternative specification. The dominance of CHAR is even more pronounced on normal volatility days, where it attains substantially lower losses than all other models and very high RC. During high volatility days, forecast losses increase sharply for all models and relative performance becomes more heterogeneous, with HAR-J exhibiting slightly lower average losses, particularly under MSE. Never-

theless, CHAR remains among the top-performing models and continues to achieve the strongest RC outcomes, especially under QLIKE.

One natural question that arises in the empirical analysis concerns the sensitivity of the forecasting results to the choice of the estimation window size. To examine how changes in the window length affect out-of-sample predictive performance, we conduct an additional robustness exercise in which the estimation sample is reduced to 1,023 observations, while the out-of-sample evaluation period is held fixed. The resulting out-of-sample forecasts are reported in [Table A6](#). Compared to the baseline results based on a larger estimation window, most models exhibit a noticeable deterioration in out-of-sample forecasting accuracy, as shown in [Table A5](#). Importantly, however, the relative ranking of the models is largely preserved. In particular, the CHAR model continues to exhibit superior out-of-sample performance, indicating that its forecasting advantage is robust to a substantial reduction in the estimation window size. Due to computational constraints, this robustness test is not extended to the remainder of the analyses in this study. Nevertheless, at least for the benchmark models, the results indicate that the main findings are robust to changes in the length of the in-sample estimation window.

Table A4: Parameter Estimates of HAR-family of Models

	AR1	HAR	HAR-J	CHAR	SHAR	ARQ	HARQ	HARQ-F
β_0	3.6436 ^a	1.8528	1.4401	1.2273	1.8444	2.8734	1.6127	0.6807
	3.6436 ^b	1.8530	1.4408	1.2479	1.8447	2.8734	1.6135	0.8452
	(1.6305) ^c	(0.9216)	(0.6446)	(0.6357)	(0.9213)	(1.3585)	(0.8758)	(0.8382)
	(100, 0) ^d	(100, 0)	(99.9, 0.1)	(98.7, 1.3)	(99.9, 0.1)	(100, 0)	(99.9, 0.1)	(77.2, 22.8)
β_1	0.1428	0.0394	0.6544			0.3653	0.2136	0.1695
	0.1428	0.0421	0.6544			0.3653	0.2136	0.1702
	(0.1090)	(0.0382)	(0.2743)			(0.2028)	(0.1093)	(0.1193)
	(100, 0)	(93.8, 6.2)	(100, 0)			(100, 0)	(100, 0)	(99.3, 0.7)
β_1^+					0.0625			
					0.0638			
					(0.0942)			
				(92.8, 7.2)				
β_1^-					0.0346			
					0.0397			
					(0.0390)			
				(88.4, 11.6)				
β^w		0.1471	0.0523		0.1449		0.1123	0.2076
		0.1642	0.0925		0.1616		0.1341	0.2197
		(0.1805)	(0.1305)		(0.1774)		(0.1568)	(0.1731)
		(77.2, 22.8)	(60.2, 39.8)		(77.0, 23.0)		(72.6, 27.4)	(89.6, 10.4)
β^m		0.3566	0.2510		0.3527		0.3090	0.5367
		0.3566	0.2529		0.3530		0.3097	0.5368
		(0.1754)	(0.1562)		(0.1767)		(0.1675)	(0.1956)
		(100, 0)	(97.1, 2.9)		(98.7, 1.3)		(98.1, 1.9)	(100, 0)
β_{jump}			-0.7353					
			0.7353					
			(0.2840)					
			(0, 100)					
β_{BPV}^d				0.4136				
				0.4161				
				(0.2526)				
			(98.3, 1.7)					
β_{BPV}^w				0.3434				
				0.3697				
				(0.2926)				
			(91.2, 8.8)					
β_{BPV}^m				0.4336				
				0.4433				
				(0.3329)				
			(92.5, 7.5)					
β_Q						-0.0004	-0.0003	-0.0002
						0.0004	0.0003	0.0002
						(0.0004)	(0.0003)	(0.0003)
					(0.4, 99.6)	(0.6, 99.4)	(2.0, 98.0)	
β_Q^w								-0.0008
								0.0011
								(0.0013)
							(22.0, 78.0)	
β_Q^m								-0.0064
								0.0068
								(0.0080)
							(7.4, 92.6)	
<i>Adj. R²(avg)</i>	0.0318	0.0721	0.0984	0.1000	0.0731	0.0583	0.0818	0.0871
<i>Adj. R²(med)</i>	0.0104	0.0404	0.0673	0.0692	0.0406	0.0406	0.0505	0.0552
<i>MSE (avg)</i>	173.3761	165.6939	161.0308	160.7043	165.4823	168.4723	163.9610	162.7886
<i>MSE (med)</i>	127.6872	124.0916	120.5695	119.9260	124.0427	125.2517	121.4500	120.8497
<i>QLIKE (avg)</i>	0.6139	0.5619	0.5177	0.5167	0.5615	0.5773	0.5481	0.5599
<i>QLIKE (med)</i>	0.6223	0.5670	0.5187	0.5236	0.5656	0.5813	0.5452	0.5737

Notes: For each parameter in each model, the mean of coefficients^[a], the mean of absolute coefficients^[b], the standard deviation^[c], and the proportions of positive and negative coefficients^[d] are computed using 36,892 daily estimations (1,604 days \times 23 stocks). ‘HAR-J’ is HAR with jump, ‘CHAR’ stands for continuous HAR, and ‘SHAR’ denotes semivariance HAR. ‘ARQ’, ‘HARQ’, and ‘HARQ-F’ are the introduced models in [Bollerslev et al. \(2016\)](#). β_0 is the constant term, β_1 is the coefficient of the first lag of RV, β_1^+ and β_1^- are the coefficients of the first lag of RV for the positive and negative returns, β^w and β^m are the coefficients of the daily average of RV over the last week and last month, β_{jump} is the coefficient of the jump term of ‘HAR-J’ model, β_{BPV}^d , β_{BPV}^w , and β_{BPV}^m are the coefficients of continuous terms of the ‘CHAR’ model, and β_Q , β_Q^w , and β_Q^m stand for the coefficients of the first lag of RQ, and the daily average of RQ for the last week and last month, respectively. In the lower section of this table, bolded values represent the highest performance for each metric. For each stock, *MSE* and *QLIKE* are initially calculated as the average (or median) in-sample errors. These values are subsequently aggregated across all 23 stocks, using either the overall average (or median).

Table A5: HAR-family Out-of-Sample Forecasting Performance

Full Out-of-Sample Period		AR1	HAR	HAR-J	CHAR	SHAR	ARQ	HARQ	HARQ-F
MSE	Avg	218.957	208.345	199.070	198.924	209.478	210.459	204.707	207.962
	Med	144.744	137.001	130.463	129.495	138.829	142.448	136.673	147.108
RC ^a		(52.17,86.96)	(73.91,95.65)	(95.65,100)	(100,100)	(73.91,95.65)	(47.83,69.57)	(69.57,86.96)	(82.61,95.65)
QLIKE	Avg	0.693	0.608	0.552	0.543	0.608	0.641	0.590	0.607
	Med	0.687	0.612	0.560	0.537	0.606	0.650	0.591	0.601
RC		(0,0)	(0,0)	(86.96,86.96)	(100,100)	(0,0)	(0,8.70)	(8.70,8.70)	(13.04,17.39)
Normal Volatility Days									
MSE	Avg	11.745	11.228	9.030	7.730	12.230	10.115	10.364	10.808
	Med	7.798	7.000	5.947	5.091	7.489	7.478	7.101	7.392
RC		(47.83,56.52)	(52.17,60.87)	(52.17,69.57)	(95.65,95.65)	(56.52,78.26)	(26.09,30.44)	(26.09,47.83)	(26.09,30.44)
QLIKE	Avg	0.399	0.340	0.313	0.298	0.339	0.364	0.327	0.318
	Med	0.362	0.327	0.296	0.269	0.330	0.339	0.314	0.303
RC		(0,0)	(4.35,4.35)	(21.74,34.78)	(95.65,95.65)	(0,0)	(0,0)	(13.04,17.39)	(43.48,56.52)
High Volatility Days									
MSE	Avg	2131.361	2028.059	1954.202	1964.630	2030.282	2060.872	1999.278	2027.084
	Med	1293.253	1223.783	1171.940	1163.489	1236.025	1266.151	1218.390	1334.427
RC		(47.83,91.30)	(69.57,91.30)	(100,100)	(91.30,100)	(69.57,95.65)	(69.57,91.30)	(91.30,91.30)	(100,100)
QLIKE	Avg	3.329	3.008	2.690	2.739	3.015	3.126	2.946	3.184
	Med	3.275	2.905	2.618	2.691	2.914	3.109	2.902	3.108
RC		(43.48,73.91)	(52.17,56.52)	(95.65,95.65)	(100,100)	(47.83,56.52)	(69.57,82.61)	(43.48,52.17)	(26.09,52.17)

Notes: Following Equation (12), the modelling functions are $f_{AR}(RV_t)$, $f_{HAR}(RV_t, \overline{RV}_t^w, \overline{RV}_t^m)$, $f_{HAR-J}(RV_t, \overline{RV}_t^w, \overline{RV}_t^m, J_t)$, $f_{CHAR}(BPV_t, \overline{BPV}_t^w, \overline{BPV}_t^m)$, $f_{SHAR}(RV_t^+, RV_t^-, \overline{RV}_t^w, \overline{RV}_t^m)$, $f_{ARQ}(RV_t, RQ_t)$, $f_{HARQ}(RV_t, \overline{RV}_t^w, \overline{RV}_t^m, RQ_t)$, and $f_{HARQ-F}(RV_t, \overline{RV}_t^w, \overline{RV}_t^m, RQ_t, \overline{RQ}_t^w, \overline{RQ}_t^m)$, where RV_t is the realised variance, \overline{RV}_t^w is the average of RV_t for the last week, \overline{RV}_t^m is the average RV_t of the last month, J_t is the jump component, BPV_t , \overline{BPV}_t^w , and \overline{BPV}_t^m are the bipower variation, the average BPV_t of the last week, and the average BPV_t of the last month. RV_t^+ and RV_t^- denote the RV aggregated from positive and negative intraday returns. RQ_t , \overline{RQ}_t^w , and \overline{RQ}_t^m are the realised quarticity, the average RQ_t of the last week, and the average RQ_t of the last month. ^a The RC denotes the percentage of tickers for which we reject, at the 5% (or 10%) significance level, the null hypothesis that the specified model does not outperform the best-performing model within the HAR-family benchmark set, excluding the model under assessment.

Table A6: HAR-family Out-of-Sample Forecasting Performance (1,023 Estimation Sample Size)

Full Out-of-Sample Period		AR1	HAR	HAR-J	CHAR	SHAR	ARQ	HARQ	HARQ-F
MSE	Avg	217.611	209.478	200.948	200.631	211.665	206.889	204.719	212.313
	Med	144.957	139.762	136.629	135.86	141.447	138.695	137.645	143.170
RC ^a		(69.57,95.65)	(86.96,95.65)	(100,100)	(100,100)	(86.96,95.65)	(86.96,95.65)	(91.30,95.65)	(91.30,91.30)
QLIKE	Avg	0.661	0.604	0.557	0.549	0.607	0.619	0.586	0.646
	Med	0.643	0.602	0.551	0.556	0.602	0.612	0.589	0.644
RC		(0,4.35)	(4.35,17.39)	(95.65,95.65)	(100,100)	(0,8.70)	(8.70,26.09)	(21.74,30.44)	(21.74,39.13)
Normal Volatility Days									
MSE	Avg	10.552	11.637	9.632	8.462	13.874	9.015	10.758	15.372
	Med	6.269	7.457	5.592	5.116	8.326	6.821	6.917	8.336
RC		(91.30,100)	(52.17,82.61)	(56.52,69.57)	(82.61,91.30)	(60.87,86.96)	(56.52,73.91)	(39.13,60.87)	(26.09,34.78)
QLIKE	Avg	0.342	0.324	0.304	0.292	0.323	0.319	0.312	0.331
	Med	0.316	0.306	0.294	0.279	0.308	0.299	0.300	0.327
RC		(4.35,4.35)	(4.35,4.35)	(39.13,47.83)	(95.65,95.65)	(0,4.35)	(30.44,30.44)	(26.09,34.78)	(21.74,34.78)
High Volatility Days									
MSE	Avg	2127.649	2035.158	1966.077	1973.312	2037.025	2034.627	1995.393	2030.749
	Med	1307.010	1252.836	1232.057	1225.938	1257.860	1236.097	1226.840	1313.707
RC		(60.87,86.96)	(69.57,82.61)	(100,100)	(100,100)	(73.91,91.30)	(73.91,82.61)	(86.96,95.65)	(91.30,100)
QLIKE	Avg	3.514	3.110	2.810	2.841	3.139	3.303	3.037	3.451
	Med	3.486	3.058	2.731	2.778	3.038	3.305	2.923	3.339
RC		(26.09,34.78)	(39.13,52.17)	(100,100)	(100,100)	(39.13,52.17)	(39.13,56.52)	(47.83,56.52)	(43.48,82.61)

Notes: Following Equation (12), the modelling functions are $f_{AR}(RV_t)$, $f_{HAR}(RV_t, \overline{RV}_t^w, \overline{RV}_t^m)$, $f_{HAR-J}(RV_t, \overline{RV}_t^w, \overline{RV}_t^m, J_t)$, $f_{CHAR}(BPV_t, \overline{BPV}_t^w, \overline{BPV}_t^m)$, $f_{SHAR}(RV_t^+, RV_t^-, \overline{RV}_t^w, \overline{RV}_t^m)$, $f_{ARQ}(RV_t, RQ_t)$, $f_{HARQ}(RV_t, \overline{RV}_t^w, \overline{RV}_t^m, RQ_t)$, and $f_{HARQ-F}(RV_t, \overline{RV}_t^w, \overline{RV}_t^m, RQ_t, \overline{RQ}_t^w, \overline{RQ}_t^m)$, where RV_t is the realised variance, \overline{RV}_t^w is the average of RV_t for the last week, \overline{RV}_t^m is the average RV_t of the last month, J_t is the jump component, BPV_t , \overline{BPV}_t^w , and \overline{BPV}_t^m are the bipower variation, the average BPV_t of the last week, and the average BPV_t of the last month. RV_t^+ and RV_t^- denote the RV aggregated from positive and negative intraday returns. RQ_t , \overline{RQ}_t^w , and \overline{RQ}_t^m are the realised quarticity, the average RQ_t of the last week, and the average RQ_t of the last month. ^a The RC denotes the percentage of tickers for which we reject, at the 5% (or 10%) significance level, the null hypothesis that the specified model does not outperform the best-performing model within the HAR-family benchmark set, excluding the model under assessment.

A.6 Stability of News Volume During the Out-of-Sample Period

Figure A1 and Figure A2 provide complementary evidence on the evolution of news volume over the out-of-sample period. Figure A1 shows that the monthly word count of stock-related news is broadly stable across time for the majority of stocks, indicating a relatively constant level of stock-related media attention. To improve readability, only series that deviate from this common pattern are highlighted, revealing that a small number of highly visible stocks, such as MU, AMZN, AAPL, and MSFT, exhibit persistently higher word counts rather than short-lived spikes. Figure A2 similarly indicates that the aggregate volume of general hot news remains stable at the monthly frequency, suggesting no systematic expansion or contraction in overall news production during the evaluation window. Taken together, these figures imply that subsequent empirical results are unlikely to be mechanically driven by changes in the quantity of textual data, and instead reflect variation in the informational content or relevance of news.

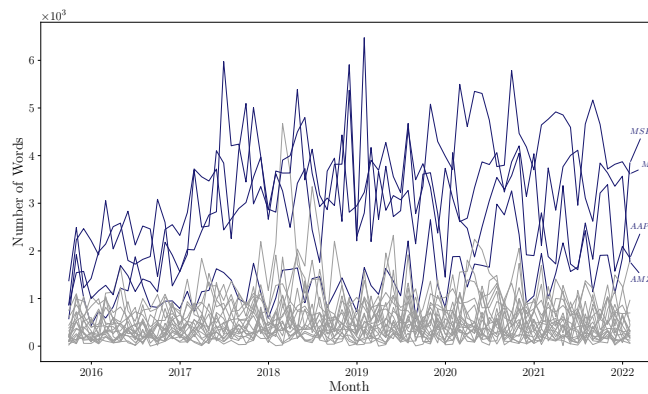


Figure A1: Stock-Related News Word Count During the Out-of-Sample Period

Notes: The figure presents the monthly word count of stock-related news stories during the out-of-sample period. To enhance clarity, we have used bold lines in a different colour and labelled only those lines that deviate from the general trend, as most stocks follow similar patterns.

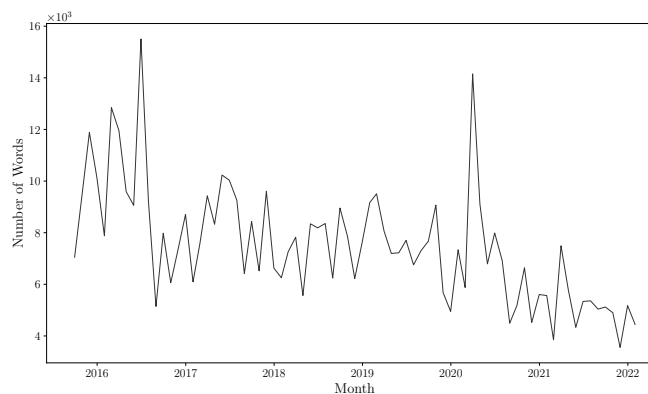


Figure A2: General Hot News Word Count During the Out-of-Sample Period

Notes: The figure presents the monthly word count of general hot news stories during the out-of-sample period.

A.7 Evolution of High Volatility Day Counts Over Time

Figure A3 presents the evolution of the monthly frequency of high volatility days across individual tickers during the out-of-sample period. The horizontal axis denotes calendar months, while the vertical axis reports the number of days classified as high volatility within each month for a given ticker. Individual tickers are displayed as black markers, allowing for a granular view of cross-sectional dispersion, whereas the solid line summarises the average monthly count across all assets. The shaded band surrounding this line represents one standard deviation, providing a measure of cross-ticker variability in high volatility occurrences over time.

The figure reveals pronounced temporal variation in the incidence of high volatility days, with clear spikes during periods of elevated market stress, most notably around the COVID-19 pandemic. Importantly, however, high volatility days are not exclusively concentrated in these extreme episodes. Instead, they occur throughout the sample, indicating that elevated volatility is a recurrent feature rather than a phenomenon confined to crisis periods. Additionally, the substantial month-to-month and cross-sectional dispersion underscores heterogeneity in volatility dynamics across assets, suggesting that both systematic shocks and idiosyncratic factors contribute to the observed distribution of high volatility days.

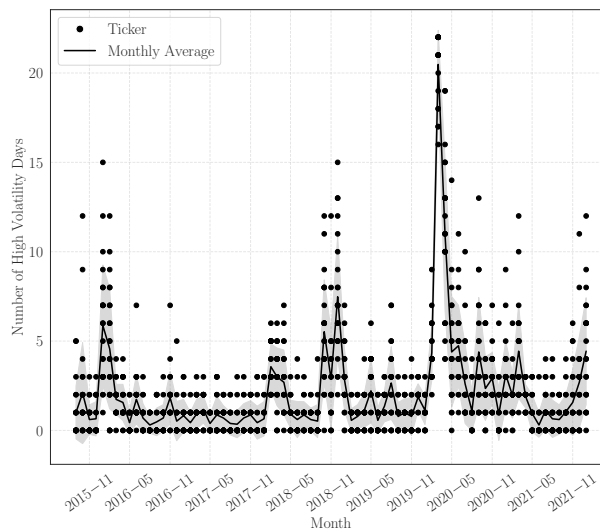


Figure A3: Number of High Volatility Days per Month over the Out-of-Sample Period

Notes: The x-axis represents the out-of-sample months, whereas the y-axis shows the count of days identified as high volatility days for each ticker in the respective month. Black-filled circles depict the tickers. The trend on a monthly average basis is represented by the line, and the areas shaded around this monthly average line signify the standard deviation.

A.8 NLP-based RV forecasting: Model Structure Details

Following [Kim \(2014\)](#), let $X_i \in \mathbb{R}^d$ be the d -dimensional token vector corresponding to the i^{th} token in the news headline, with $d = 300$. Daily (stock-related) news input sequence (concatenated headlines) with fewer than 500 tokens are padded with the placeholder token NONE to ensure a fixed input length.³¹

Let $X_{i:i+j}$ refer to the concatenation of token vectors $X_i, X_{i+1}, \dots, X_{i+j}$ as follows:

$$X_{i:i+j} = X_i \oplus X_{i+1} \oplus \dots \oplus X_{i+j}, \quad (\text{A3})$$

where \oplus denotes the concatenation operator. A convolution operation involves a filter $W \in \mathbb{R}^{hd}$, which is applied over a window of size h tokens to produce a new feature:

$$C_i = f(W \cdot X_{i:i+h-1} + b), \quad (\text{A4})$$

where $b \in \mathbb{R}$ is a bias term and $f(\cdot)$ is a nonlinear activation function. This filter is applied to each possible window of tokens $\{X_{1:h}, X_{2:h+1}, \dots, X_{n-h+1:n}\}$ to produce a feature map $C \in \mathbb{R}^{n-h+1}$:

$$C = \{C_1, C_2, \dots, C_{n-h+1}\}. \quad (\text{A5})$$

As the next step, global max-pooling is applied to the feature map:

$$\hat{C} = \max\{C_1, C_2, \dots, C_{n-h+1}\}, \quad (\text{A6})$$

which retains the most informative feature detected by the filter ([Collobert et al. 2011](#)). When multiple convolutional filters are employed, indexed by $k = 1, \dots, K$, the pooled outputs are stacked to form a fixed-length feature vector:

$$\mathbf{z}_t = \begin{bmatrix} \hat{C}^{(1)} & \hat{C}^{(2)} & \dots & \hat{C}^{(K)} \end{bmatrix}^\top \in \mathbb{R}^K. \quad (\text{A7})$$

The vector \mathbf{z}_t is passed to a FCNN. Let the FCNN consist of L hidden layers. For layer $\ell = 1, \dots, L$, the transformation is given by

$$\mathbf{h}^{(\ell)} = \text{ReLU}\left(W^{(\ell)}\mathbf{h}^{(\ell-1)} + \mathbf{b}^{(\ell)}\right), \quad (\text{A8})$$

where $\mathbf{h}^{(0)} = \mathbf{z}_t$, $W^{(\ell)}$ and $\mathbf{b}^{(\ell)}$ denote the weight matrix and bias vector of layer ℓ , and $\text{ReLU}(x) =$

³¹The padding value referenced here applies exclusively to stock-related news. For general hot news, a padding value of 2,000 is used. Additional details are provided in [Section 4.2](#).

$\max(0, x)$. The output layer maps the final hidden representation to a scalar forecast of next-day RV:

$$\widehat{RV}_{t+1} = \text{ReLU}(\mathbf{w}^\top \mathbf{h}^{(L)} + b), \quad (\text{A9})$$

where \mathbf{w} and b are the parameters of the output layer. The ReLU activation ensures non-negativity of the RV forecast. Model parameters are estimated by minimising the mean squared error (MSE) objective function:

$$\mathcal{L} = \frac{1}{T} \sum_{t=1}^T \left(RV_{t+1} - \widehat{RV}_{t+1} \right)^2, \quad (\text{A10})$$

where RV_{t+1} and \widehat{RV}_{t+1} denote the observed and forecasted RV, respectively. To prevent overfitting, L^2 regularisation is applied to the CNN and FCNN parameters:

$$\mathcal{L}_{\text{reg}} = \mathcal{L} + \lambda \sum_{\theta \in \Theta} \|\theta\|_2^2, \quad (\text{A11})$$

where Θ denotes the set of all trainable parameters of the NLP model. Optimisation is carried out using the Adam algorithm (Kingma & Ba 2014). All models are trained using a fixed random number generator (RNG) seed to ensure reproducibility.

A.9 LM Dictionary Results

A key question underlying this study is whether the additional complexity required to develop NLP models is justified for RV forecasting, or whether simpler dictionary-based sentiment measures already capture the relevant information in news. The LM dictionary in [Loughran & McDonald \(2011\)](#) provides a transparent and well-established benchmark that has been widely used to extract economically meaningful sentiment from financial text. Comparing NLP-based with LM-based signals therefore serves two important purposes. First, it allows us to assess whether the added modelling flexibility and computational cost of NLP models translate into incremental predictive gains. Second, it anchors our analysis to the existing literature by evaluating performance relative to a familiar and highly interpretable textual framework.

The LM dictionary categorises words into financially meaningful sentiment classes. In this study, we focus on the standard LM sentiments: ‘Negative’, ‘Positive’, ‘Uncertainty’, ‘Litigious’, and ‘Constraining’, as well as the modal sentiments ‘Modal Weak’, ‘Modal Moderate’, and ‘Modal Strong’, which capture the strength of commitment in forward-looking statements. ‘Negative’ and ‘Positive’ reflect unfavourable and favourable tone, respectively, while ‘Uncertainty’ captures ambiguity, imprecision, and lack of clarity regarding future outcomes. ‘Litigious’ words proxy for legal, judicial, and regulatory risk, and ‘Constraining’ words reflect language associated with limitations or restrictions on managerial actions and discretion. ‘Modal Weak’ and ‘Modal Moderate’ terms indicate low to intermediate levels of certainty and conditional or qualified intentions, whereas ‘Modal Strong’ terms signal a high degree of certainty or obligation. In addition to sentiment-based measures, we include a simple news volume proxy, denoted as ‘News Count’, defined as the daily number of stock-related news stories. This variable captures the intensity of information arrival independently of tone.

Sentiment scores are computed on a daily, stock-related basis using term frequency–inverse document frequency (tf–idf) weighting. For each stock and trading day, tf–idf–weighted counts of words belonging to a given LM sentiment are first computed at the news story level and then aggregated across all stock-related news items published during that day by simple averaging. The resulting daily sentiment measure, denoted by $S_{i,t}$, summarises the overall tone of stock-related news within the daily information set. The sentiment measures are constructed over a one-day horizon, with the start and end times exactly matching the news aggregation window described in [Section 4.2](#). As a result, the information content and temporal coverage of the LM-based sentiment variables are fully aligned with those of the NLP-derived signals. These sentiment variables are incorporated into the forecasting framework by extending the baseline CHAR model, which is identified as the best-performing speci-

fication in [Section 5](#). Building on the general HAR-family specification in [Equation \(12\)](#), the CHAR model augmented with dictionary-based sentiment is given by

$$RV_{i,t+1} = \beta_0 + \beta_1 BPV_{i,t} + \beta_2 BPV_{i,t}^w + \beta_3 BPV_{i,t}^m + \gamma S_{i,t} + \varepsilon_{i,t+1}, \quad (\text{A12})$$

where $RV_{i,t+1}$ denotes next-day RV, $BPV_{i,t}$ is daily bipower variation, and $BPV_{i,t}^w$ and $BPV_{i,t}^m$ are the corresponding weekly and monthly averages, respectively. The coefficient γ captures the incremental predictive content of LM-based sentiment for RV. Each sentiment is added individually, yielding a parsimonious extended CHAR specification that mirrors the structure used for the NLP models and facilitates a clean comparison across textual approaches. This specification is comparable to the results reported in [Section 5.2](#), specifically in [Table 8](#), which combine NLP models with the CHAR benchmark, thereby jointly exploiting both information sources for RV forecasting.

[Table A7](#) shows that dictionary-based signals yield, at best, modest gains relative to the CHAR benchmark. Over the full out-of-sample period, most dictionary sentiments produce loss ratios that are effectively at parity, with the best-performing entries remaining very close to one. This pattern indicates that any improvements delivered by dictionary-based sentiment measures are small in magnitude. The RC results are more promising, as they are generally high, typically ranging from about 83–100% depending on the sentiment measure and significance level. By contrast, the simple stock-related ‘News Count’ proxy stands out clearly. It reduces the full out-of-sample MSE ratio to 0.985 and the QLIKE ratio to 0.947, and it achieves 100% RC at both the 5% and 10% levels in the full out-of-sample MSE comparison and above 91% for QLIKE loss function. These results point to a broad-based and statistically robust improvement relative to the CHAR benchmark, highlighting the importance of information intensity rather than tone alone. Consequently, ‘News Count’ provides the best-performing baseline against which the incremental predictive value of more sophisticated textual representations can be assessed.

Comparing the dictionary-based results in [Table A7](#) with the stock-related ensemble forecasting performance in [Table 8](#) shows whether greater language level complexity delivers improved forecasting performance. In [Table A7](#), most LM sentiments are essentially indistinguishable from the CHAR benchmark in terms of loss ratios, whereas the simple information-intensity proxy ‘News Count’ yields the only meaningful full out-of-sample improvement (average MSE ratio 0.985; average QLIKE ratio 0.947) and attains uniformly strong RC performance. Against this stronger baseline, the ensemble model in [Table 8](#) delivers additional gains: for example, the FinText Word2Vec (skip-gram) ensemble achieves an average MSE ratio of 0.961 and an average QLIKE ratio of 0.937, with RC rates that

Table A7: Dictionary-Based Out-of-Sample Forecasting Performance

Full Out-of-Sample Period	p-value		Negative	Positive	Uncertainty	Litigious	Modal _{weak}	Modal _{moderate}	Modal _{strong}	Constraining	News Count
MSE ^a		Avg	1.001	1.000	1.000	1.001	1.001	1.000	1.000	1.000	0.985
		Med	1.001	1.000	1.000	1.000	1.000	1.000	1.000	1.000	0.992
RC ^c	5%		95.65	95.65	95.65	82.61	91.30	95.65	91.30	86.96	100
	10%		100	100	100	95.65	100	95.65	100	86.96	100
QLIKE ^b		Avg	0.999	1.000	1.004	1.003	0.998	1.001	1.008	1.006	0.947
		Med	1.003	1.001	1.000	1.002	1.001	1.001	1.001	1.001	0.941
RC	5%		91.30	91.30	100	91.30	95.65	95.65	86.96	91.30	91.30
	10%		95.65	91.30	100	95.65	100	95.65	95.65	91.30	95.65
Normal Volatility Days											
MSE		Avg	1.019	1.005	1.040	1.015	1.031	1.010	1.011	1.010	1.340
		Med	0.997	1.005	1.012	1.006	1.011	1.006	1.005	1.003	1.123
RC	5%		73.91	65.22	47.83	47.83	47.83	52.17	52.17	73.91	43.48
	10%		73.91	73.91	47.83	60.87	56.52	56.52	60.87	82.61	43.48
QLIKE		Avg	0.997	1.002	1.007	1.003	1.006	1.004	1.004	1.005	0.992
		Med	0.995	1.001	1.001	1.002	1.003	1.003	1.002	1.003	0.988
RC	5%		78.26	78.26	73.91	69.57	69.57	82.61	69.57	78.26	73.91
	10%		78.26	82.61	82.61	69.57	73.91	82.61	82.61	82.61	73.91
High Volatility Days											
MSE		Avg	1.000	1.000	0.999	1.000	0.999	1.000	1.000	1.000	0.970
		Med	1.001	1.000	1.000	1.000	1.000	1.000	1.000	1.000	0.986
RC	5%		91.30	100	95.65	86.96	95.65	91.30	86.96	100	100
	10%		91.30	100	95.65	91.30	95.65	91.30	91.30	100	100
QLIKE		Avg	1.003	0.998	1.005	1.003	0.992	0.997	1.012	1.007	0.903
		Med	1.007	1.001	1.000	1.001	0.988	1.000	1.001	0.998	0.911
RC	5%		78.26	95.65	100	91.30	91.30	91.30	91.30	100	100
	10%		82.61	100	100	95.65	100	100	100	100	100

Notes: ^a The ratio of the average (or median) MSE of the specified model to that of the CHAR model, averaged across 23 tickers. ^b The ratio of the average (or median) QLIKE of the specified model to that of the CHAR model, averaged across 23 tickers. ^c The RC denotes the percentage of tickers for which we reject, at the 5% (or 10%) significance level, the null hypothesis that the specified model does not outperform the best-performing model within the HAR-family benchmark set.

Table A8: Realised Utility of Dictionary-Based Models

Category	Realised Utility
Negative	2.7524
Positive	2.7532
Uncertainty	2.7485
Litigious	2.7492
Modal _{weak}	2.7592
Modal _{moderate}	2.7531
Modal _{strong}	2.7406
Constraining	2.7437
News Count	2.8367

Notes: This table reports realised utility values from the utility-based approach in [Section 5.3](#) for dictionary-based RV forecasting models. In [Equation \(20\)](#), the maximum attainable realised utility is 4%. All values are expressed in percentage terms.

are near-universal under MSE and remain high under QLIKE. Since these improvements exceed those achieved by ‘News Count’, they indicate that the ensemble is not merely proxying for variation in the volume of stock-related news, but is extracting incremental predictive content from the linguistic structure of news that complements the RV dynamics.

The utility-based results in [Table A8](#) reinforce and sharpen the conclusions drawn from the statistical forecasting evidence.³² With the exception of ‘News Count’, all LM sentiments deliver realised utilities tightly clustered around the CHAR benchmark of 2.7540%, ranging from 2.7406% to 2.7592%. These magnitudes indicate that sentiment-based dictionary signals, while occasionally marginally improving or matching CHAR in loss-based metrics, do not translate into economically meaningful gains once evaluated through the lens of investor utility. This finding is fully consistent with the loss ratios in [Table A7](#). By contrast, ‘News Count’ stands out economically, achieving a realised utility of 2.8367%, which exceeds CHAR by 0.0827%. However, when compared with the ensemble results reported in the right panel of [Table 10](#), even this specification falls short of the realised utilities achieved by ensemble models based on stock-related news; for example, the Word2Vec (skip-gram) ensemble attains a realised utility of 2.9321%. Taken together, the utility-based evidence confirms that while simple dictionary measures largely fail to improve economic gain beyond CHAR, both news volume and, more strongly, NLP-based ensemble models deliver economically meaningful gains, highlighting the incremental value of richer textual representations over sentiments.

Moving to XAI in [Section 5.4](#) and extending it to the LM dictionary, [Figure A4](#) shows the Shapley values for the three most frequent negative words in the LM dictionary, namely *loss*, *termination*, and *against*, displayed in the top, middle, and bottom rows, respectively.³³ Each selected word is also

³²Details of the economic gain approach are provided in [Section 5.3](#).

³³Negative sentiment is selected from the LM dictionary as it encompasses the largest number of terms compared to

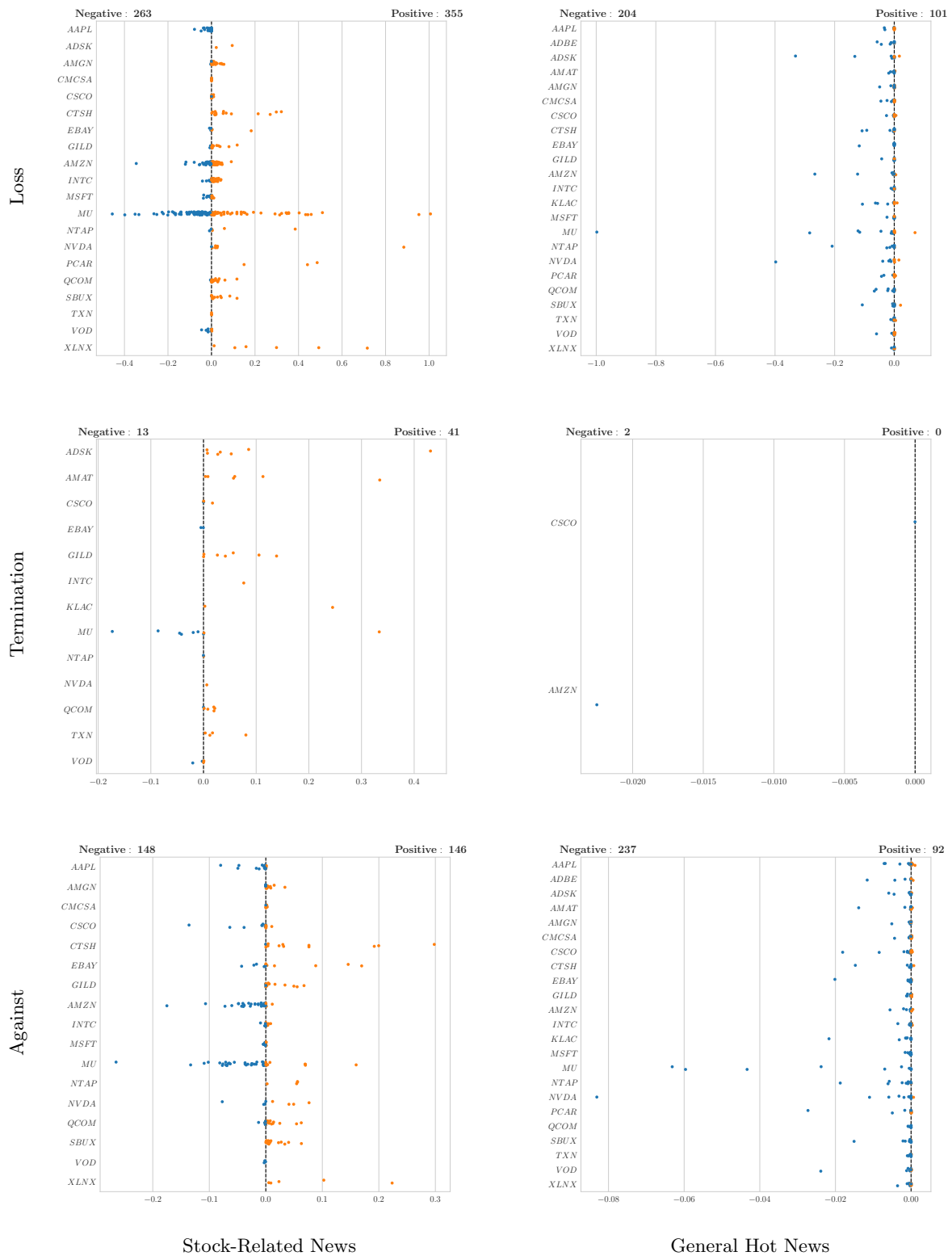


Figure A4: Shapley Values for Top Negative LM Words

Notes: Rows represent the most frequently occurring negative words in the LM dictionary. The left (right) column shows the Shapley values for stock-related (general hot) news published during the out-of-sample period. The x-axis displays the Shapley values, while the y-axis represents the ticker names. The vertical line indicates no impact on the RV forecast, with the left (right) side indicating a negative (positive) impact of the specified group of words. The total number of negative and positive Shapley values is displayed at the top of each figure.

grouped with its variations from the LM dictionary; thus, $\{loss, losses\}$, $\{termination, terminate, terminates, terminated\}$, and $\{against\}$ represent *loss*, *termination*, and *against* words, respectively. The Shapley values for these words in each group are displayed individually in [Figure A4](#). The left (right) column shows the Shapley values for stock-related (general hot) news. A dot on the vertical zero line indicates cases where the word has no impact on the RV forecast. The left (right) side represents the negative (positive) impact of the specified word group, where a larger positive (negative) value indicates a larger increase (decrease) in the RV forecast. The y-axis displays the ticker name; if a ticker is absent from the y-axis, it implies that the specified word group either did not appear in the news stories or SHAP method did not identify words from that group as contributors to RV forecasting for that ticker. The total number of negative and positive Shapley values is indicated at the top of each figure.

[Figure A4](#) reveals important properties about using textual information to forecast RV based on a fixed LM dictionary approach versus our NLP model. First, the LM dictionary approach counts occurrences of negative words such as *loss*, *termination*, and *against*, including their variations. The higher the word counts, the stronger the impact on RV. In contrast, [Figure A4](#) shows a wide variety of relationships of these top word groups on RV forecast. For example, the ‘Loss’ group in stock-related news increases RV in 355 appearances and decreases RV in 263 appearances (see top left subfigure). Similar patterns are observed for the other two top word groups in stock-related news and also in general hot news. Additionally, substantial variations exist across stocks. In the same subfigure, ‘Loss’ group has a negative impact on the RV of the AAPL ticker but a predominantly positive impact on the RV of the CTSB ticker. As previously noted, some of these words did not appear at all in news stories for certain stocks, or when they did, they had no discernible impact on the RV forecasts. This shows how the NLP model is able to capture more nuances in news, which ultimately translate into better statistical and economic performance compared with dictionary-based sentiments.

other sentiments. This dictionary is primarily designed for analysing financial reports, which typically convey a positive tone. Consequently, the negative sentiment category is more extensive, with a broader range of terms, to capture the nuances necessary for effective financial report analysis.

A.10 Nonlinear modelling of HAR-Family Predictors

An important benchmarking consideration is whether the gains obtained by adding news to RV forecasting models reflect the incremental informational content of news, or whether similar improvements could be achieved through a more flexible specification of the benchmark models themselves. The HAR-family of models in Equation (12) is typically estimated under linear functional forms, despite the possibility that RV dynamics exhibit nonlinear interactions across horizons. If a nonlinear reformulation of the HAR framework were able to deliver forecasting performance comparable to, or exceeding, that of the proposed NLP models, the incremental contribution of news would be less clearly identified. This consideration motivates a direct assessment of how forecasting performance changes when the HAR-family specification is extended from a linear to a nonlinear form, while holding the information set fixed.

To address this concern, the linear HAR-family of models is generalised by allowing for a nonlinear functional form while preserving the same information set:

$$RV_{t+1} = f_{\text{FCNN}}\left(RV_t, \overline{RV}_t^w, \overline{RV}_t^m, J_t, BPV_t, \overline{BPV}_t^w, \overline{BPV}_t^m, \right. \\ \left. RV_t^+, RV_t^-, RQ_t, \overline{RQ}_t^w, \overline{RQ}_t^m\right), \quad (\text{A13})$$

where all variables are defined in Section 4.1. The function $f_{\text{FCNN}}(\cdot)$ is implemented as a simple FCNN. An important advantage of this specification is that it accommodates, within a single unified framework, all predictors introduced across the HAR, SHAR, HAR-J, CHAR, ARQ, HARQ, and HARQ-F models, while allowing for nonlinear interactions among them. As a result, this specification provides a stringent benchmark for assessing whether nonlinear transformations of the full HAR-family information set can account for the forecasting gains. The nonlinear model is trained using the same forecasting design as the linear HAR benchmarks in Section 5. In particular, training is conducted using a daily rolling-window with identical in-sample and out-of-sample periods and the same forecasting horizon, ensuring full comparability across models. To assess the role of model complexity, the FCNN is trained using different numbers of hidden units, specifically 5, 10, 15, 20, and 25. This allows for a systematic evaluation of how increasing nonlinear flexibility affects forecasting performance. Given 23 stocks, 1,604 out-of-sample trading days, and five model complexities, a total of 184,460 FCNN models are trained and evaluated under this specification.

The results in Table A9 indicate that introducing nonlinearity into the HAR-family framework does not lead to an overall improvement in forecasting performance over the full out-of-sample period.

Across both loss functions, the nonlinear HAR specification exhibits systematically higher loss ratios relative to the CHAR benchmark, together with generally weak RC results. For example, under MSE, the average loss ratios over the full out-of-sample period range between 1.200 and 1.219 across different network sizes, while the corresponding QLIKE ratios range from 4.474 to 7.402. Consistent with these results, RC values remain low, particularly under QLIKE. These findings indicate that greater model flexibility alone does not translate into superior average forecasting performance when evaluated across the full out-of-sample period. A more granular decomposition by volatility regime, however, reveals a pronounced state dependence. During normal volatility days, the nonlinear HAR model delivers clear improvements relative to the linear HAR-family benchmarks. Under MSE, average loss ratios fall well below unity and decline monotonically with model complexity, reaching values as low as 0.689 for the largest specification, with RC statistics exceeding 90% for most configurations. Nevertheless, under QLIKE, with average ratios ranging from 2.873 to 5.184 and slightly higher RC values compared to the full out-of-sample results, the deterioration in performance is evident. In contrast, performance deteriorates substantially during high volatility days. In this regime, loss ratios exceed unity across all specifications, with MSE ratios averaging 1.226 and QLIKE ratios averaging 7.7838 across different model complexities, accompanied by uniformly weak RC statistics. These large forecast errors during high volatility days dominate the aggregate evaluation and account for the observed deterioration in full out-of-sample period. Overall, the results suggest that while nonlinear transformations of the HAR-family predictors are informative in normal market conditions, they lack robustness in periods of elevated volatility, limiting their effectiveness as standalone alternatives to the HAR-family of models.

Although nonlinear transformations of HAR-type regressors can deliver incremental forecasting gains relative to linear specifications, particularly during normal volatility days, their overall performance remains systematically inferior to that of the standalone NLP models. This underperformance is especially pronounced when compared with ensemble forecasts that combine news-based signals with volatility-history benchmarks over the full out-of-sample period. A comparison with the NLP models reported in [Table 6](#) indicates that, while both the nonlinear HAR models and the NLP models exhibit some degradation in performance over the full out-of-sample window, the magnitude of underperformance is substantially larger for the nonlinear models. This result holds consistently across MSE and QLIKE loss ratios, as well as RC metrics. Furthermore, comparing these nonlinear specifications with the ensemble model results in [Table 8](#) reveals a clear advantage of the ensemble approach. In the vast majority of cases, ensemble forecasts deliver unambiguous improvements over the full out-of-sample period, accompanied by materially higher RC values relative to the nonlinear models.

[Table A10](#) reports the realised utility associated with the nonlinear HAR model variants evaluated

in the out-of-sample period, using the utility-based approach described in [Section 5.3](#). The results show that all nonlinear HAR specifications deliver negative realised utility, indicating a deterioration in economic performance. This stands in contrast to the positive and high realised utility gains documented in [Table 10](#) for the NLP models and, in particular, for the ensemble models. From a theoretical perspective, realised utility measures the ex post welfare gain from using a given volatility forecast in an optimal decision rule relative to a benchmark. A negative realised utility therefore implies that forecast errors are not only larger on average but are also systematically misaligned with the investor’s loss function, leading to inferior volatility-timing decisions. The observed results here suggest that the additional nonlinear structure does not enhance the decision-relevant content of volatility forecasts and instead amplifies estimation noise and overfitting, such that increased model flexibility fails to translate into economic gain, which, from the results in [Table A9](#), stems from the underperformance of the models during high volatility days.

Overall, the results show that introducing nonlinear transformations within the HAR-family framework does not replicate the forecasting or economic gains obtained by incorporating news through the NLP models. While nonlinear HAR specifications show improvements in forecasting performance during normal volatility days, their lack of robustness in high volatility days leads to inferior full out-of-sample forecasting performance and worse realised utility. This indicates that increased functional flexibility applied solely to volatility-history variables is insufficient to generate economic value. In contrast, the high realised utility achieved by the NLP and ensemble models reflects genuinely incremental information contained in news. Moreover, these results support research that questions the robustness of ML models for RV forecasting when they rely on broadly the same set of volatility-based predictors, suggesting limited gains in the absence of genuinely new information ([Hillebrand & Medeiros 2010](#), [Aldrino & Knaus 2016](#), [Branco et al. 2024](#), [Aldrino & Chassot 2025](#))

Table A9: FCNN Out-of-Sample Forecasting Performance

		Full Out-of-Sample Period					Normal Volatility Days					High Volatility Days				
		5	10	15	20	25	5	10	15	20	25	5	10	15	20	25
MSE ^a	Avg	1.215	1.214	1.219	1.211	1.200	0.972	0.853	0.824	0.783	0.689	1.224	1.228	1.233	1.226	1.219
	Med	1.191	1.188	1.197	1.177	1.165	0.919	0.755	0.776	0.702	0.662	1.212	1.211	1.206	1.207	1.188
RC ^c	0.05	26.09	13.04	21.74	26.09	30.44	78.26	91.30	91.30	95.65	100	17.39	13.04	4.35	8.70	8.70
	0.10	60.87	60.87	56.52	60.87	65.22	78.26	91.30	95.65	95.65	100	52.17	43.48	34.78	34.78	39.13
QLIKE ^b	Avg	5.221	6.152	7.402	5.141	4.474	3.255	4.271	5.184	3.091	2.873	7.376	8.302	9.870	7.225	6.146
	Med	5.017	5.352	6.554	4.320	4.433	3.008	3.492	3.776	2.106	2.571	6.267	7.172	10.009	6.506	5.645
RC	0.05	0.00	0.00	0.00	0.00	0.00	8.70	4.35	4.35	8.70	21.74	0.00	0.00	0.00	0.00	0.00
	0.10	4.35	0.00	4.35	8.70	0.00	8.70	4.35	4.35	8.70	21.74	8.70	0.00	4.35	4.35	0.00

Notes: Columns report FCNN specifications with increasing numbers of hidden units (5–25), with larger values indicating greater model complexity.

^a The ratio of the average (or median) MSE of the specified model to that of the CHAR model, averaged across 23 tickers. ^b The ratio of the average (or median) QLIKE of the specified model to that of the CHAR model, averaged across 23 tickers. ^c The RC denotes the percentage of tickers for which we reject, at the 5% (or 10%) significance level, the null hypothesis that the specified model does not outperform the best-performing model within the HAR-family benchmark set.

Table A10: Realised Utility of Nonlinear HAR Models

Complexity	Realised Utility
5	-4.4668
10	-6.1599
15	-8.5773
20	-4.6595
25	-3.3510

Notes: This table reports realised utility values from the utility-based approach in [Section 5.3](#) for nonlinear HAR forecasting models. Complexity column lists the number of units in FCNN, including 5, 10, 15, 20, and 25, with larger values indicating greater model complexity. In [Equation \(20\)](#), the maximum attainable realised utility is 4%. All values are expressed in percentage terms.

A.11 Hyperparameter Effects on NLP Model Forecasts

[Table A11](#) examines the sensitivity of the NLP models to the length of the input window used to aggregate stock-related news. Specifically, this table reports out-of-sample forecasting performance when headlines from the preceding one, three, five, and seven days are incorporated as model inputs, evaluated over the full sample as well as across normal and high volatility days. The purpose of this exercise is twofold. First, it assesses whether extending the information set beyond the previous day improves forecasting performance, thereby testing the temporal persistence of news effects on RV. Second, by increasing the input window, the analysis reduces the incidence of days without news coverage, thereby providing an indirect evaluation of the trainable word embedding block presented in [Figure 3](#). We select the Word2Vec (skip-gram) specification from FinText, which performs among the best models in [Section 5.1](#), for this analysis. The 1-Day specification is equivalent to the results reported in [Table 6](#).

The results indicate that extending the input window increases loss ratios relative to the CHAR benchmark, specially for MSE, even though RC statistics remain high. Over the full out-of-sample period, the average MSE ratio rises from 1.106–1.108 (1-Day) to 1.164–1.165 (7-Days). However, the average QLIKE ratio decreases from 1.566–1.640 to 1.508–1.518. At the same time, RC values are generally strongest for the 1-Day specification (e.g., MSE RC reaches 82.61% at 5% and 100% at 10%), while QLIKE RC remains low (21.74% at 5% across all windows). Across regimes, normal volatility days generally show improved performance when longer input windows are used, particularly in terms of MSE. However, this comes at the cost of generally lower forecasting performance during high volatility days. The RC values generally reinforce these findings. Overall, the results imply that volatility-relevant news is largely short-lived: incorporating older headlines tends to dilute the timely signal that is most relevant for forecasting RV, particularly during high volatility days. This result accords with established evidence on volatility dynamics, indicating that volatility responds predominantly to recent information and short-horizon components, with the marginal predictive contribution of older or longer-horizon components declining over time ([Andersen et al. 2003](#), [Corsi 2009](#)).

[Table A12](#) focuses on the role of model architecture by evaluating the impact of alternative convolutional filter sizes on forecasting performance when stock-related news is used. The table contrasts results obtained from three distinct sets of filters, corresponding to shorter and longer n-gram representations of textual information, again reported for the full out-of-sample period and conditional on volatility regimes. The motivation for this analysis is to investigate whether allowing the model to

capture longer linguistic patterns enhances its ability to extract volatility-relevant information from news. By holding the remaining components of the model fixed and varying only the filter sizes, this table isolates the effect of textual granularity on RV forecasting performance. Similar to the previous analysis, we select the Word2Vec (skip-gram) specification from FinText, which performs among the best models in [Section 5.1](#). Additionally, the $\{1, 2, 3\}$ filter sizes are equivalent to the results reported in [Table 6](#).

The results indicate that increasing textual granularity beyond short n-grams does not lead to material improvements in RV forecasting performance. Over the full out-of-sample period, loss ratios are generally lower under the baseline filter set $\{1, 2, 3\}$ for MSE but not for QLIKE, relative to extending the filters to $\{4, 5, 6\}$ or $\{7, 8, 9\}$; in contrast, RC statistics relative to the HAR-family benchmarks tend to be similar or to increase slightly with longer filter sizes. This divergence is more pronounced across volatility regimes. During normal volatility days, longer filters yield lower MSE and QLIKE ratios. However, RC values for QLIKE remain close to zero, and no material change is evident for MSE. During high volatility days, MSE ratios but not QLIKE generally increase as filter sizes lengthen, despite slight improvements in RC. Overall, the evidence is mixed, with changes in performance across normal and high volatility days largely offsetting each other; consequently, the results generally favour retaining shorter filters.

While these robustness checks suggest that the baseline, out-of-the-box NLP architecture is not highly sensitive to changes in the input window or filter configuration, they also indicate that RV forecasting performance could, in principle, be improved through a more extensive hyperparameter search. Such optimisation would require substantially greater computational resources and careful experimentation (e.g., tuning window construction, filter sets, regularisation, and learning dynamics), which is beyond the scope of this study. Moreover, moving toward heavily tuned architectures would depart from the deliberately simple and transparent modelling philosophy that underpins the HAR-family of models.

Table A11: Out-of-Sample RV Forecasting Performance: Stock-Related News with Varying Input Windows

Full Out-of-Sample Period	p-value		1-Day				3-Days				5-Days				7-Days			
			25	50	75	100	25	50	75	100	25	50	75	100	25	50	75	100
MSE ^a		Avg	1.106	1.108	1.108	1.107	1.154	1.153	1.153	1.153	1.159	1.159	1.159	1.159	1.164	1.165	1.164	1.164
		Med	1.101	1.092	1.096	1.093	1.122	1.125	1.123	1.123	1.124	1.127	1.125	1.124	1.124	1.127	1.125	1.125
RC ^c	0.05		82.61	82.61	82.61	82.61	73.91	73.91	73.91	73.91	69.57	65.22	65.22	65.22	65.22	65.22	65.22	65.22
	0.10		100	100	100	100	100	100	100	100	95.65	95.65	95.65	95.65	95.65	91.30	95.65	91.30
QLIKE ^b		Avg	1.566	1.640	1.571	1.571	1.503	1.504	1.497	1.494	1.510	1.508	1.500	1.498	1.516	1.518	1.511	1.508
		Med	1.570	1.579	1.563	1.567	1.440	1.441	1.430	1.439	1.453	1.449	1.438	1.453	1.475	1.473	1.460	1.464
RC	0.05		21.74	21.74	21.74	21.74	17.39	17.39	17.39	17.39	13.04	17.39	17.39	17.39	8.70	8.70	8.70	13.04
	0.10		39.13	34.78	39.13	30.44	21.74	21.74	21.74	21.74	21.74	21.74	21.74	21.74	21.74	21.74	21.74	21.74
Normal Volatility Days																		
MSE		Avg	1.683	1.703	1.702	1.690	1.108	1.176	1.178	1.200	1.106	1.173	1.169	1.192	1.090	1.151	1.147	1.164
		Med	1.101	1.092	1.096	1.093	1.053	1.142	1.138	1.176	1.057	1.122	1.115	1.145	1.072	1.130	1.124	1.119
RC	0.05		69.57	65.22	65.22	65.22	65.22	56.52	56.52	47.83	65.22	56.52	56.52	47.83	65.22	56.52	52.17	52.17
	0.10		69.57	69.57	73.91	69.57	73.91	60.87	56.52	56.52	69.57	56.52	56.52	56.52	69.57	65.22	65.22	60.87
QLIKE		Avg	1.345	1.370	1.363	1.354	1.299	1.321	1.322	1.331	1.299	1.320	1.321	1.331	1.299	1.320	1.321	1.330
		Med	1.570	1.579	1.563	1.567	1.285	1.302	1.317	1.329	1.317	1.337	1.346	1.353	1.330	1.354	1.350	1.355
RC	0.05		4.35	4.35	4.35	4.35	4.35	4.35	4.35	4.35	4.35	4.35	4.35	4.35	4.35	4.35	4.35	4.35
	0.10		4.35	4.35	4.35	4.35	4.35	4.35	4.35	4.35	4.35	4.35	4.35	4.35	4.35	4.35	4.35	4.35
High Volatility Days																		
MSE		Avg	1.081	1.082	1.082	1.082	1.155	1.151	1.151	1.150	1.160	1.158	1.158	1.157	1.166	1.164	1.164	1.163
		Med	1.095	1.094	1.096	1.093	1.129	1.130	1.128	1.129	1.130	1.132	1.130	1.130	1.129	1.132	1.130	1.130
RC	0.05		65.22	69.57	69.57	69.57	65.22	65.22	65.22	65.22	65.22	65.22	65.22	65.22	60.87	65.22	65.22	65.22
	0.10		95.65	95.65	95.65	95.65	91.30	91.30	91.30	91.30	91.30	91.30	91.30	91.30	91.30	91.30	91.30	91.30
QLIKE		Avg	1.804	1.960	1.794	1.812	1.705	1.685	1.671	1.656	1.720	1.697	1.681	1.668	1.735	1.720	1.705	1.690
		Med	1.749	1.771	1.788	1.784	1.646	1.664	1.670	1.665	1.642	1.649	1.634	1.626	1.661	1.655	1.658	1.645
RC	0.05		43.48	43.48	43.48	43.48	43.48	43.48	43.48	34.78	39.13	43.48	43.48	30.44	30.44	30.44	30.44	
	0.10		60.87	69.57	65.22	65.22	60.87	65.22	65.22	65.22	56.52	69.57	65.22	65.22	47.83	56.52	56.52	52.17

Notes: Using the FinText with Word2Vec (skip-gram) specification, identified as one of the best-performing models in Section 5.1, the ‘1-Day,’ ‘3-Days,’ ‘5-Days,’ and ‘7-Days’ columns incorporate stock-related news from the preceding one, three, five, and seven days, respectively, as model inputs. The ‘1-Day’ specification corresponds to the results reported in Table 6.

^a The ratio of the average (or median) MSE of the specified model to that of the CHAR model, averaged across 23 tickers. ^b The ratio of the average (or median) QLIKE of the specified model to that of the CHAR model, averaged across 23 tickers. ^c The RC denotes the percentage of tickers for which we reject, at the 5% (or 10%) significance level, the null hypothesis that the specified model does not outperform the best-performing model within the HAR-family benchmark set.

Table A12: Out-of-Sample RV Forecasting Performance: Stock-Related News with Varying Filter Sizes

Full Out-of-Sample Period	p-value		{1, 2, 3}				{4, 5, 6}				{7, 8, 9}			
			25	50	75	100	25	50	75	100	25	50	75	100
MSE ^a		Avg	1.106	1.108	1.108	1.107	1.131	1.128	1.128	1.129	1.125	1.125	1.124	1.125
		Med	1.101	1.092	1.096	1.093	1.112	1.112	1.111	1.112	1.106	1.108	1.109	1.109
RC ^c	0.05		82.61	82.61	82.61	82.61	86.96	86.96	86.96	86.96	86.96	86.96	86.96	86.96
	0.10		100	100	100	100	100	100	100	100	100	100	100	100
QLIKE ^b		Avg	1.566	1.640	1.571	1.571	1.478	1.478	1.470	1.472	1.486	1.487	1.481	1.478
		Med	1.570	1.579	1.563	1.567	1.424	1.432	1.427	1.426	1.435	1.453	1.451	1.432
RC	0.05		21.74	21.74	21.74	21.74	21.74	21.74	21.74	21.74	17.39	17.39	21.74	
	0.10		39.13	34.78	39.13	30.44	43.48	43.48	43.48	43.48	43.48	43.48	43.48	
Normal Volatility Days														
MSE		Avg	1.683	1.703	1.702	1.690	1.140	1.188	1.178	1.192	1.172	1.221	1.211	1.226
		Med	1.101	1.092	1.096	1.093	1.107	1.133	1.133	1.148	1.118	1.155	1.142	1.178
RC	0.05		69.57	65.22	65.22	65.22	65.22	60.87	60.87	60.87	65.22	60.87	65.22	56.52
	0.10		69.57	69.57	73.91	69.57	73.91	60.87	65.22	60.87	65.22	65.22	65.22	65.22
QLIKE		Avg	1.345	1.370	1.363	1.354	1.283	1.297	1.295	1.301	1.278	1.293	1.291	1.298
		Med	1.570	1.579	1.563	1.567	1.266	1.285	1.287	1.296	1.259	1.275	1.283	1.290
RC	0.05		4.35	4.35	4.35	4.35	4.35	4.35	4.35	8.70	4.35	4.35	4.35	
	0.10		4.35	4.35	4.35	4.35	4.35	4.35	4.35	8.70	4.35	4.35	4.35	
High Volatility Days														
MSE		Avg	1.081	1.082	1.082	1.082	1.128	1.124	1.124	1.124	1.120	1.119	1.118	1.119
		Med	1.095	1.094	1.096	1.093	1.133	1.131	1.130	1.127	1.126	1.124	1.117	1.124
RC	0.05		65.22	69.57	69.57	69.57	73.91	78.26	78.26	78.26	82.61	82.61	82.61	78.26
	0.10		95.65	95.65	95.65	95.65	95.65	95.65	95.65	95.65	95.65	95.65	95.65	95.65
QLIKE		Avg	1.804	1.960	1.794	1.812	1.673	1.659	1.645	1.643	1.696	1.683	1.672	1.658
		Med	1.749	1.771	1.788	1.784	1.700	1.694	1.652	1.648	1.706	1.708	1.686	1.644
RC	0.05		43.48	43.48	43.48	43.48	43.48	39.13	47.83	43.48	43.48	43.48	43.48	
	0.10		60.87	69.57	65.22	65.22	73.91	73.91	73.91	73.91	73.91	73.91	73.91	

Notes: Using the FinText with Word2Vec (skip-gram) specification, identified as one of the best-performing models in Section 5.1, the sets {1, 2, 3}, {4, 5, 6}, and {7, 8, 9} correspond to different filter sizes discussed in Section 4.2. The {1, 2, 3} group aligns with the results presented in Table 6.

^a The ratio of the average (or median) MSE of the specified model to that of the CHAR model, averaged across 23 tickers. ^b The ratio of the average (or median) QLIKE of the specified model to that of the CHAR model, averaged across 23 tickers. ^c The RC denotes the percentage of tickers for which we reject, at the 5% (or 10%) significance level, the null hypothesis that the specified model does not outperform the best-performing model within the HAR-family benchmark set.

A.12 DeepLIFT (Deep Learning Important FeaTures)

DeepLIFT (Shrikumar et al. 2017) explains a prediction by comparing the model output at the observed input to the output at a reference (baseline) input, and then attributing the difference to the inputs via additive contribution scores. In our setting, we apply DeepLIFT to the FCNN and attribute changes in the RV forecast to changes in the FCNN inputs z_t , where each component of z_t is a pooled convolutional activation and hence corresponds to an n -gram detector. The FCNN produces a nonnegative RV forecast through a final ReLU:

$$\widehat{RV}_{t+1} = \text{ReLU}(u_{t+1}), \quad u_{t+1} = w^\top h^{(L)} + b. \quad (\text{A14})$$

Following Shrikumar et al. (2017), we take the DeepLIFT target to be the pre-activation $t := u_{t+1}$, and interpret attributions as explaining how inputs shift u_{t+1} , which then maps into \widehat{RV}_{t+1} via the ReLU. Given a reference input producing (z_t^0, t^0) , define differences from the reference as

$$\Delta z_{t,k} = z_{t,k} - z_{t,k}^0, \quad \Delta t = t - t^0. \quad (\text{A15})$$

DeepLIFT assigns contribution scores $C_{\Delta z_{t,k} \rightarrow \Delta t}$ such that the total change in the target is exactly decomposed into additive input contributions:

$$\sum_k C_{\Delta z_{t,k} \rightarrow \Delta t} = \Delta t. \quad (\text{A16})$$

Computationally, these contributions are obtained efficiently using a single backward pass with finite-difference-style propagation rules. In Deep SHAP, DeepLIFT-style attributions are averaged over a background set of reference inputs to approximate SHAP values (Lundberg & Lee 2017).

References

- Adämmer, P. & Schüssler, R. A. (2020), ‘Forecasting the Equity Premium: Mind the News!’, *Review of Finance* **24**(6), 1313–1355.
- Agirre, E., Alfonseca, E., Hall, K., Kravalova, J., Pasca, M. & Soroa, A. (2009), A Study on Similarity and Relatedness Using Distributional and WordNet-based Approaches, *in* ‘Proceedings of Human Language Technologies: The 2009 Annual Conference of the North American Chapter of the Association for Computational Linguistics’, pp. 19–27.
- Andersen, T. G. & Bollerslev, T. (1998), ‘Answering the Skeptics: Yes, Standard Volatility Models do Provide Accurate Forecasts’, *International Economic Review* pp. 885–905.
- Andersen, T. G., Bollerslev, T. & Diebold, F. X. (2007), ‘Roughing It up: Including Jump Components in the Measurement, Modeling, and Forecasting of Return Volatility’, *The Review of Economics and Statistics* **89**(4), 701–720.
- Andersen, T. G., Bollerslev, T., Diebold, F. X. & Labys, P. (2003), ‘Modeling and Forecasting Realized Volatility’, *Econometrica* **71**(2), 579–625.
- Andersen, T. G., Bollerslev, T., Diebold, F. X. & Vega, C. (2007), ‘Real-Time Price Discovery in Global Stock, Bond and Foreign Exchange Markets’, *Journal of International Economics* **73**(2), 251–277.
- Audrino, F. & Chassot, J. (2025), ‘HARd to Beat: The Overlooked Impact of Rolling Windows in the Era of Machine Learning’, *International Journal of Forecasting* .
- Audrino, F. & Knaus, S. D. (2016), ‘Lassoing the HAR Model: A Model Selection Perspective on Realized Volatility Dynamics’, *Econometric Reviews* **35**(8-10), 1485–1521.
- Barndorff-Nielsen, O. E. & Shephard, N. (2002), ‘Estimating Quadratic Variation Using Realized Variance’, *Journal of Applied Econometrics* **17**(5), 457–477.
- Barndorff-Nielsen, O., Hansen, P. R., Lunde, A. & Shephard, N. (2009), ‘Realised Kernels in Practice: Trades and Quotes’, *The Econometrics Journal* **12**(3), C1–C32.
- Bates, J. M. & Granger, C. W. (1969), ‘The Combination of Forecasts’, *Journal of the Operational Research Society* **20**(4), 451–468.
- Bernanke, B. S. & Kuttner, K. N. (2005), ‘What Explains the Stock Market’s Reaction to Federal Reserve Policy?’, *The Journal of Finance* **60**(3), 1221–1257.

- Bojanowski, P., Grave, E., Joulin, A. & Mikolov, T. (2017), ‘Enriching Word Vectors with Subword Information’, *Transactions of the Association for Computational Linguistics* **5**, 135–146.
- Bollerslev, T., Hood, B., Huss, J. & Pedersen, L. H. (2018), ‘Risk Everywhere: Modeling and Managing Volatility’, *The Review of Financial Studies* **31**(7), 2729–2773.
- Bollerslev, T., Patton, A. J. & Quaedvlieg, R. (2016), ‘Exploiting the Errors: A Simple Approach for Improved Volatility Forecasting’, *Journal of Econometrics* **192**(1), 1–18.
- Branco, R. R., Rubesam, A. & Zevallos, M. (2024), ‘Forecasting Realized Volatility: Does Anything Beat Linear Models?’, *Journal of Empirical Finance* **78**, 101524.
- Bybee, L., Kelly, B., Manela, A. & Xiu, D. (2024), ‘Business News and Business Cycles’, *The Journal of Finance* **79**(5), 3105–3147.
- Caldara, D. & Iacoviello, M. (2022), ‘Measuring Geopolitical Risk’, *American Economic Review* **112**(4), 1194–1225.
- Chen, Y., Kelly, B. T. & Xiu, D. (2022), ‘Expected Returns and Large Language Models’, *Available at SSRN 4416687*.
- Christensen, K., Siggaard, M. & Veliyev, B. (2023), ‘A Machine Learning Approach to Volatility Forecasting’, *Journal of Financial Econometrics* **21**(5), 1680–1727.
- Collobert, R., Weston, J., Bottou, L., Karlen, M., Kavukcuoglu, K. & Kuksa, P. (2011), ‘Natural Language Processing (Almost) from Scratch’, *Journal of Machine Learning Research* **12**(ARTICLE), 2493–2537.
- Corsi, F. (2009), ‘A Simple Approximate Long-Memory Model of Realized Volatility’, *Journal of Financial Econometrics* **7**(2), 174–196.
- Ederington, L. H. & Lee, J. H. (1993), ‘How Markets Process Information: News Releases and Volatility’, *The Journal of Finance* **48**(4), 1161–1191.
- Engle, R. F. & Ng, V. K. (1993), ‘Measuring and Testing the Impact of News on Volatility’, *The Journal of Finance* **48**(5), 1749–1778.
- French, K. R. & Roll, R. (1986), ‘Stock Return Variances: The Arrival of Information and the Reaction of Traders’, *Journal of Financial Economics* **17**(1), 5–26.
- Gallo, G. M. & Pacini, B. (2000), ‘The Effects of Trading Activity on Market Volatility’, *The European Journal of Finance* **6**(2), 163–175.

- Gentzkow, M., Kelly, B. & Taddy, M. (2019), ‘Text as Data’, *Journal of Economic Literature* **57**(3), 535–74.
- Groß-Klußmann, A. & Hautsch, N. (2011), ‘When Machines Read the News: Using Automated Text Analytics to Quantify High Frequency News-Implied Market Reactions’, *Journal of Empirical Finance* **18**(2), 321–340.
- Gu, S., Kelly, B. & Xiu, D. (2020), ‘Empirical Asset Pricing via Machine Learning’, *The Review of Financial Studies* **33**(5), 2223–2273.
- Han, B., Liu, A., Chen, J. & Knottenbelt, W. (2025), ‘Can Machine Learning Models Better Volatility Forecasting? A Combined Method’, *The European Journal of Finance* pp. 1–22.
- Hill, F., Reichart, R. & Korhonen, A. (2015), ‘SimLex-999: Evaluating Semantic Models With (Genuine) Similarity Estimation’, *Computational Linguistics* **41**(4), 665–695.
- Hillebrand, E. & Medeiros, M. C. (2010), ‘The Benefits of Bagging for Forecast Models of Realized Volatility’, *Econometric Reviews* **29**(5-6), 571–593.
- Huang, A. H., Wang, H. & Yang, Y. (2023), ‘FinBERT: A Large Language Model for Extracting Information from Financial Text’, *Contemporary Accounting Research* **40**(2), 806–841.
- Huang, R. & Polak, T. (2011), ‘LOBSTER: Limit Order Book Reconstruction System’, *Available at SSRN 1977207*.
- Kalev, P. S., Liu, W.-M., Pham, P. K. & Jarnecic, E. (2004), ‘Public Information Arrival and Volatility of Intraday Stock Returns’, *Journal of Banking & Finance* **28**(6), 1441–1467.
- Karpoff, J. M. (1987), ‘The Relation Between Price Changes and Trading Volume: A Survey’, *Journal of Financial and Quantitative Analysis* **22**(1), 109–126.
- Kim, Y. (2014), ‘Convolutional Neural Networks for Sentence Classification’, *arXiv preprint arXiv:1408.5882*.
- Kingma, D. P. & Ba, J. (2014), ‘Adam: A Method for Stochastic Optimization’, *arXiv preprint arXiv:1412.6980*.
- Lamoureux, C. G. & Lastrapes, W. D. (1990), ‘Heteroskedasticity in Stock Return Data: Volume versus GARCH Effects’, *The Journal of Finance* **45**(1), 221–229.
- LeCun, Y., Bengio, Y. & Hinton, G. (2015), ‘Deep learning’, *Nature* **521**(7553), 436–444.

- Li, S. Z. & Tang, Y. (2025), ‘Automated Volatility Forecasting’, *Management Science* **71**(7), 6248–6274.
- Liu, L. Y., Patton, A. J. & Sheppard, K. (2015), ‘Does Anything Beat 5-Minute RV? A Comparison of Realized Measures Across Multiple Asset Classes’, *Journal of Econometrics* **187**(1), 293–311.
- Loughran, T. & McDonald, B. (2011), ‘When Is a Liability Not a Liability? Textual Analysis, Dictionaries, and 10-Ks’, *The Journal of Finance* **66**(1), 35–65.
- Lundberg, S. M. & Lee, S.-I. (2017), ‘A Unified Approach to Interpreting Model Predictions’, *Advances in Neural Information Processing Systems* **30**.
- Manela, A. & Moreira, A. (2017), ‘News Implied Volatility and Disaster Concerns’, *Journal of Financial Economics* **123**(1), 137–162.
- McGill, R., Tukey, J. W. & Larsen, W. A. (1978), ‘Variations of Box Plots’, *The American Statistician* **32**(1), 12–16.
- Mikolov, T., Chen, K., Corrado, G. & Dean, J. (2013), ‘Efficient Estimation of Word Representations in Vector Space’, *arXiv preprint arXiv:1301.3781*.
- Mikolov, T., Sutskever, I., Chen, K., Corrado, G. S. & Dean, J. (2013), ‘Distributed Representations of Words and Phrases and their Compositionality’, *Advances in Neural Information Processing Systems* **26**.
- Moreno-Pino, F. & Zohren, S. (2024), ‘DeepVol: Volatility Forecasting from High-Frequency Data with Dilated Causal Convolutions’, *Quantitative Finance* **24**(8), 1105–1127.
- Morin, F. & Bengio, Y. (2005), Hierarchical Probabilistic Neural Network Language Model, in ‘International Workshop on Artificial Intelligence and Statistics’, PMLR, pp. 246–252.
- Patton, A. J. (2011), ‘Volatility Forecast Comparison Using Imperfect Volatility Proxies’, *Journal of Econometrics* **160**(1), 246–256.
- Patton, A. J. & Sheppard, K. (2015), ‘Good Volatility, Bad Volatility: Signed Jumps and The Persistence of Volatility’, *Review of Economics and Statistics* **97**(3), 683–697.
- Patton, A. J. & Zhang, H. (2025), ‘Bespoke Realized Volatility: Tailored Measures of Risk for Volatility Prediction’, *Journal of Econometrics* **In Press**.
- Pennington, J., Socher, R. & Manning, C. D. (2014), GloVe: Global Vectors for Word Representation,

- in ‘Proceedings of the 2014 Conference on Empirical Methods in Natural Language Processing (EMNLP)’, pp. 1532–1543.
- Politis, D. N. & Romano, J. P. (1994), ‘The Stationary Bootstrap’, *Journal of the American Statistical Association* **89**(428), 1303–1313.
- Rahimikia, E. & Drinkall, F. (2024), ‘Re(Visiting) Large Language Models in Finance’, *Available at SSRN* .
- Rahimikia, E. & Poon, S.-H. (2020), ‘Machine Learning for Realised Volatility Forecasting’, *Available at SSRN* **3707796**.
- Ross, S. A. (1989), ‘Information and Volatility: The No-Arbitrage Martingale Approach to Timing and Resolution Irrelevancy’, *The Journal of Finance* **44**(1), 1–17.
- RoyChowdhury, A., Sharma, P., Learned-Miller, E. & Roy, A. (2017), Reducing Duplicate Filters in Deep Neural Networks, in ‘NIPS Workshop on Deep Learning: Bridging Theory and Practice’, Vol. 1, p. 1.
- Sermpinis, G., Laws, J. & Dunis, C. L. (2013), ‘Modelling and Trading the Realised Volatility of the FTSE100 Futures with Higher Order Neural Networks’, *The European Journal of Finance* **19**(3), 165–179.
- Shrikumar, A., Greenside, P. & Kundaje, A. (2017), Learning Important Features Through Propagating Activation Differences, in ‘International Conference on Machine Learning’, PMLR, pp. 3145–3153.
- Sirignano, J. & Cont, R. (2019), ‘Universal Features of Price Formation in Financial Markets: Perspectives from Deep Learning’, *Quantitative Finance* **19**(9), 1449–1459.
- Tetlock, P. C. (2007), ‘Giving Content to Investor Sentiment: The Role of Media in the Stock Market’, *The Journal of Finance* **62**(3), 1139–1168.
- Timmermann, A. (2006), ‘Forecast Combinations’, *Handbook of Economic Forecasting* **1**, 135–196.
- Tukey, J. W. (1977), *Exploratory Data Analysis*, Addison-Wesley, Reading, MA.
- Van Binsbergen, J. H., Bryzgalova, S., Mukhopadhyay, M. & Sharma, V. (2024), (Almost) 200 Years of News-Based Economic Sentiment, Technical report, National Bureau of Economic Research.
- White, H. (2000), ‘A Reality Check for Data Snooping’, *Econometrica* **68**(5), 1097–1126.

Womack, K. L. (1996), ‘Do Brokerage Analysts’ Recommendations Have Investment Value?’, *The Journal of Finance* **51**(1), 137–167.

Zhao, W., Joshi, T., Nair, V. N. & Sudjianto, A. (2020), ‘SHAP Values for Explaining CNN-based Text Classification Models’, *arXiv preprint arXiv:2008.11825* .